PB82-196866

Flux Force/Condensation Scrubbing for Collecting Fine Particulate from Iron Melting Cupolas

Air Pollution Technology, Inc.
San Diego, CA

Prepared for

Industrial Environmental Research Lab.
Research Triangle Park, NC

Sep 81

U.S. Department of Commerce
National Technical Information Service
NTIS

United States
Environmental Protection
Agency

EPA-600/7-81-148

September 1981

EPA

Research and Development

PB82-196866

FLUX FORCE/CONDENSATION SCRUBBING FOR COLLECTING FINE PARTICULATE FROM IRON MELTING CUPOLAS

Prepared for

Office of Environmental Engineering and Technology

Prepared by

Industrial Environmental Research
Laboratory
Research Triangle Park NC 27711

REPRODUCED BY
NATIONAL TECHNICAL
INFORMATION SERVICE
U.S. DEPARTMENT OF COMMERCE
SPRINGFIELD, VA 22161

TECHNICAL REPORT DATA
(Please read Instructions on the reverse before completing)

1. REPORT NO. EPA-600/7-81-148	2.	3. RECIPIENT'S ACCESSION NO. PB82 196866
4. TITLE AND SUBTITLE Flux Force/Condensation Scrubbing for Collecting Fine Particulate from Iron Melting Cupolas		5. REPORT DATE September 1981 6. PERFORMING ORGANIZATION CODE
7. AUTHOR(S) Richard D. Chmielewski and Seymour Calvert		8. PERFORMING ORGANIZATION REPORT NO.
9. PERFORMING ORGANIZATION NAME AND ADDRESS Air Pollution Technology, Inc. 4901 Morena Boulevard, Suite 402 San Diego, California 92117		10. PROGRAM ELEMENT NO. EHE624A 11. CONTRACT/GRANT NO. 68-02-2191
12. SPONSORING AGENCY NAME AND ADDRESS EPA, Office of Research and Development Industrial Environmental Research Laboratory Research Triangle Park, NC 27711		13. TYPE OF REPORT AND PERIOD COVERED Final; 10/76-8/81 14. SPONSORING AGENCY CODE EPA/600/13

15. SUPPLEMENTARY NOTES IERL-RTP project officer is Dale L. Harmon, Mail Drop 61, 919/541-2925.

16. ABSTRACT The report gives results of a 6-month test, demonstrating the industrial feasibility of a flux force/condensation (F/C) scrubbing system for controlling particulate emissions from an iron and steel melting cupola. The demonstration, conducted by A.P.T., Inc., under EPA contract, was part of a sequence of research and development projects for this method of particulate pollution control. A particle collection efficiency of 84% was required to meet the emission limit for a melting rate of about 12,500 kg/hr. The demonstration plant was designed to enable experimental determination of operating characteristics when attaining efficiencies around the emission limit. Particle size distributions, flow rates, pressure drops, temperatures, and other parameters were measured and utilized for performance analysis and comparison with theoretical predictions. After an initial period during which equipment and operating methods were refined, the system performed well and without significant difficulty. An optimized F/C scrubbing system for this application would require only about 65% of the predicted power requirement for a conventional high energy system. The total annual operating cost for an F/C scrubber system was estimated to be $131,000, compared to $150,000 for a new conventional venturi scrubber system.

17. KEY WORDS AND DOCUMENT ANALYSIS

a. DESCRIPTORS	b. IDENTIFIERS/OPEN ENDED TERMS	c. COSATI Field/Group
Pollution Dust Aerosols Iron and Steel Industry Melting Furnace Cupolas Scrubbers Flux Density Condensing	Pollution Control Stationary Sources Particulate Flux Force/Condensation	13B 07A 11G 14G 07D 11F 13H 13I

18. DISTRIBUTION STATEMENT Release to Public	19. SECURITY CLASS *(This Report)* Unclassified	21. NO. OF PAGES 135
	20. SECURITY CLASS *(This page)* Unclassified	22. PRICE

EPA Form 2220-1 (9-73)

EPA 600/7-81-148
September 1981

Flux Force/Condensation Scrubber System

For Collection of Fine Particulate

Emissions From An Iron Melting Cupola

by

Richard D. Chmielewski and Seymour Calvert

Air Pollution Technology, Inc.
4901 Morena Blvd., Suite 402
San Diego, California 92117

Contract No. 68-02-2191

EPA Project Officer: Dale L. Harmon

ABSTRACT

A flux force/condensation (F/C) scrubbing system for the control of particulate emissions from an iron and steel melting cupola demonstrated its industrial feasibility during a six month test period. This demonstration program was conducted by A.P.T., Inc. under an E.P.A. contract and was part of a sequence of research and development projects for this method of particulate pollution control.

A particle collection efficiency of 84% was required to meet the emission limit for a melting rate which ranged around 12,500 kg/hr. The demonstration plant was designed so as to enable experimental determination of operating characteristics when attaining efficiencies around the emission limit. Measurements of particle size distributions, flow rates, pressure drops, temperatures, and other parameters were made and utilized for performance analysis and comparison with theoretical predictions.

After an initial period during which equipment and operating methods were refined, the system performed well and without significant difficulty. An optimized F/C scrubbing system for this application would require only about 65% of the predicted power requirement for a conventional high energy system. The total annual operating cost for an F/C scrubber system was estimated to be $131,000 compared to $150,000 for a new conventional Venturi scrubber system.

TABLE OF CONTENTS

iii.	ABSTRACT	ii
v.	LIST OF FIGURES	iv
viii.	LIST OF TABLES	vii
ix.	SYMBOLS AND ABBREVIATIONS	viii
xii.	NOMENCLATURE	xi
xv.	ACKNOWLEDGEMENT	xiv
I.	INTRODUCTION	1
II.	SUMMARY, CONCLUSIONS, RECOMMENDATIONS	7
III.	SITE SELECTION	10
IV.	SYSTEM DESIGN	18
V.	PERFORMANCE TESTING	42
VI.	SYSTEM PERFORMANCE MODEL	48
VII.	COMPARISON OF EXPERIMENTAL RESULTS AND PERFORMANCE MODEL	61
VIII.	ECONOMIC ANALYSIS	83
	APPENDIX	96

LIST OF FIGURES

Figure		Page
3-1	Particle Size Distribution Site One	13
3-2	Particle Size Distribution Site Two	14
3-3	Particle Size Distribution Site Three	15
4-1	F/C Demonstration Plant Flow Diagram Induced Draft	19
4-2	F/C Demonstration Plant Flow Diagram Forced Draft	20
4-3	Induced Draft System (Plan View)	21
4-4	Induced Draft System (Elevation View)	22
4-5	Forced Draft System (Plan View)	23
4-6	Forced Draft System (Elevation View)	24
4-7	Process Flow Sheet Induced Draft System	25
4-8	Process Flow Sheet Forced Draft System	26
5-1	Modified EPA Sampling System with In-Stack Cascade Impactor	47
6-1	Simplified F/C Scrubber System	49
6-2	Example of Initial and Grown Size Distribution	56
6-3	Example of Condenser, Scrubber and Combined Penetration	57
7-1	Histogram of Condenser Inlet Mass Concentration	69
7-2	Average Condenser Inlet Size Distribution	69
7-3	Average Condenser Inlet Cumulative Size Distribution	69

LIST OF FIGURES (cont.)

Figure		Page
7-4	Predicted and Experimental Pt Run 36/1	72
7-5	Predicted and Experimental Pt Run 36/2	72
7-6	Predicted and Experimental Pt Run 36/3	72
7-7	Predicted and Experimental Pt Run 36/4	72
7-8	Predicted and Experimental Pt Run 36/6	73
7-9	Predicted and Experimental Pt Run 36/7	73
7-10	Predicted and Experimental Pt Run 36/8	73
7-11	Predicted and Experimental Pt Run 36/9	73
7-12	Predicted and Experimental Pt Run 36/10	74
7-13	Predicted and Experimental Pt Run 36/11	74
7-14	Predicted and Experimental Pt Run 36/12	74
7-15	Predicted and Experimental Pt Run 36/13	74
7-16	Predicted and Experimental Pt Run 36/14	75
7-17	Predicted and Experimental Pt Run 36/15	75
7-18	Predicted and Experimental Pt Run 36/16	75
7-19	Predicted and Experimental Pt Run 36/17	75
7-20	Predicted and Experimental Pt Run 36/18	76
7-21	Predicted and Experimental Pt Run 36/19	76
7-22	Predicted and Experimental Pt Run 36/20	76
7-23	Predicted and Experimental Pt Run 36/21	76
7-24	Predicted and Experimental Pt Run 36/22	77
7-25	Predicted and Experimental Pt Run 37/1	77
7-26	Predicted and Experimental Pt Run 37/3	77
7-27	Predicted and Experimental Pt Run 37/4	77

LIST OF FIGURES (cont.)

Figure		Page
7-28	Predicted and Experimental Pt Run 37/5	78
7-29	Predicted and Experimental Pt Run 37/6	78
7-30	Predicted and Experimental Pt Run 37/7	78
7-31	Predicted and Experimental Pt Run 37/8	78
7-32	Predicted and Experimental Pt Run 37/9	79
7-33	Predicted and Experimental Pt Run 37/10	79
7-34	Predicted and Experimental Pt Run 37/11	79
7-35	Predicted and Experimental Pt Run 37/12	79
7-36	Predicted and Experimental Pt Run 37/13	80
7-37	Predicted and Experimental Pt Run 37/15	80
7-38	Predicted and Experimental Pt Run 37/16	80
7-39	Predicted and Experimental Pt Run 37/17	80
7-40	Predicted and Experimental Pt Run 37/18	81
7-41	Predicted and Experimental Pt Run 37/19	81
7-42	Predicted and Experimental Pt Run 37/21	81
7-43	Predicted and Experimental Pt Run 37/23	81
7-44	Predicted and Experimental Pt Run 37/24	82
7-45	Predicted and Experimental Pt Run 37/25	82
7-46	Predicted and Experimental Pt Run 37/26	82
7-47	Predicted and Experimental Pt Run 37/27	82
8-1	Optimum F/C Scrubber System Flow Diagram	86

LIST OF TABLES

No.		Page
1-1	F/C Scrubbing Studies by A.P.T. for EPA	2
1-2	F/C Scrubbing Performance Data Sources	5
3-1	Summary of Alternate Cupola Operations	11
4-1	Pump Specifications	35
6-1	Input Variables for Prediction of Scrubber Performance	55
6-2	Example Calculation	55
7-1	F/C Scrubber System Operating Parameters for 36 Series	63
7-2	F/C Scrubber System Operating Parameters for 37 Series	64
7-3	Gas Flow Rates, Temperatures and Measured Condensation Ratio for 36 Series	65
7-4	Gas Flow Rates, Temperatures and Measured Condensation Ratio for 37 Series	66
7-5	Particulate Mass Concentrations	70
7-6	Particulate Mass Concentrations	71
8-1	Summary of Equipment Costs F/C Scrubber System	87
8-2	Summary of Equipment Losts Conventional Scrubber	88
8-3	Direct and Indirect Cost F/C System	90
8-4	Direct and Indirect Cost Conventional Scrubber	91
8-5	Summary of Power Requirements	92
8-6	Summary of Annual Operating Costs	92

ABBREVIATIONS FOR UNITS

I. S.I. Units

Quantity	Unit	SI Symbol	Formula
Base Units:			
length	metre	m	
mass	kilogram	kg	
time	second	s ("sec" in Eng.)	
power	watt	W	J/s
pressure	pascal	Pa	N/m^2
quantity of heat	joule	J	N·m

II. Additional Metric Units ***

mass	gram	g
volume	liter	
pressure	atmosphere	atm
	length of water column	cm W.C.
	length of mercury column	cm Hg
time	minute	min
	hour	hr
	day	day
	month	mo
	year	yr
temperature	degree Celsius	°C

* Reference: ASTM Standard E380

** A dash is preferred although the Standard uses dots; e.g., A-s/v

*** The units of poise, stoke, erg, calorie, and dyne are not acceptable S.I. units, but their corresponding formulae are acceptable.

III. English Units

Quantity	Unit	Symbol
mass	pound mass	lbm
force	pound force	lbf
length	inch	in.
temperature	degree Fahrenheit	°F
energy	British thermal units	BTU
power	horsepower	HP
flow rate	gallons per min.	GPM
	cubic feet per min.	CFM
pressure	pounds per sq. in.	lbf/in^2 or (psia, psig)
	length of water column	in. W.C.
	length of mercury column	in. Hg

IV. Other Abbreviations

Quantity	Abbreviations
molecular weight	M.W.
average	avg
barrel	bbl
cubic meter, cubic foot, etc	m^3, ft^3, etc
natural logarithm	ln
common logarithm (base 10)	log
parts per million	ppm
Air Pollution Technology, Inc.	A.P.T.
entrainment separator	E.S.
cascade impactor	C.I.

Prefixes for English units:

actual (at system T, P. and humidity)	A
dry	D
standard (at 68°F and 29.9 in. Hg	S
hundred	C
thousand	M

Prefixes for S.I. units:

actual	A
dry	D
normal (at 20°C and 76 cm Hg)	N

NOMENCLATURE

Latin

C - Mass concentration, g/DNm³

C' - Cunningham slip correction factor, dimensionless

C_D - Drag coefficient, dimensionless

d_c - Collector diameter, m or cm

d_d - Drop diameter, m, cm, or μm

d_p - Particle diameter, m, cm, or μ

d_{pa} - Particle aerodynamic diameter, μmA
where $d_{pa} \equiv d_p (C'\varrho_p)^{\frac{1}{2}}$ and the units used are:

d_p in μm, ϱ_p in g/cm³ and μmA = μm(g/cm³)$^{\frac{1}{2}}$

d_{pc} - Particle aerodynamic cut (50%) diameter, μm (g/cm³)$^{\frac{1}{2}}$

d_{pg} - Mass mean geometric diameter, cm, μm, or μmA

DNm^3 - Dry normal cubic meters at 20°C and 1 atm pressure

f_p - Fraction of water condensed on particles, dimensionless

f_v - Mol fraction of gas condensing, dimensionless

H_d - Liquid holdup fraction, dimensionless

j - Channel width fraction, dimensionless

K - Coagulation constant, cm³/S

K_p - Inertial impaction parameter = $\dfrac{\mu_G \, d^2_{pa}}{9\mu_G \, d_c}$

L_t - Throat length, m or cm

n_p - Particle number concentration, number/m^3 or no./cm^3
P - Pressure, Pa, atm, or cm W.C., etc.
Pt - Penetration, fraction or %

$\overline{Pt}$ - Overall penetration, fraction or %

q' - Mass vapor condensed per mass or dry, kg/kg or g/g
Q_G - Gas Volumetric flow rate, m^3/s
Q_L - Liquid volumetric flow rate, m^3/s
t - Time, s
u_G - Gas velocity, m/s or cm/s
W_{cum} - Cumulative mass concentration, g/DNm^3 or mg/Dnm^3
Z - Distance or height, m

Greek

ΔP - Pressure drop or loss, Pa, atm, or cm W.C., etc.
ε - Volume fraction or voids (porosity), dimensionless
μ_G - Gas viscosity, kg/m-s or g/cm-s
μm - Micrometer (micron)
μmA - Micrometers, aerodynamic, $\mu mA\ (g/cm^3)^{\frac{1}{2}}$
ϱ - Density, kg/m^3 or g/cm^3
ϱ_G - Gas density, kg/m^3 or g/cm^3
ϱ_p - Particle density, kg/m^3 or g/cm^3
σ_g - Geometric standard deviation of particle size distribution

Subscripts

c - Condenser
c_D - Condenser, diffusiophoresis
c_i - Condenser inlet
c_I - Condenser, impaction
c_o - Condenser outlet

Subscripts

s - Scrubber
si - Scrubber inlet
so - Scrubber outlet
o - Original condition

ACKNOWLEDGEMENT

A.P.T., Inc. expresses its appreciation to Mr. Dale Harmon, EPA Project Officer, for excellent technical coordination and assistance in support of all our efforts under this contract.

SECTION 1
INTRODUCTION

Flux force/condensation (F/C) scrubbing has been developed by Air Pollution Technology under EPA-sponsorship for the past several years (see Table 1-1). The objectives of (F/C) scrubbing involve reducing the power requirement for collection of fine particles compared to conventional high energy scrubbers. The improvement in scrubber performance due to condensation effects is most apparent in the submicron size range where the mechanism of inertial impaction is difficult to apply economically.

There are three condensation effects which are utilized in F/C scrubbing. The condensation of water vapor from a hot saturated gas can be caused by contacting the gas with cold liquid. The suspended particles in the gas act as condensation nuclei, resulting in growth of the particles due to condensation of water vapor.

The transfer of water vapor toward the cold liquid results in diffusiophoresis. This mechanism collects particles by movement of the condensing water vapor toward the cold surface. Simultaneously, the temperature gradient established in the condenser causes a thermal force which leads to collection by thermophoresis. The particle growth due to condensation plus the flux forces of diffusiophoresis and thermophoresis enhance the particle collection efficiency of the F/C scrubber system.

TABLE 1-1

F/C SCRUBBING STUDIES BY A.P.T. FOR EPA

Title	Contract Report No. and Date	Subject
Wet Scrubber System Study - Scrubber Handbook (Vol. 1)	CPA-70-95 NTIS #PB 213-016 (1972)	F/C scrubbing principles and potential discussed.
Feasibility of Flux Force/Condensation Scrubbing for Fine Particulate Control	68-02-0256 EPA 650/2-73-036 NTIS #PB 227-307 (1973	Theoretical analysis, mathematical modeling, computer predictions, experimental data from bench-scale F/C scrubbers.
Study of Flux Force/ Condensation Scrubbing of Fine Particles	68-02-1082 EPA 600/2-75-018 (1975)	Laboratory pilot-plant study of F/C scrubbing in sieve plate and spray apparatus.
Study of Horizontal Spray Flux Force/Condensation Scrubber	68-02-1328 Task #10 EPA 600/2-76-200 (1976)	Laboratory pilot-plant study of F/C scrubbing in horizontal spray apparatus.
Fine Particle Collection by a Flux Force/ Condensation Scrubber: Pilot Demonstration	68-02-1869 EPA 600/2-77-238 (1977)	Pilot demonstration of F/C scrubbing with a sieve plate column on a secondary metal recoveryfurnace, analysis of results, and further development of mathematical modeling.

Background

Flux force effects on particles have been known for many years and the background is reviewed and discussed in depth by authors such as Waldmann and Schmitt (1966), Goldsmith and May (1966), Hidy and Brock (1970) and Calvert et al. (1972). The research and development work supported by the E.P.A. had the objectives of first assessing the potential of F/C scrubbing, then developing rational means for exploiting it, and then demonstrating the technology.

Calvert and Jhaveri (1974) presented the results of experimental studies of bench- and pilot-scale F/C scrubbers and compared them with the results obtained by other investigators for a variety of scrubbers in which condensation occurred. Table 1-2 indicates the type of apparatus which had been used by others who had reported their findings publicly. These references were located by means of extensive literature searches and were the only ones found which presented useful experimental data.

First Demonstration Plant

The feasibility of F/C scrubbing and a rational design basis were established in the first four studies listed in Table 1-1. The next step was a pilot-scale demonstration, which was carried out on a secondary metal recovery furnace. Control of the entire source effluent, a maximum flow rate of 200 Am^3/min (7,000 ACFM) at temperatures up to 800°C, required both particle collection and acid gas absorption. Demonstration plant performance was consistent with the preceeding laboratory, bench scale, and pilot-plant studies.

The nature of the source emissions entering the scrubber depended greatly on the operating conditions and on the type of

scrap copper wire or other metal scrap being incinerated to remove the insulation. A conventional high energy scrubber would be incapable of controlling emissions at a practically feasible pressure drop from anything but the premium grade of scrap. An F/C scrubber system would be feasible for the control of lower (more polluting) grade scrap; the type of scrap which had more commercial importance.

The system was generally capable of about 90% to 95% efficiency on particles with a mass median aerodynamic diameter of 0.7 to 0.8 μmA (about 0.3 μm physical diameter for particles with a density of 4.0 g/cm^3). This efficiency was achieved with a 68 cm (27 in.) W.C. gas phase pressure drop. A conventional high energy scrubber without F/C effects would require pressure drops of roughly 250 cm (98 in.) W. C. for 90% and 535 cfm (210 in.) W.C. for 95% particle collection efficiency.

Earlier studies (Calvert et al., 1973 and 1975) included theoretical development of design equations for F/C scrubbing and the development of a computer mathematical model to predict particle collection in a sieve plate F/C scrubber. The predictions compared well with experimental results, but the computerized model had certain limitations. Its usefulness for quick and overall design calculations was limited since solutions for each sieve plate and for each different set of operating conditions had to be calculated individually. In the first demonstration study, a revised mathematical model was developed from the same basic relationships and the design procedures were greatly simplified for prediction of F/C scrubber performance.

TABLE 1-2. F/C SCRUBBING PERFORMANCE DATA SOURCES

Fahnoe, Lindroos, and Abelson (1951)	(A) Cyclone, or (B) Peabody (1 plate)
Goldsmith and May (1966)	Tubular condenser
Lancaster and Strauss (1971)	Steam nozzle + spray + Cyclone
Litvinov (1967)	Venturi + 2 sieve plates
Prakash and Murray (1973)	Steam nozzle and Dry duct
Rozen and Kostin (1967)	Sieve plate with alternate hot and cold plates
Schauer (1952)	Steam nozzle + Peabody (5 plates)
Stinchombre and Goldsmith (1966)	Tubular Condenser
Terebenin and Bykov (1972)	Vertical wetted planes

We arrived at the conclusion that the flux force effects could be treated separately from the condensation effects in many scrubber situations. While the condensation-induced improvement in inertial impaction efficiency could be handled conveniently, the flux force deposition prediction remained cumbersome. Then we became aware of a concept developed by Whitmore (1977) which provided the key to simplifying the prediction of the diffusional effects in F/C scrubbing. By incorporating Whitmore's concept into our model we developed a much simpler design method which is convenient to use. Agreement between experimental data and predictions made with the revised model was good and illustrated the utility of the design method.

Present Project

This report presents the results of a demonstration project to test further the design methods and economics of flux force/condensation scrubbing on a large scale in an industrial environment. The F/C system was designed, built and tested on the total exhaust gas stream from a 12,500 Kg/hr iron and steel melting cupola. The demonstration experience involved six months of operation. This included summer, fall and winter in a demanding environment and resulted in a good test of the equipment design and materials selection.

SECTION 2
SUMMARY, CONCLUSIONS, AND RECOMMENDATIONS

SUMMARY

The objectives of this program were to demonstrate the performance and economics of a flux force/condensation scrubber system in an industrial environment. The major tasks were:

1. Select a company in the iron and steel industry suitable for the demonstration scrubber.
2. Design the demonstration scrubber system for the chosen site.
3. Prepare a test plan.
4. Fabricate, install and start up F/C system.
5. Conduct test program.
6. Maintain laboratory capability to support test program.
7. Analyze system performance.
8. Restore site, if needed.

All of the required tasks were completed. Because the system was appraised and then purchased by the host company, no site restoration was required.

A survey of three iron melting cupolas revealed that the main process parameters of exhaust gas temperature, flow rate and particulate concentration varied from site to site. Even for similar sized cupolas the gas flow rate, temperature, particle mass concentration, and size distribution varied. The site chosen had the largest production rate and uncontrolled mass emission rate of the three investigated.

The process weight limit required that the overall system penetration be less than 0.16 (16%) based on measured emission rates after the spray saturator. The mass mean aerodynamic diameter was found to average about 1.2 μmA. An optimized F/C scrubber system would require a total power expenditure of 223 kW

(299 HP) while 345 kW (462 HP) is predicted for a conventional high energy scrubber to meet the 16% penetration. This power saving was obtained by (1) reducing the necessary pressure drop for the F/C system and by (2) reducing the volumetric flow rate of the exhaust gas which occurs during the F/C process due to cooling.

The total annual operating cost for an F/C system operating on this source was estimated to be $131,000 compared to $150,000 for a new conventional venturi system. Fixed capital investments for F/C and conventional systems were $348,000 and $250,000, respectively.

CONCLUSIONS

The following conclusions can be drawn from the results of this study:

1. The performance data were in general accord with predictions based on design methods developed by A.P.T. on previous EPA contracts.
2. The F/C scrubber system was built, operated for six months, and shown to be in compliance with all applicable air pollution regulations for that site.
3. The F/C scrubber system needed only about 65% of the predicted power requirement of a conventional high energy scrubber to achieve the same performance.
4. The particle mass concentration and size distribution emitted during the cupola charging cycle varied greatly. Continuous or semicontinuous cupola charging with a conveyor system would probably reduce the variation in emissions and gas temperature.
5. The solids/liquid separation presented some maintenance problems. Additional attention should be given to equipment

design, both to prevent settling in the scrubber equipment and to improve solids separation in the water treatment system.

6. Corrosion of the cooling tower packing was severe. Sulfuric and sulfurous acids from the sulfur in the coke must be neutralized in order to prevent significant deterioration of steel components in the system. Maintenance of the proper circulating water pH is also important if stainless steel is used because of the chloride compounds present.
7. Operation over a six-month period showed that the F/C system is capable of performing well and without significant difficulty in the demanding conditions of a ferrous foundry. During the entire test period there were no production stoppages due to the F/C scrubbing system.
8. F/C scrubbing becomes more economically advantageous than conventional scrubbing as either power cost or plant operating time increases.

SECTION 3
SITE SELECTION

The site selection for the F/C demonstration plant involved preliminary investigation of three foundry operations. The first candidate was a foundry department in a shipyard which produced grey iron castings for use in the shipbuilding activities. The cupola had an internal diameter of 0.94 m and a melting rate of approximately 2,700 kg/hr (3 ton/hr). This cupola was operated with an iron to coke ratio which ranged from 5.6 to 7.2, depending upon the type of material being charged. The average iron to coke ratio was about 6.

This foundry operation produced a number of castings which required close attention to the composition of the metal produced. As a consequence each charge of coke, flux, iron and steel was weighed before charging and close control of melt rate and temperature was maintained.

Molten metal was taken from the cupola into a ladle which was used to pour the castings. This resulted in intermittent withdrawl of metal from the cupola, consequently the tuyere blower was operated in an on and off manner. The result was a wide variation in exhaust gas flows, temperature and particle concentration.

Table 3-1 summarizes the operating parameters for this foundry as well as two additional foundries which were evaluated. Particulate matter samples were taken at a location downstream of the hot gas quencher.

The second foundry produced cast iron pipe and fittings. The cupola was significantly larger than the first, having an internal diameter of 1.67 m and a melt rate of approximately 10,250 kg/hr. Table 3-1 shows the process conditions for this

TABLE 3-1. SUMMARY OF ALTERNATE CUPOLA OPERATIONS

	Site 1	Site 2	Site 3
Cupola Diameter (m)	0.94	1.67	1.67
Charge Wt. (kg)	438	682	1,815
Melt Rate (kg/hr)	2,700	10,250	12,500
Iron to Coke Ratio	6	7	6
Tuyere Air (DNm^3/s)	1.0	2.5	3.5
Exhaust Gas Flow (DNm^3/s)	2.5	5.8	6.6
Exhaust Gas Temperture (°C)	600-950	350-1,050	350-1,100
*Exhaust Gas Particle Concentration (g/DNm^3)	1.0	1.5	1.8

*Measured after quencher

cupola. The iron to coke ratio for this cupola averaged about 7. The charges were weighed before being loaded into the cupola. The tuyere air flow rate was controlled with an orifice meter, damper and an automatic controller.

The molten metal from this cupola was withdrawn continuously into a holding ladle from which metal was taken for various casting operations. This continous operation resulted in process conditions which were more uniform.

The third site investigated was a foundry which produced metal shot. The cupola had an internal diameter of 1.67 m. The production rate varied from about 8,200 kg/hr to 13,500 kg/hr depending upon the charging rate. The metal was withdrawn continuously from the cupola. Neither the charge weight nor the tuyere air flow rate was measured regularly by the foundry personnel.

PARTICULATE DATA FROM PRELIMINARY TESTS

Particle sampling were done at each of the three sites in order to measure particle size distribution . Sampling was performed using the University of Washington cascade impactors. A few E.P.A. Method 5 total filter runs were made to determine particle concentration and mass flow rate. Figures 3-1, 3-2, and 3-3, show the particle size distributions measured with the U.W. impactors at the three sites. In each case the sampling was done at a location downstream of the spray quenchers, which were used to cool the hot cupola exhaust gas. The design of the quench systems varied from plant to plant, however, each of the quench systems utilized preformed sprays, which probably resulted in some collection of larger particulate matter.

The particle size distribution measurements at each site were found to be reasonably consistent from run to run. At the first site the average mass mean particle aerodynamic diameter

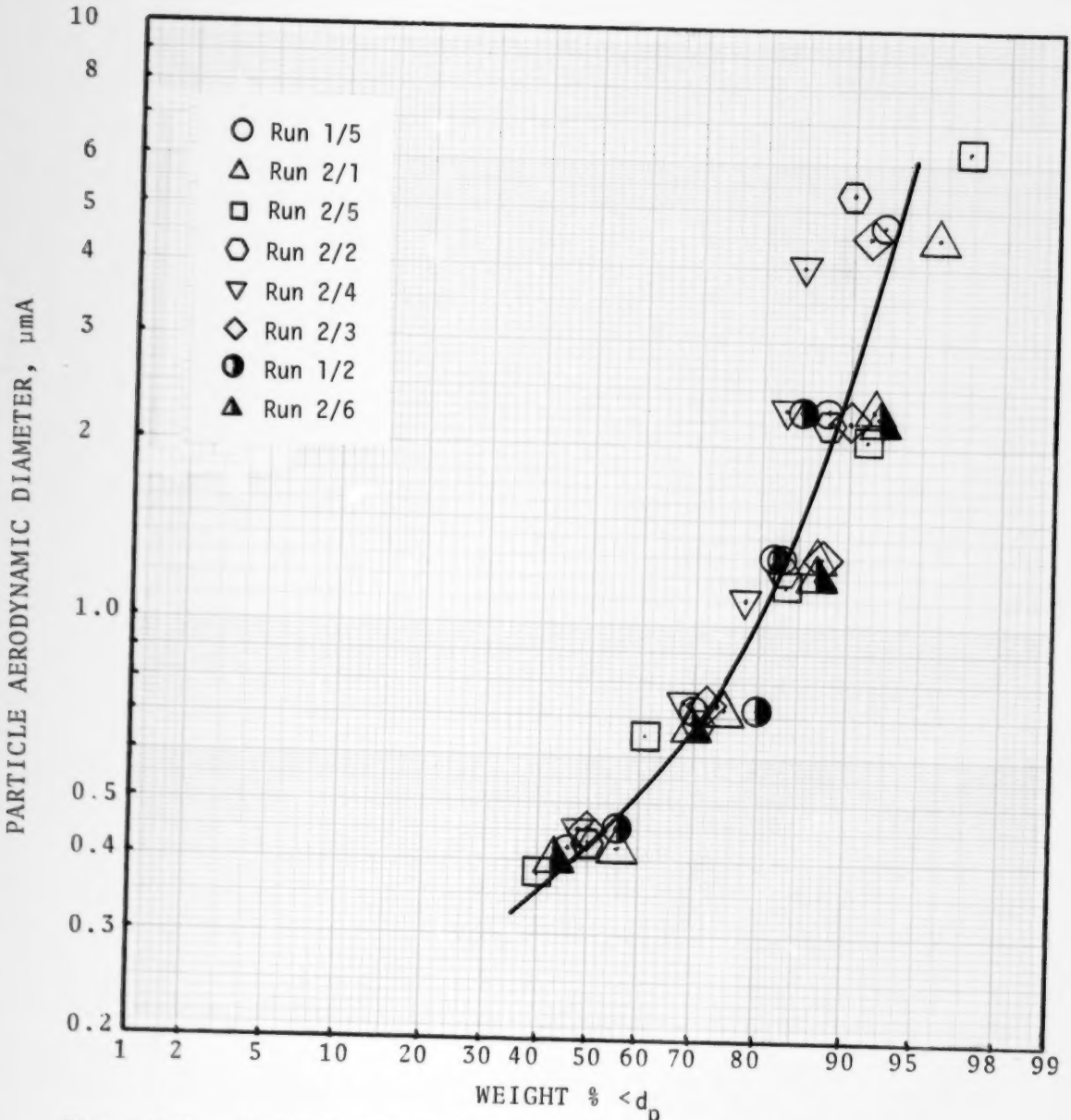

Figure 3-1. Particle size distribution after Quencher at site one.

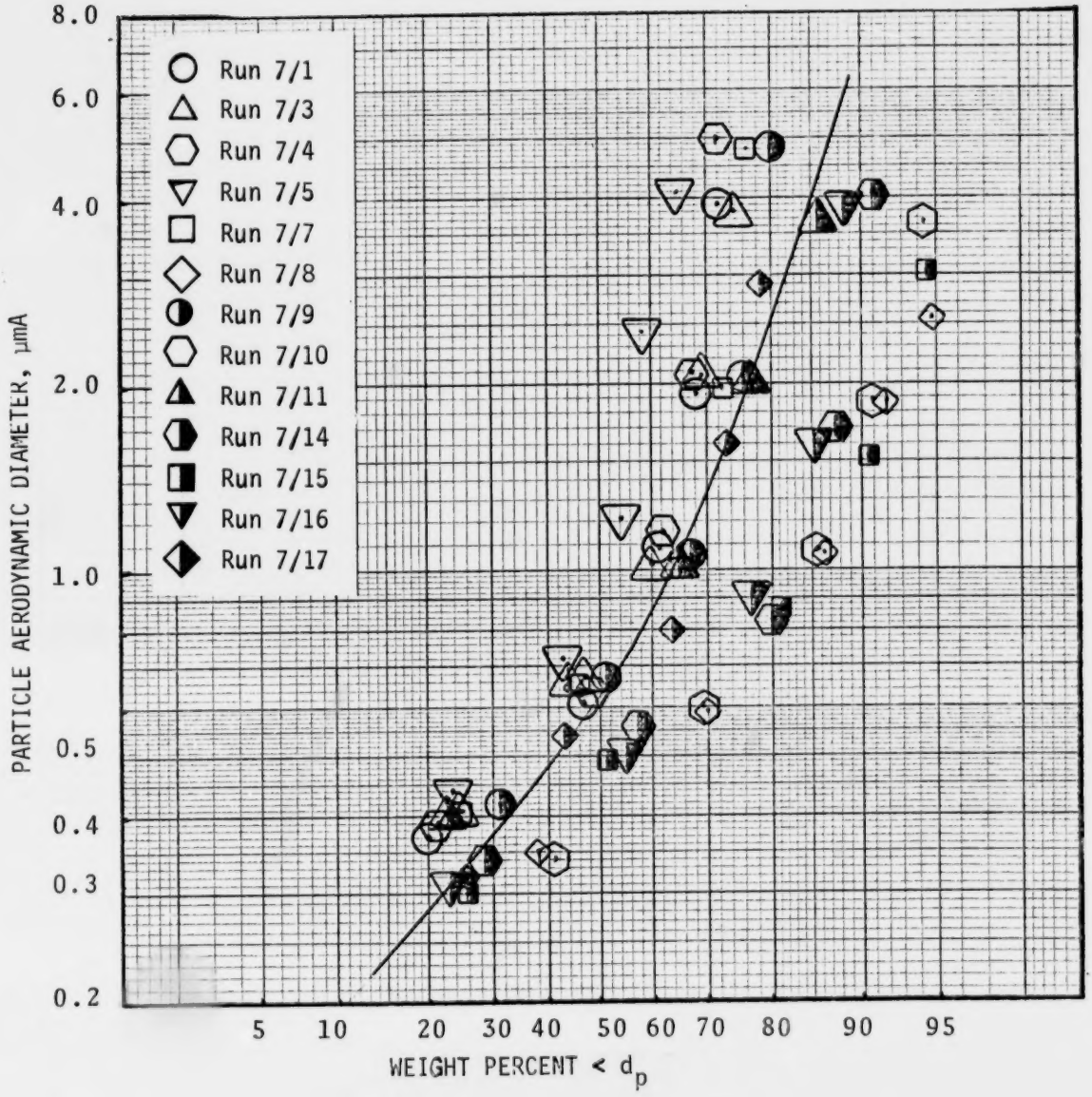

Figure 3-2. Particle size distribution after Quencher at site two.

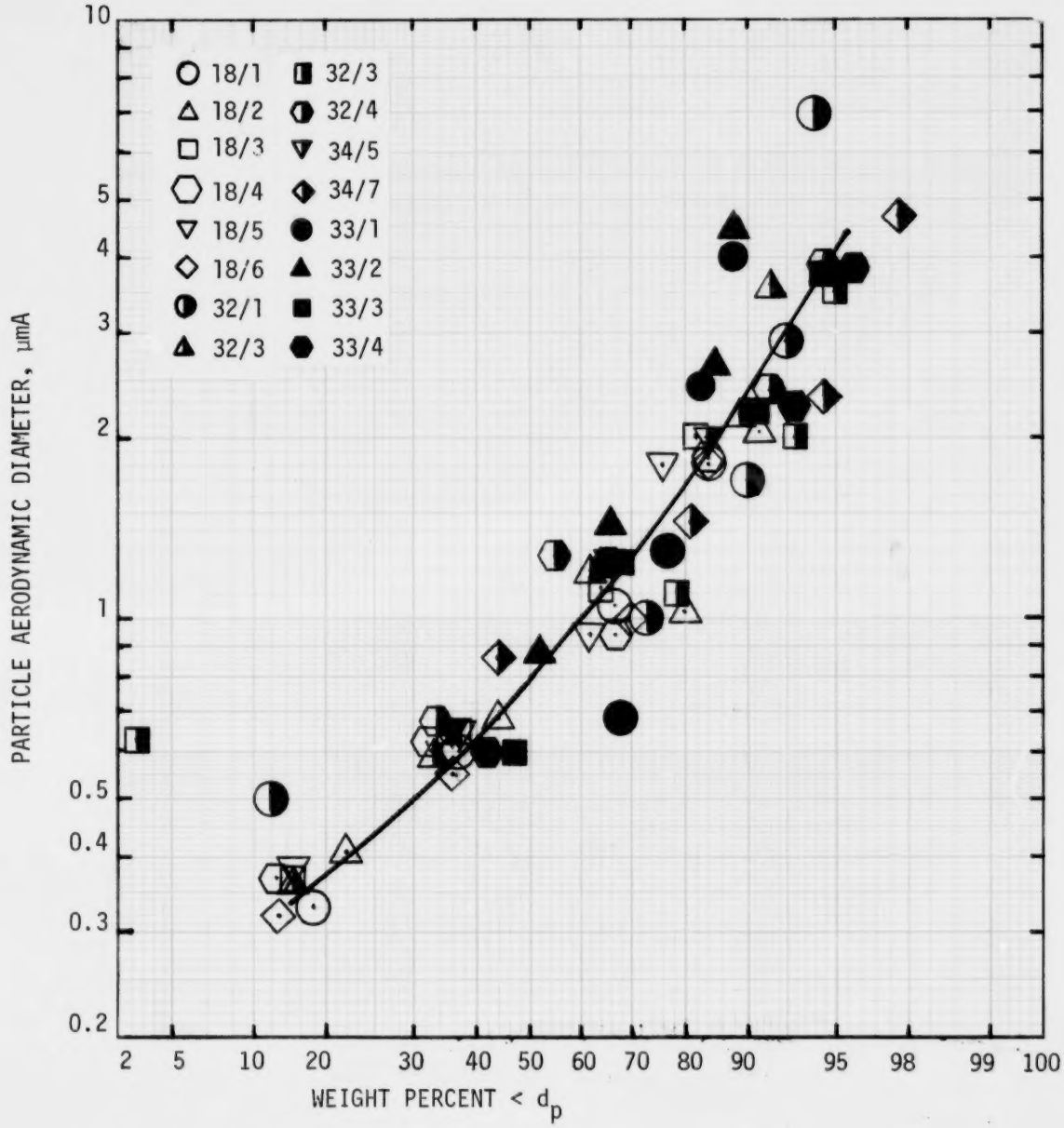

Figure 3-3. Particle size distribution after Quencher at site three.

was found to be about 0.45 μmA. The average mass concentration was 1.0 g/DNm³. This was the smallest cupola tested and the scrap charge was weighed very closely. The combination of small cupola and a closely controlled charge may contribute to the small particle size distribution measured. For the second site the average mass mean particle aerodynamic diameter was 0.6 μmA. The average particulate mass concentration was 1.5 g/DNm³. The third site was found to have a mass mean particle aerodynamic diameter which averaged 0.9 μmA. This large cupola had the highest particle concentration of 1.8 g/DNm³. No wieghing of the charges was performed at this foundry. The third site had the largest charge weight, as shown in Table 3-1.

SITE SELECTION

The site finally chosen for the demonstration plant was site 3. The first site proved to be unacceptable when the production schedule dropped to six hours per week. Discussion with the plant management indicated that while there was considerable interest in the project, the production level was not expected to increase in the near future. The size of the cupola was relatively small and not typical of large industrial sources. These two factors resulted in a decision to seek an alternative host company.

The second site was a better candidate for the demonstration system. The cupola was significantly larger and the production schedule was five days per week. The management of the plant allowed preliminary testing in order to obtain design data, however, A.P.T. could not convince the owners of the foundry to continue with the demonstration project. The lack of available space for the proposed equipment was one contributing factor to the decision to reject the second site.

The third site was found and proved to be the better choice for building the demonstration plant. This site had a cupola which is representative of the larger cupolas in operation.

The foundry had an existing air pollution system consisting of an afterburner tank, quencher, Venturi scrubber and exhaust fan. The existing system was 12 years old and capable of only marginal performance. As a consequence the plant management had a keen interest in hosting the demonstration plant.

SECTION 4
SYSTEM DESIGN

INTRODUCTION

This section describes the system process design, the component design functions, and the structural details of the F/C scrubbing demonstration plant. The system flow diagrams are shown in Figures 4-1 and 4-2 for the induced draft and forced draft configuration, respectively. Both configurations draw the hot gas from the cupola through the breeching and afterburner tank to the saturator and condenser vessels. In the induced draft system the blower is located downstream of the scrubber, while in the forced draft mode the blower is located between the condenser and the scrubber. Figures 4-3 and 4-4 show the system layouts for the induced draft system. Figures 4-5 and 4-6 show the layout for the forced draft system. Note that only the ducting is modified to switch from forced to induced draft; the other components remained stationary.

PROCESS DESCRIPTION

Figures 4-7 and 4-8 show the process flow sheet for both the induced draft and forced draft configurations. The design conditions were set to maximize F/C effects, given the cupola emission parameters which were measured in preliminary tests.

The cupola converts scrap iron and steel to the molten state using heat generated by combustion of coke. The combustion air is supplied to tuyeres in the bottom of the cupola by a tuyere air blower. The cupola is a cylindrical vessel, brick lined internally and water cooled externally. The melting rate is determined by the charging rate and tuyere air flow rate. Raw materials are composed of scrap structural steel, engine blocks,

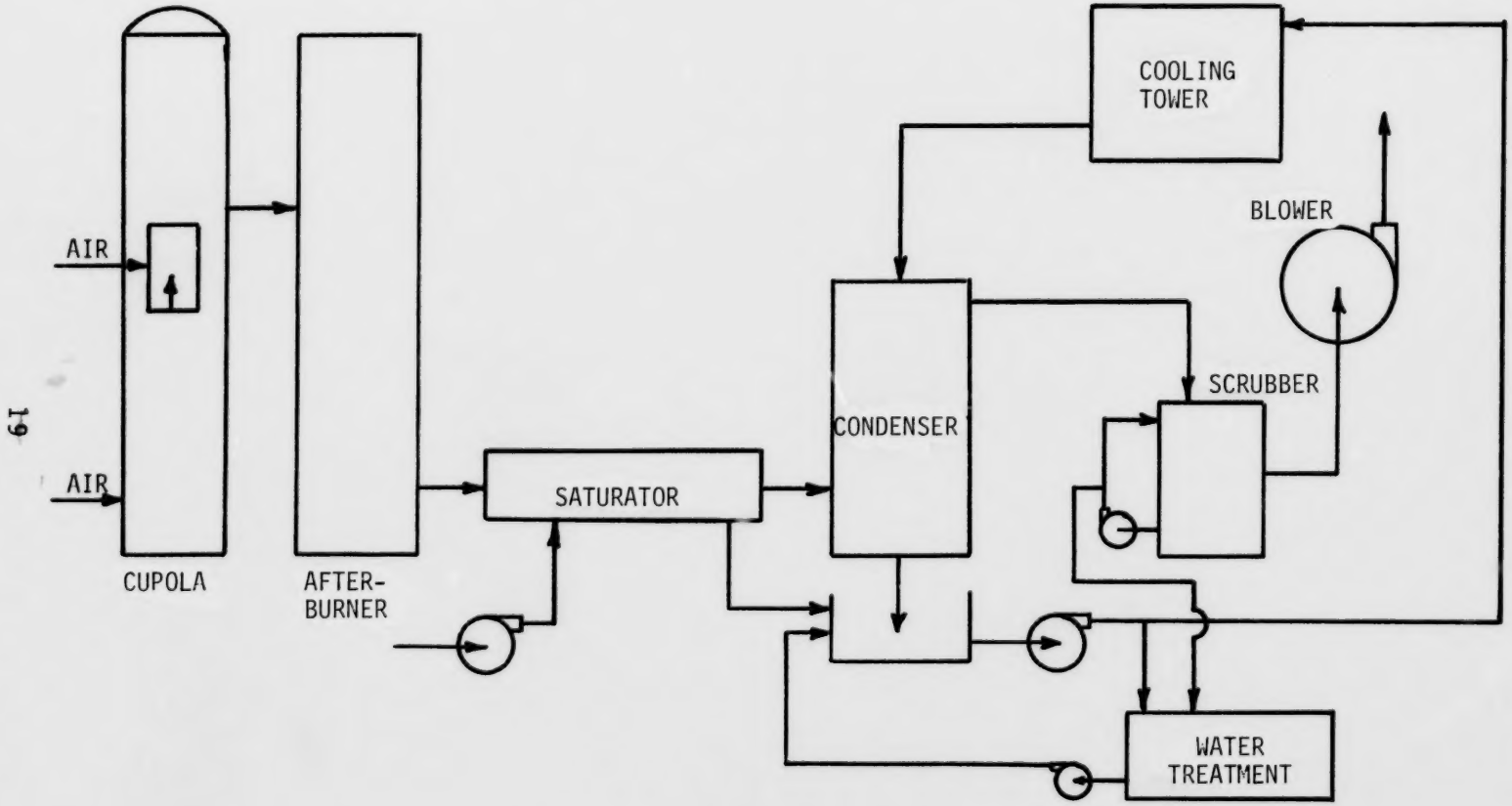

Figure 4-1. F/C demonstration plant flow diagram, induced draft.

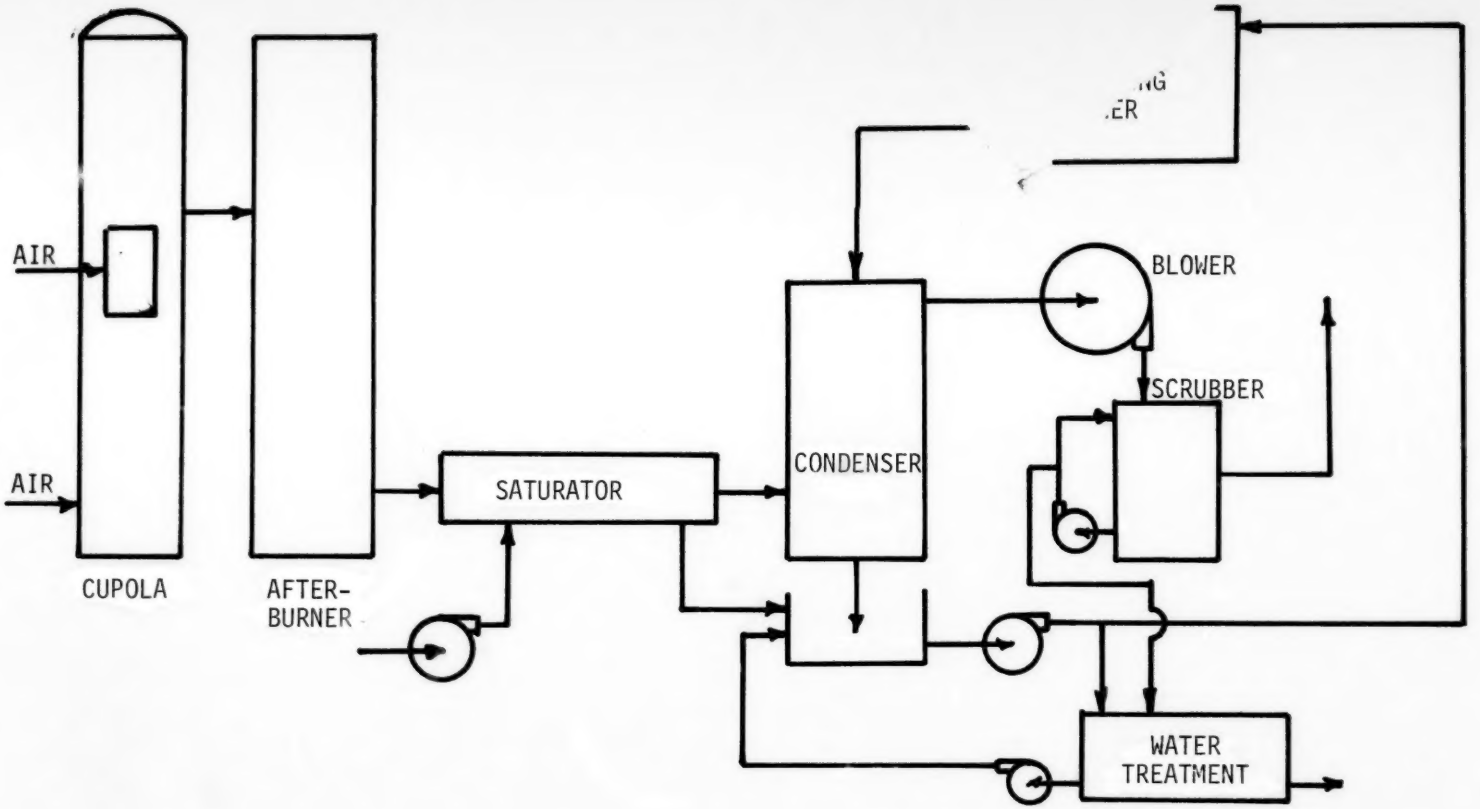

Figure 4-2. F/C Demonstration plant flow diagram, forced draft

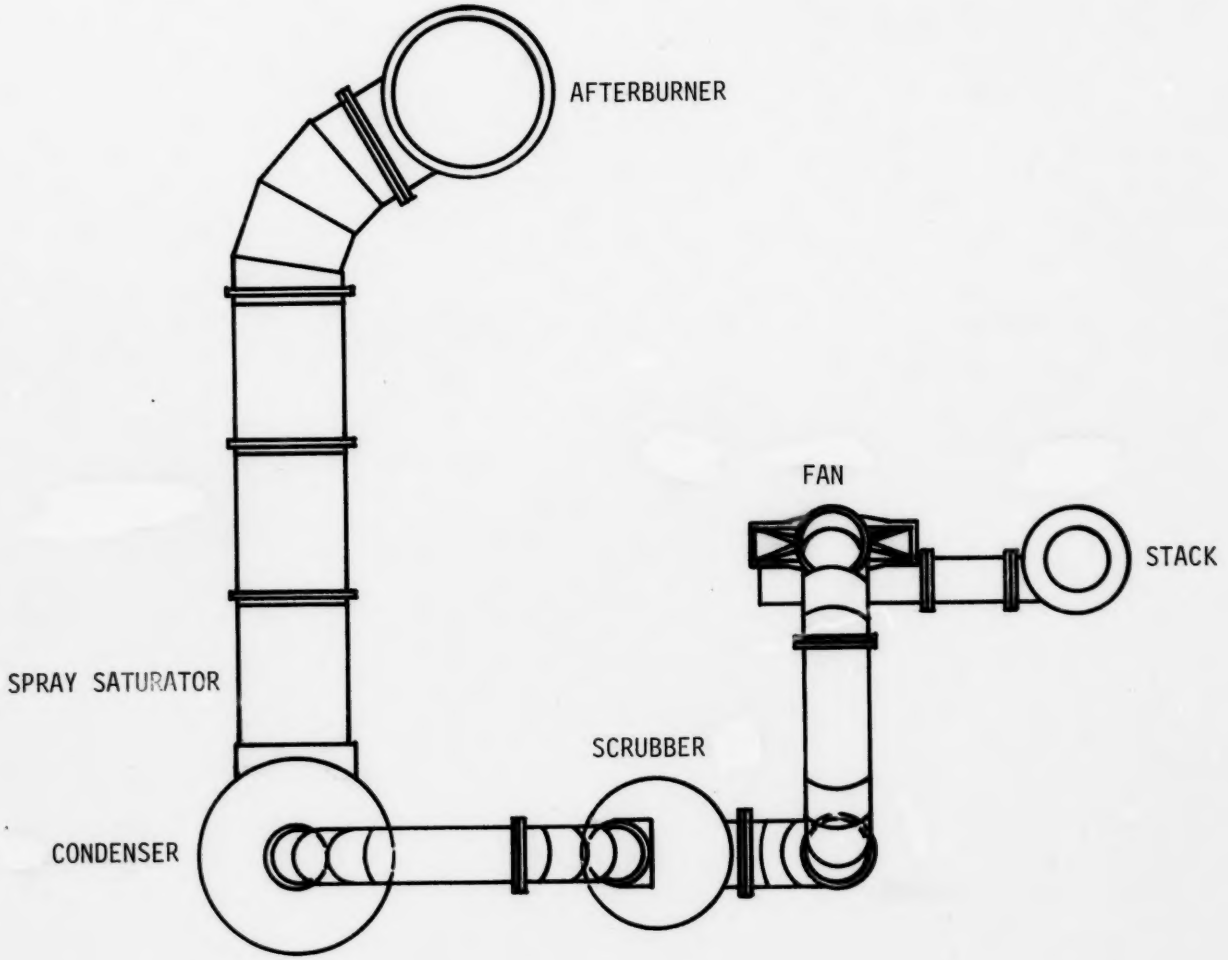

Figure 4.3 Induced draft system (Plan View).

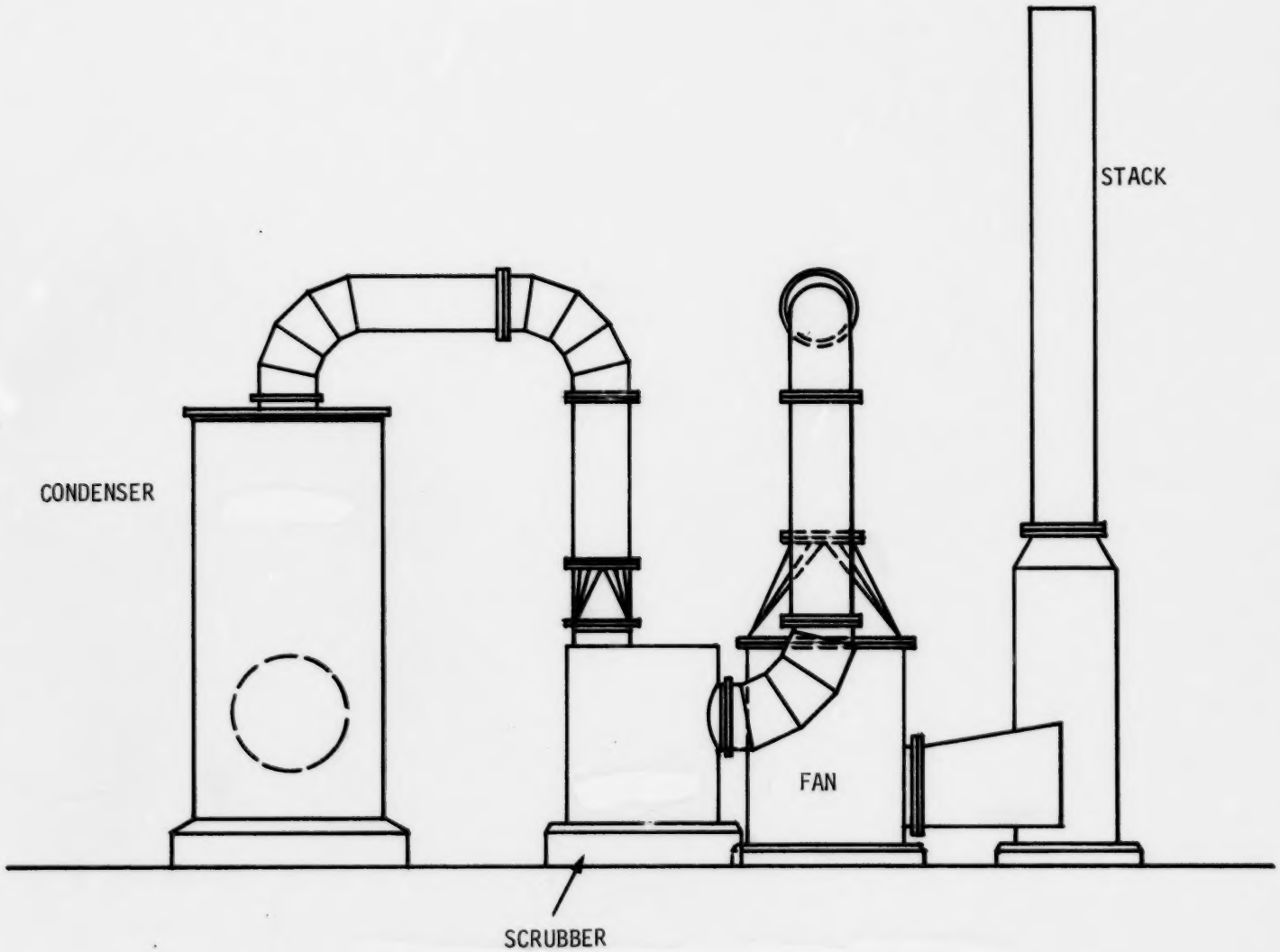

Figure 4-4. Induced draft system (Elevation View).

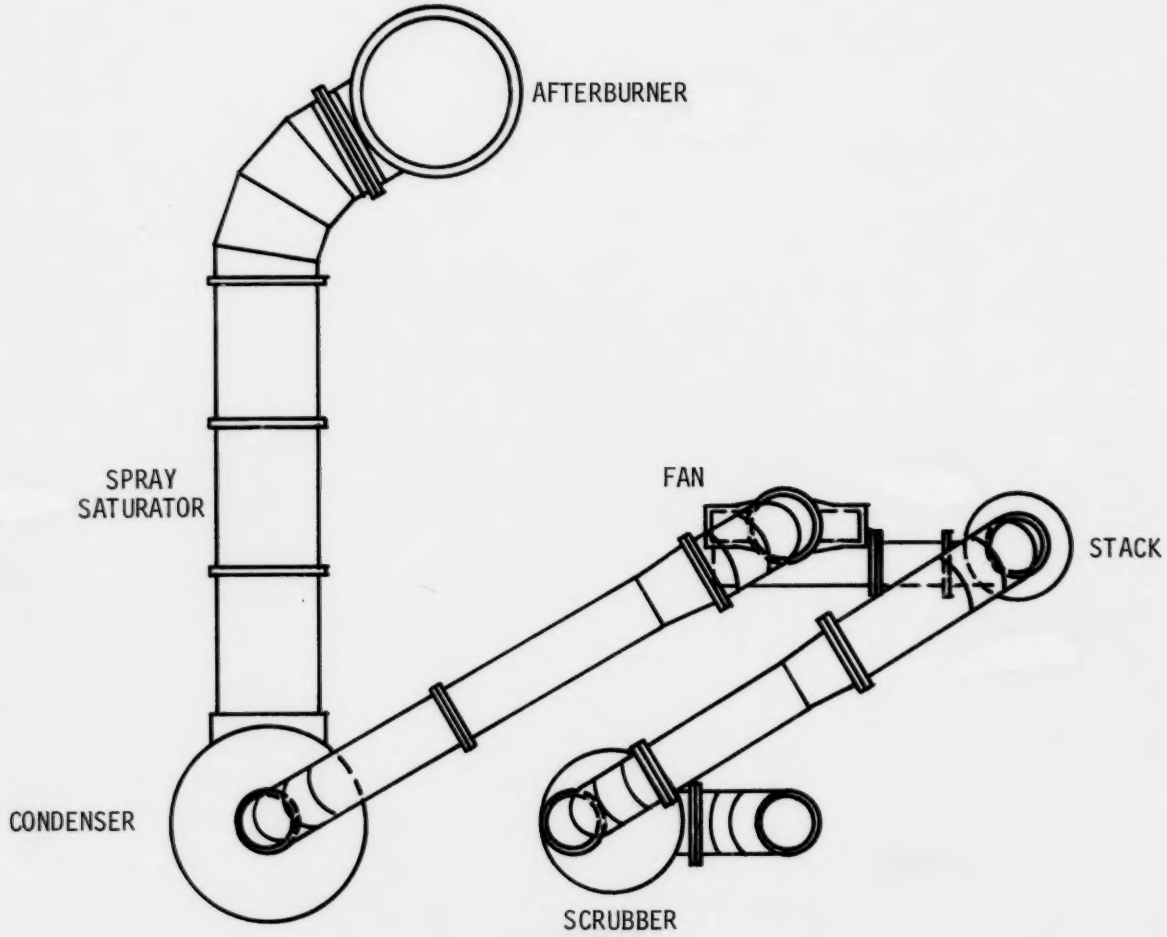

Figure 4-5. Forced draft F/C system (Plan View).

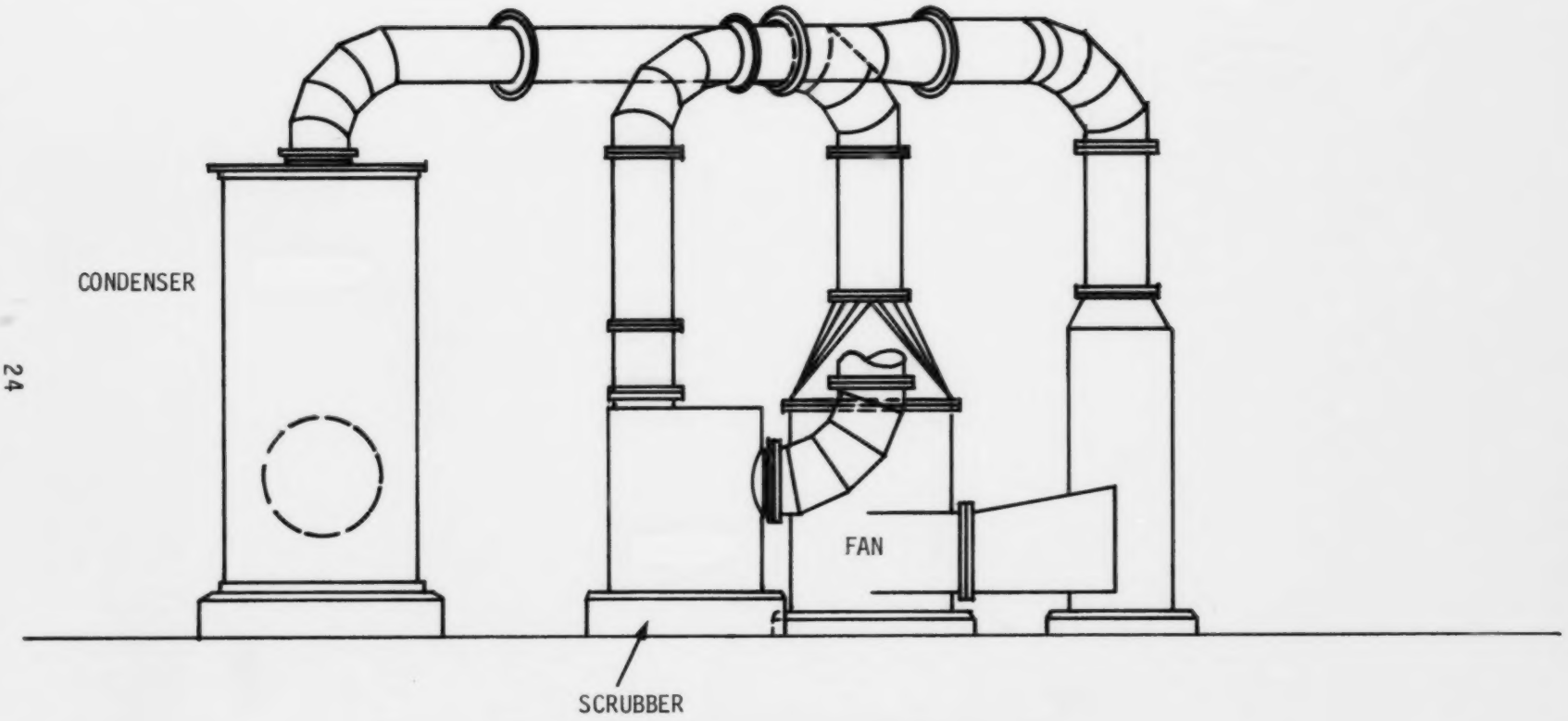

Figure 4-6. Forced draft F/C system (Elevation View).

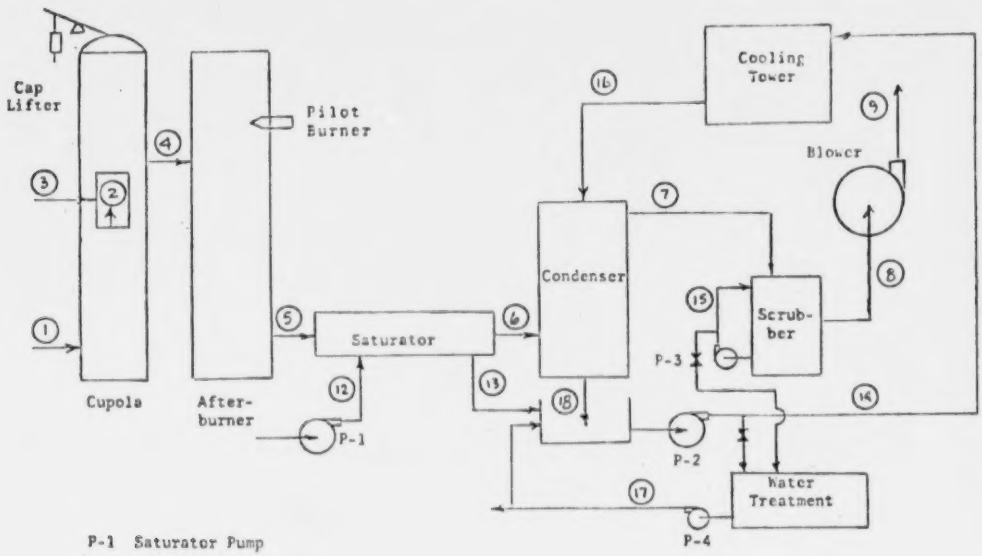

P-1 Saturator Pump
P-2 Cooling Tower Pump
P-3 Scrubber Pump
P-4 Water Treatment Pump

PROCESS FLOWS

GAS

	1	2	3	4	5	6	7	8	9	10
Mass Flow Rate (Dry) kg/min	318	360	149	508	508	508	508	508	508	
Mass Flow Rate (Wet) kg/min	322	360	151	---	515	729	565	565	565	
Composition										
O_2, kg/min	74.0	---	34.5		6.8	6.8	6.8	6.8	6.8	
N_2, kg/min	244	244	114		358	358	358	358	358	
CO, kg/min	---	49.0	---		---	---	---	---	---	
CO_2, kg/min	---	67.0	---		148	143	143	143	143	
H_2O, kg/min	4.54	0.73	2.3		6.8	220	56.8	56.8	56.8	
Temperature, °C	32.2		32.2		982	76.7	54.4	54.4	54.4	
Abs. Press., cm Hg	84.0	76.0	76.0		75.8	75.6	74.7	70.0	76.2	
Ga. Press, cm W.C.	107	-1.3	0		-2.5	-5.0	-18.0	-81.0	+2.5	
Am^3/min	259		145		1,720	855	566	603	555	
Nm^3/min	291		140		402					
DNm^3/min	264		137		393	393	393	393	393	

LIQUID

	11	12	13	14	15	16	17	18
Mass Flow Rate, kg/min		281	68.1	4,140	1,360	4,070	34-68	4,280
Temperature °C		26.7	76.7	65.6	54.4	37.8	32.2	65.6
Pressure, k Pa		1,380	0	138-207	0	0	0	

Figure 4-7. Process Flow Sheet, Induced Draft System.

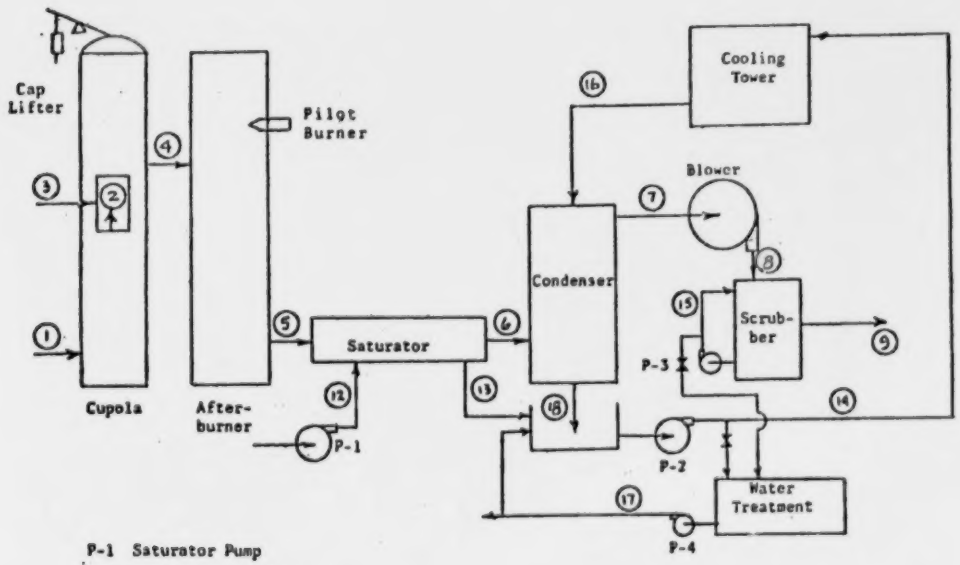

P-1 Saturator Pump
P-2 Cooling Tower Pump
P-3 Scrubber Pump
P-4 Water Treatment Pump

PROCESS FLOWS

GAS

	1	2	3	4	5	6	7	8	9	10
Mass Flow Rate (Dry) kg/min	318	360	149	508	508	508	508	508	508	
Mass Flow Rate (Wet) kg/min	322	360	151	---	515	729	565	565	565	
Composition										
O_2, kg/min	74.0	---	34.5		6.8	6.8	6.8	6.8	6.8	
N_2, kg/min	244	244	114		358	358	358	358	358	
CO, kg/min	---	49.0	---		---	---	---	---	---	
CO_2, kg/min	---	67.0	---		143	143	143	143	143	
H_2O, kg/min	4.54	0.73	2.3		6.8	220	56.8	56.8	56.8	
Temperature, °C	32.2		32.2		982	76.7	54.4	54.4	54.4	
Abs. Press., cm Hg	84	76	76.0		75.8	75.6	74.7	79.3	76.2	
Ga. Press., cm W.C.	107	-1.3	0		-2.5	-5	-17.8	+45.7	+2.5	
Am^3/min	264		145		1,720	855	566	532	555	
Nm^3/min (Wet)	291		140		402					
DNm^3/min	264		137		393	393	393	393	393	

LIQUID

	11	12	13	14	15	16	17	18
Mass Flow Rate, kg/min		281	68.1	4,140	1,360	4,070	34-68	4,280
Temperature, °C		26.7	76.7	65.6	54.4	37.8	32.2	65.6
Pressure, kPa		1,380	0	138-207	0	0	0	

Figure 4-8. Process Flow Sheet, Forced Draft System.

metal stamping and turnings,cast iron pipe and fittings and other miscellaneous metal parts.

The scrap and coke are charged together in 1,800 kg charges (2 tons) with an iron to coke mass ratio of 6. Small amounts of limestone, 20-30 kg, are also charged to act as a fluxing agent in the formation of slag. The nominal melting rate is 12,500 kg/hr. The tuyere air flow rate can be varied by means of a damper on the blower. The normal tuyere air flow rate is 3.5 DNm^3/s.

The exhaust gases from the bed of material in the cupola are composed of carbon monoxide, carbon dioxide and nitrogen. The gas analysis is typically 14% CO, 13% CO_2, and 73% N_2. Additional combustion air at a rate of 2.3 DNm^3/s enters the charging door to allow for complete conversion of carbon monoxide to carbon dioxide. An ignition burner is required to ensure that a flame source is available for combustion of the CO to CO_2.

Combustion is completed in a brick lined afterburner tank. The exhaust gases leave the afterburner tank at a temperature ranging from 800 to 1,000°C. The exhaust gas flow rate at this point is about 6.6 DNm^3/s.

The hot gases leave the afterburner and are cooled in the saturator by means of water sprays. The gas is cooled and the temperature approaches the adiabatic saturation temperature, which depends upon the hot gas temperature. Typically, the saturation temperature achieved ranges from 71°C to 77°. The maximum water spray rate in the saturator is 4.5 l/s (75 gpm).

The saturated gases next enter the condenser which further cools the gases causing condensation of water vapor. The cooling capacity of the condenser depends upon the rate of cooling water flow and the cold water temperature, which depends upon the cooling tower performance. The condenser and cooling tower system has a design heat rejection rate of 9.6×10^6 J/s (33 x

10^6 BTU/hr). The water flow rate can be varied up to 69 l/S (1,100 gpm). The cold gas temperature leaving the condenser is about 55°C at design flow rates. The condenser is a counter-current packed bed.

Particle collection occurs in the condenser by the mechanisms of inertial impaction, diffusion, thermophoresis and diffusiophoresis. The condensation of water vapor on the particles results in substantial growth of the submicron particles. This growth phenomenon is a primary aspect of F/C scrubbing which differentiates this process from other scrubbing applications.

The exhaust gases leave the condenser and enter either the exhaust fan or the scrubber, depending on the ducting configuration. The system is designed to allow testing with the scrubber either in the induced draft or forced draft mode. The scrubber is the primary particle collection device in the system. The design is a gas atomized scrubber with variable area throat. The design incorporates an integral water sump and entrainment separator.

The exhaust fan provides the draft for the system. The fan used in the demonstration plant was re-built from that used in the previous system and is a straight radial blade design. The flow rate of the fan is approximately 14 Am^3/s (30,000 cfm) at -96 cm W.C. (-38 in. W.C.).

The cooling tower cools the water to be pumped into the condenser. It is designed to cool 69 l/s (1,100 gpm) of water from 66°C to 38°C using ambient air. This is accomplished by evaporative cooling.

The settler is designed to remove particles collected by the scrubbing liquid. A 1.3 l/s (20 gpm) stream of sump water is clarified by the settler. The thickened sludge (10-30% by wt.)

is disposed of as land fill. The clarified water (100 ppm solids) is returned to the sump.

MECHANICAL DESIGN

The major F/C scrubber system components which are listed below will be described in detail:

1. Afterburner
2. Saturator
3. Condenser
4. Cooling tower
5. Venturi Scrubber
6. Settler
7. Fan
8. Pumps
9. Piping & ducting
10. Instrumentation
11. Structure & foundation

Afterburner

The afterburner vessel is a cylindrical steel shell 7.3 m high with a diameter of 2.4 m. The top third of the afterburner which was added in a plant expansion is made of stainless steel while the lower portion is carbon steel. The shell is lined with 7.6 cm of castable insulation. Gas from the cupola enters the top portion and flows out the bottom into the saturator. The ignition burner is located in the duct coming out of the cupola before the afterburner vessel. The ignition burner is a Hauck gas pilot size #3 and operates on 0.057 m^3/min (2 cfm) of natural gas at a pressure of 15.24 cm W.C. (6 in W.C.). A 2.54 cm pipe tapped off a foundry gas line is used. The burner unit also requires a flow of air of about 0.7 m^3/min (25 cfm) which was tapped off the tuyere air fan with a 3.8 cm pipe.

Saturator

The saturator is a horizontal cylinder rolled from 3.5 mm (10 gauge) 216 stainless steel sheet. The saturator has a

straight section and an elbow section which connects to the afterburner tank. The cylinder is 9.1 m long and has a diameter of 1.5 m. The vessel is built in three sections and connected by flanges. The elbow section of the vessel is welded to the afterburner while the other end forms an expansion joint at the condenser inlet. The section of the saturator leaving the afterburner is insulated with firebrick because of the high temperatures at that location.

The spray pattern in the saturator is determined by the arrangement of spray nozzles. The spray banks are designed to provide easy access to the nozzles. Three nozzles with radial sprays are located in the first (elbow) section of the saturator. A spray header with 4 nozzles transverses the duct. Forty nozzles are located on 12 header pipes in the straight section of the saturator. Three or four nozzles are mounted on 2.54 cm diameter stainless steel pipes. These pipes can be removed from outside for maintenance. A flow switch has also been installed on the main water supply line to the nozzles. When the flow to the saturator nozzles decreases below 75.8 l/min (20 gpm), the switch activates an alarm system and shuts off the main exhaust blower. This is to prevent high gas temperatures from damaging the spray bank and saturator gaskets.

The mechanical design of the saturator was based on two constraints. First, the vessel has to have enough volume so the residence time is sufficient for evaporation of the water drops. The second constraint involves the available space for construction of the F/C system. The primary equipment area was to be located north of the existing sump; hence, a long, horizontal spray chamber was designed to connect the afterburner with the condenser.

Condenser

The condenser vessel is a 3161 stainless steel cylindrical shell, which is 2.75 m in diameter and 6.1 m high. The wall thickness is 3.5 m (10 gauge). The gas enters the bottom of the condenser from the saturator and is distributed by turning vanes. Counter current contact is made with cold water in a packed bed having a packing depth of 1.2 m. Intalox saddles of 5.0 cm nominal diameter are used as packing. This packed bed is irrigated by water falling from a trough type distribution plate. Some of the water droplets are entrained in the rising gas and a second packed bed, 0.3 m deep, is used as an entrainment separator. The gas flows out the top of the condenser through a 0.8 m diameter duct to the scrubber or fan. The water drains down to the condenser reservoir at the bottom of the condenser and is drained through a 0.3 m diameter pipe back into the sump.

Scrubber

The scrubber consists of a cylindrical shell 2.1 m in diameter and 2.7 m high. The scrubber shell was rolled from 3.5 mm (10 gauge) stainless steel sheet. The shell houses both a gas atomized scrubber section and the entrainment separators.

The inlet ducting is bolted to the gas atomized scrubber section which in turn is bolted to the scrubber shell. The scrubber section has a variable area throat with hydraulic or manual control which allows the area to be varied from 0.08 m^2 to 0.22 m^2. Scrubber water is pumped to six distribution headers located just upstream of the converging section of the scrubber. The gas is directed downward through the scrubber. Scrubber water is collected in the bottom of the scrubber shell and recirculated to the scrubber throat.

Drops of water generated in the scrubber throat are entrained in the gas stream. To remove these drops entrainment separators

are required at the outlet to the scrubber shell. A tube bank entrainment separator is used in this application. The entrainment separators consist of six rows of 4.1 cm dia. stainless steel tubes spaced 4.1 cm from center to center. These rows are offset to force the gas stream to weave its way through the tubes before leaving the scrubber housing. The entrained drops impact on the tubes and drain to the scrubber reservoir. The entrainment separator cross-sectional area is 5.1 m^2 and is made of 1,080 tubes 76.2 cm long.

Cooling Tower

The cooling tower consists of a 3.7 m x 2.7 m x 5.2 m epoxy coated steel shell. The tower is a standard commercial design. Ambient air is forced through the packed tower by a fan. Hot water is distributed across the top of the tower packing by means of multiple headers and spray nozzles. Cold water temperature is controlled by an automatic adjustment of the air flow by means of a fan damper.

The cooling tower is designed to cool 69 l/s of water from 66°C to 38°C. The cooling tower incorporates a baffle type entrainment separator to remove entrained drops from the exhaust air.

Settler

Solids are removed from the circulating water system by means of a gravity settler. The settler which was used had a settling area of 11 m^2. The design incorporates parallel plates inclined at a 55° angle to minimize the required area for the unit.

The cleaned liquid (overflow) flows upward along the plates and overflows through flow distribution orifices. The solids collect on the plates and slide downward into a sludge hopper.

The sludge is discharged periodically through a sludge valve and disposed of as landfill.

A flocculant aid is used to increase the settling rate of the solids. A chemical feed system involving a mix tank and metering pump supplies the flocculant at a dose rate of 5-10 ppm. The settler design incorporates a flash mix tank and a floc growth tank as well as agitators with speed controllers. The nominal flow rate through the settler is 1.3 l/s. The settler reduces the solids content of the circulating water from several thousand ppm to a few hundred ppm.

Blower

During the initial phase of the project the blower from the existing scrubber system was used to provide flow for the F/C system. The fan then had a straight radial blade design and was driven by a directly coupled 400 HP electrical motor at 1,800 rpm. The current demand was excessive, requiring 480-500 amps at 480 volts. The performance of the fan was poor and several modifications were made to obtain the required flow.

Early testing indicated that significant leakage of ambient air through the fan housing caused reduced flow through the F/C scrubber system. The entire inlet section of the fan housing was rebuilt, solving leakage problems and allowing the design flow rate through the scrubber. The fan still had poor efficiency and the developed head exceeded the F/C system requirements.

Finally, a new fan wheel was designed in order to obtain more flow and a lower head. The new fan wheel also had straight radial blades, but the wheel diameter was reduced to 1.47 m from 1.60 m and a new blade profile was designed to conform closer to the fan housing. The new fan wheel was installed and

successfully operated. The designed flow rate was attained at a lower head and the motor power requirement dropped to 360-380 amps at 480 V.

Pumps

Table 4.1 shows the pump specifications for each of the pumps used on the demonstration plant. All of the pumps are of a proven commercial design and presented no unusual operating problems.

The saturator pump supplies city water to the spray nozzles in the saturator. A two-stage centrifugal pump is used to provide the high pressure required to give fine atomization for effective evaporation.

The sump pump causes the circulation of water from the sump to the cooling tower. A vertical turbine pump with the suction submerged in the sump was used for this purpose.

Two diaphragm pumps are used in the systems. The smaller pump is used to transport sump water to the settler. The larger pump is used for maintenance purposes such as cleaning condenser and scrubber, etc. These pumps are portable, driven by compressed air available at the plant, and are capable of pumping liquids as well as sludges with a high solids content.

Piping, Ducting and Valves

The piping system is composed of four separate subsystems: (1) Saturator piping, (2) cooling water piping, (3) scrubber piping and (4) water treatment piping.

City water is used in the saturator to cool the exhaust gas. The water is piped to the saturator pump (P-1) and then passes through one of two parallel strainers which remove solids which might plug the spray nozzles. Galvanized pipe having a diameter of 6.4 cm (2.5 in.) is used up to the individual spray headers.

TABLE 4.1 PUMP SPECIFICATIONS

Pump and Type	Capacity	Driver
Saturator Pump (2-stage centrifugal)	54 l/s @15 atm	20 HP, 240V, 30 motor
Sump Pump (Vertical turbine)	750 l/s @2 atm	30 HP, 240V, 30 motor
Scrubber Pump (Centrifugal)	250 l/s @1 atm	5 HP, 240V, 30 motor
Water Treatment Pump (Diaphragm)	1.3 l/s @1 atm	Compressed Air
Sludge Pump (Diaphragm)	2.6 l/s @1 atm	Compressed Air

Flexible copper hoses (2.5 cm diameter) are used to connect to the saturator.

Cooling Water Piping

The cooling water piping runs from the sump pump to the cooling tower, from the cooling tower to the condenser and from the condenser to the sump. A bypass line around the cooling tower is also inclined. The material used for the cooling water system is schedule 40 fiberglass pipe of 20 cm diameter (8 in.).

Scrubber Piping

The scrubber piping runs from the scrubber internal sump to the gas atomized scrubber throat. Fiberglass pipe having a diameter of 10 cm (4 in.) is used. At the scrubber throat six header pipes each 5 cm (2 in.) in diameter distribute the scrubber liquor. A bypass line allows the scrubber water to be pumped to the settler.

Water Treatment Piping

The settler system is connected to the circulating water system by 5 cm diameter PVC piping.

Valves

The valves used in the system were generally for two purposes: (1) flow control and (2) shut-off. The scrubber liquid flow was controlled using a rubber lined diaphragm pump. Ball valves were used on the saturator spray lines for on-off control. Butterfly valves were used in other locations for control or shut-off.

Ducting

The ducting used on the project was Fiberglass reinforced polyester (FRP) ducting. The ducting sections between the condenser and scrubber are 0.81 m diameter. The exhaust gas ducting is 0.91 m diameter. The nominal wall thickness is 0.5 cm. The ducting system was designed to allow operation in both the forced draft and induced draft mode.

Foundations and Structural Design

A reinforced concrete foundation was required to support the condenser and scrubber vessels. The saturator and scrubber pumps are also installed on this foundation. The condenser foundation is a concrete block 3.5 m square by 1.8 m deep. The adjacent scrubber and pump foundation is a rectangular pad 3.5 m wide by 4.7 m long and 0.5 m deep.

A structural steel platform was required to support the cooling tower. The platform also included a sampling area just above the scrubber where particulate sampling could be performed both at the scrubber inlet ducting and at the scrubber outlet ducting.

INSTRUMENTATION AND CONTROL SYSTEM

Instrumentation

Temperatures were measured by means of chromel-alumel thermocouples (K type). The temperatures were reordered on a strip chart recorder and observable on a digital indicator with a 20-point selector switch.

The liquid flow rates were measured with venturi meters, equipped with transducers and indicators. Liquid pressures were measured with standard pressure gauges, both locally at the pumps and remotely in the instrument trailer.

The gas pressures and differential pressures across the condenser and scrubber were measured by means of diaphragm type gauges. Pressure tubing was used between the equipment and the instrument trailer where the gauges were located.

Saturator Process Measurements

a. Gas inlet temperature
b. Gas outlet temperature
c. Liquid flow rate
d. Liquid temperature
e. Pump suction pressure
f. Pump discharge pressure
g. Strainer discharge pressure

Condenser Process Measurements

a. Gas inlet temperature
b. Gas outlet temperature
c. Gas inlet pressure
d. Gas outlet pressure
e. Condenser total pressure drop
f. Entrainment separator pressure drop
g. Liquid flow rate
h. Liquid inlet temperature
i. Liquid outlet temperature

Cooling Tower Process Measurements

a. Liquid flow rate
b. Liquid inlet temperature
c. Liquid outlet temperature

Scrubber Process Measurements

a. Gas inlet temperature
b. Gas outlet temperature
c. Liquid flow rate
d. Liquid temperature
e. Pump discharge pressure
f. Scrubber total pressure drop
g. Entrainment separator pressure drop
h. Scrubber liquid level

Water Treatment System Process Flows

a. Liquid flow rate

Control System

Saturator Water System

The saturator water flow rate is controlled by manually opening or closing the shutoff valves located on the spray bar headers. The saturator water system also contains two liquid "Y" strainers piped in parallel to remove particulate which could clog the spray nozzles. Pressure gauges located upstream and downstream of the strainers monitored pressure loss across the strainer.

Cooling Water Flow

The cooling water low rate is controlled by means of a bypass valve. The cooling tower can be bypassed by opening the cooling tower bypass valve and closing the cooling tower valve. This allows water to be pumped directly to the condenser from the sump.

Scrubber Liquid Flow

The scrubber liquid flow is controlled by means of the flow control valve. In addition, the scrubber bypass valve allows scrubber liquid to be pumped to the sump or to the sewer.

Scrubber Liquid Level

The scrubber liquid level is controlled by means of a level controller which actuates valve on the signal of a low level.

Scrubber Flow Area

The scrubber flow area can be controlled by a hydraulic system which opens and closes the scrubber throat area. In addition, manual adjustment is possible using extension levers located outside the scrubber.

Gas Flow Rate

The gas flow rate is controlled by a combination of fan inlet damper and scrubber throat area.

Water Treatment Flow Rate

The flow rate to the water treatment system is controlled by the air regulator used on the diaphragm pump.

Circulating Water pH

The pH of the circulating water system is measured using a pH meter and controlled within the range of 6 to 9 by addition of soda ash.

Safety System

The safety system protects the equipment from excessive temperature in the event that the saturator sprays or pump fails to provide enough cooling water. The saturator water flow rate

is monitored by a flow switch. If the flow rate decreases below 25 gpm the flow switch will shut down the exhaust fan and initiate automatic opening of the cupola cap.

A backup safety system involves a temperature switch located in the ducting section coming out of the condenser. In the event gas temperature at this point exceeds the setpoint of 80°C (175°F) the exhaust fan will be shut down and the cupola cap raised.

Both of these safety switches provide an alarm and indicator light to alert operators of the malfunction.

SECTION 5
PERFORMANCE TESTING

In the course of the system start up, we encountered no significant problems with the equipment supplied for the project. The original exhaust fan, however, did cause excessive power consumption and tripping of the electrical overload device. This condition continued until the new fan, which A.P.T. designed, was installed. The system performance was quite good during the test period. No lost production time was experienced by the foundry due to problems associated with the operation of the F/C scrubber system.

Operating Modes

The F/C system was tested in two basic configurations, induced draft (I.D.) and forced draft (F.D.) modes. In the usual I.D. system the exhaust gas flows through the afterburner, saturator, condenser, scrubber, and then the exhaust fan to the stack. By using ducting modifications we could employ the F.D. mode, wherein the exhaust gas flows through the afterburner, saturator, and condenser; then through the exhaust fan, the scrubber, and the stack. The F.D. mode has the potential advantage of reducing the fan power requirement by about 6%, with the possible disadvantage of entrained liquid entering the fan.

The major operating parameters which were varied during the test program were the condenser liquid flow rate and scrubber pressure drop. The condenser liquid flow rate affected the amount of cooling in the condenser and, hence, the condensation ratio. The scrubber pressure drop could be varied by changing the scrubber throat flow area and the scrubber liquid to gas

ratio. The scrubber pressure drop determines the collection efficiency in the scrubber.

Sampling Locations

Sampling was performed at three locations in the F/C system. At each of these locations two sampling ports located 90° apart were available. The sampling ports were made of 10 cm (4 in) pipe couplings.

The sampling location was at the cold end of the saturator just before the condenser vessel. The sampling ports at this location were easily accessible from the ground. The remaining two sampling locations were in the scrubber inlet and outlet ducting. These sampling ports were accessible from a sampling platform which was constructed as part of the cooling tower platform.

Testing Methods

This section describes the test procedures that were used to determine the F/C system performance. Sampling was usually performed at the inlet to the condenser and at the scrubber outlet. For some runs samples were also taken at the scrubber inlet. Sampling at three locations allowed the condenser performance and scrubber performance to be evaluated separately.

Impactor Runs

The particle size distribution and mass concentration was obtained using University of Washington cascade impactors. Pre-cutters were used on the impactors to remove large particles and entrainment. Fiberglass and greased aluminum substrates were used in the impactors.

Modified EPA Method 5

Several modified EPA Method 5 total filter runs were made to determine total mass concentration. These tests were done for compliance tests and to confirm impactor mass loadings.

Sampling Equipment

The sampling equipment used involves four sampling trains as shown in Figure 5-1. The cascade impactor runs were made in-stack. The precutters used had cut points in the range of 6 to 9 μmA, depending upon sampling flow rate. Nozzle sizes were chosen to maintain isokinetic sampling. The filter tests were made with heated filters out-of-stack and heated sampling probes. The probes were made from 0.95 cm (3/8") stainless steel and incorporated S-type Pitot tubes. Cyclones were not used in the method 5 testing.

Data Analysis

Cascade Impactors

Cascade impactor measurements provide the cumulative mass concentration as a function of particle size. From these data, one can compute penetration as a function of particle size. The data analysis done was with a computer program developed by Dr. Leslie Sparks. The program calculated impactor cut points and cumulative mass concentrations based on weight gain per stage, impactor flow rate, and impactor calibration data.

The overall penetration was calculated from the total mass concentrations as follows:

$$\overline{Pt} = \overline{Pt_c} \times \overline{Pt_s} \qquad (5\text{-}1)$$

$$Pt = \frac{C_{si}}{C_{ci}} \times \frac{C_{so}}{C_{si}} \qquad (5\text{-}2)$$

$$\overline{Pt} = \frac{C_{so}}{C_{ci}} \qquad (5\text{-}3)$$

where $\overline{Pt}$ = overall penetration for condenser and scrubber

$\overline{Pt_c}$ = overall penetration for condenser

$\overline{Pt_s}$ = overall penetration for scrubber

C_{ci} = particle mass concentration, condenser inlet, g/DNm³

C_{si} = particle mass concentration, scrubber inlet, g/DNm³

C_{so} = particle mass concentration, scrubber outlet, g/DNm³

The penetration as a function of particle size was evaluated in two ways, each of which is based on the following equation:

$$Pt(d_{pa}) = \frac{[dC/d(d_{pa})]_{outlet}}{[dC/d(d_{pa})]_{inlet}} \qquad (5\text{-}4)$$

where $dC/d(d_{pa})$ is the rate of change of cumulative mass concentration with particle aerodynamic diameter.

The graphical method involves plotting the cumulative mass concentration versus particle diameter curves for both the inlet and outlet and determining the slopes of these curves at various

points. The fractional penetration curve is then plotted on the size range of interest by performing the division shown in equation (5-4) at several particle diameters.

The second method used, known as the discrete or finite difference method, involves approximating the slope of the cumulative mass concentration curve by use of the individual impactor stage weight gain and cut points, i.e.

$$Pt = \frac{(\Delta C/\Delta \ln d_p)_{\text{inlet}}}{(\Delta C/\Delta \ln d_p)_{\text{outlet}}} \qquad (5\text{-}5)$$

This method is described by McCain et al. (1978) and has the advantage of being easily adapted to computer calculations. It eliminates to subjective errors in determining the slope of the cumulative mass concentration curve, but introduces an approximation error.

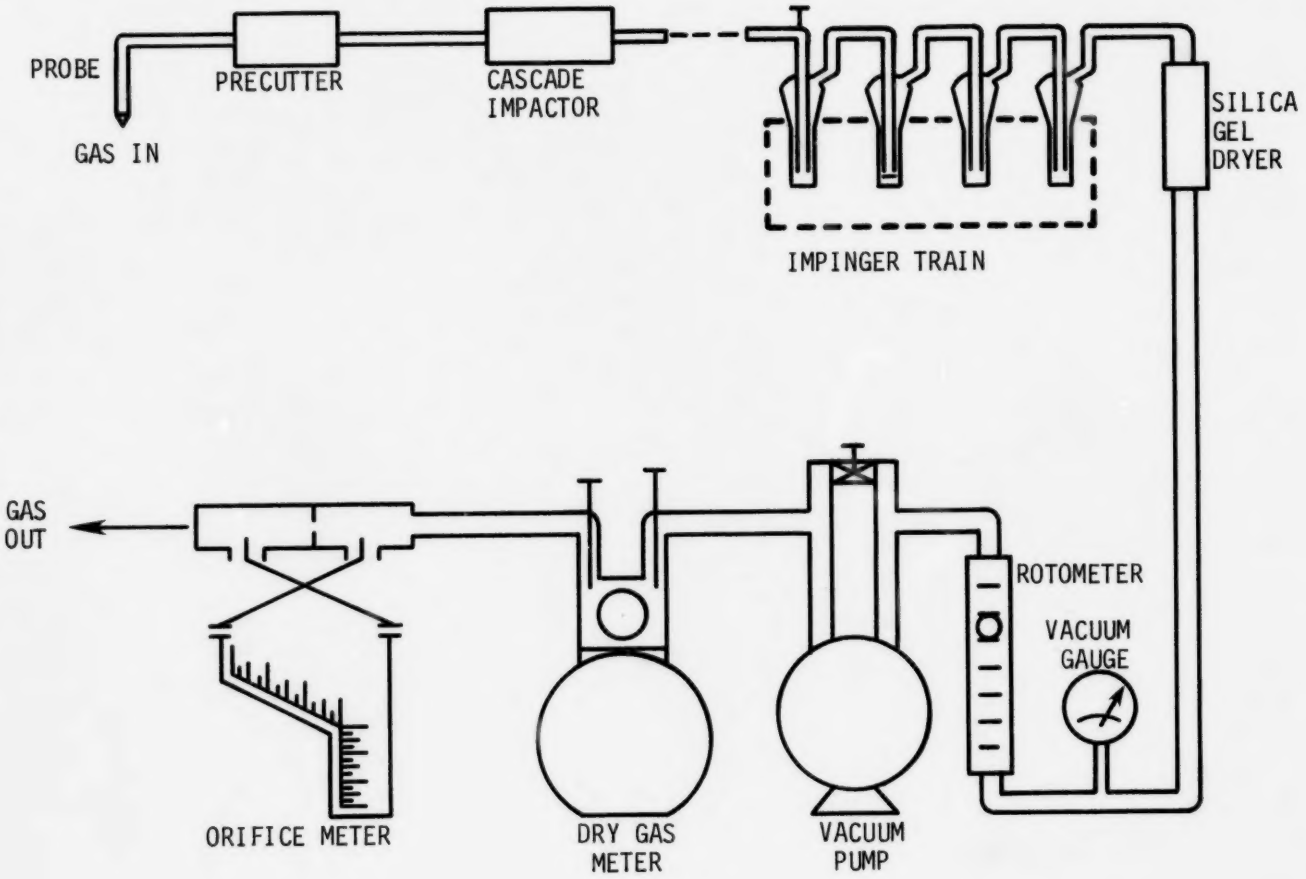

Figure 5-1. Modified E.P.A. sampling train with in-stack cascade impactor.

SECTION 6
SYSTEM PERFORMANCE MODEL

INTRODUCTION

The system performance model predicts the particle removal efficiency in the flux force/condensation scrubber system. The model can be used to predict the emission from a F/C scrubber system installed on a pollutant source with a known particle concentration and size distribution. The model allows one to study independently the two primary variables which influence the performance of the F/C system. These two variables are the condensation ratio and scrubber pressure drop.

Under previous EPA contracts, Air Pollution Technology, Inc. conducted detailed studies on the technical and economic feasibilities of F/C scrubbing (Calvert et al., 1973, '75, '77). These studies included theoretical development of design equations for F/C scrubbing as well as experimental verification of on both pilot plants and demonstration plant equipment. The model used in this project also used scrubber performance methods developed in the scrubber system study (Calvert, 1972) and recent revisions for gas atomized spray scrubbers (Yung, 1978).

BASIC CONCEPTS

Before proceeding to the details of the mathematical model, the basic concepts and outline of the approach will be discussed. If we consider a typical F/C scrubbing system, it might have the features shown in Figure 6-1. The gas leaving the source is hot and has a water vapor content which depends on the source process. The first step is to saturate the gas by quenching it with water. This will cause no condensation if the particles are insoluble, but will if they are soluble. There will be a diffusiophoretic force directed away from the liquid surface.

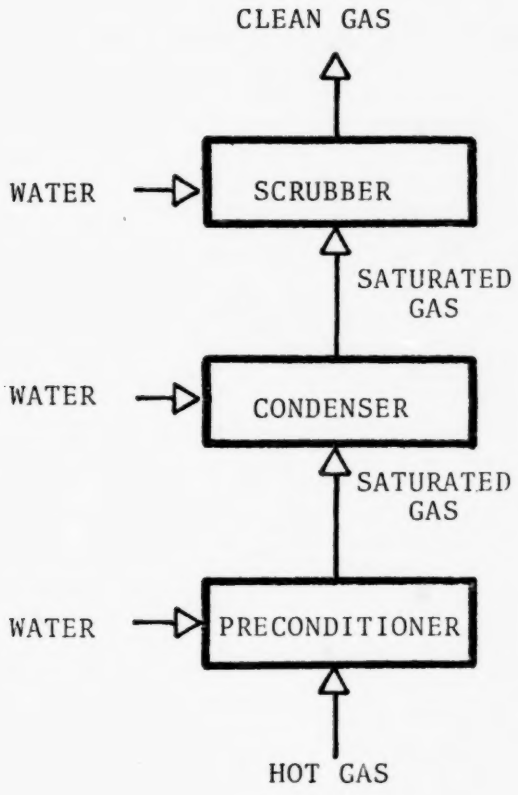

Figure 6-1. Simplified F/C scrubber system.

Condensation is required in order to have diffusiophoretic deposition, any growth on insoluble particles, and extensive growth on soluble particles. Contacting with cold water or a cold surface is employed to cause condensation. While condensation occurs there will be diffusiophoretic and thermophoretic deposition as well as some inertial impaction (and, perhaps, Brownian diffusion). The particles in the gas leaving the condenser will have grown in mass due to the layer of water they carry.

Subsequent scrubbing of the gas will result in more particle collection by inertial impaction. This will be more efficient than impaction before particle growth because of the greater inertia of the particles. There may be additional condensation, depending on water and gas temperatures, and its effects can be accounted for as discussed above.

The mathematical model for the F/C demonstration plant is outlined below:

In the saturator:

a. Gas is humified and cooled to adiabatic saturation temperature.
b. No condensation occurs (particles are assumed insoluble).
c. Particle collection is assumed to be negligible.

In the condenser:

a. Particles are collected by impaction in packing.
b. Condensation occurs, causing growth of particles.
c. Collection occurs by diffusiophoresis.

In the scrubber:

a. Grown particles are collected by impaction.

b. Negligible condensation occurs.

PREDICTION OF PENETRATION

Collection by Impaction in Condenser

The particulate collection in the condenser is primarily due to inertial impaction. The inlet (dry) particle size distribution is used for these calculations (no credit is taken for growth for collection within the condenser). The penetration is calculated with the following equation for collection in a packed bed.

$$Pt_{CI} = \exp\left[\frac{\pi}{2(j+j^2)\ (\varepsilon - H_d)}\ \frac{Z}{d_C}\ K_p\right] \qquad (6\text{-}1)$$

where K_p = impaction parameter $u_G d_{pa}^2/9\mu_G\ d_C$

μ_G = gas viscosity, g/cm-s

μ_G = gas viscosity, g/cm-s

d_C = packing diameter, cm

Z = packing depth, cm

j = channel width fraction, dimensionless

ε - void fraction, dimensionless

H_d = liquid holdup fraction, dimensionless

d_{pa} = particle aerodynamic diameter, cm $(g/cm^3)^{\frac{1}{2}}$

For the F/C demonstration plant the condenser was packed with 5.0 cm Intalox Saddle packing to a depth of 122 cm. The void fraction was 0.97 and the channel width fraction was estimated to be 0.15.

Condensation and Growth

The growth of the particles due to condensation of water vapor is predicted based on the humidity entering and leaving the condenser. The grown particle size is calculated from equation (6-2).

$$d_{p2} = \left[\frac{6\ f_p\ q'}{772\ \pi\ n_p} + d_p^3 \right]^{1/3} \qquad (6\text{-}2)$$

where d_{p1} = initial particle (physical) diameter, cm
d_{p2} = grown particle (physical) diameter, cm
f_p = particle condensation fraction
q' = condensation ratio, g H_2O/g dry gas
n_p = particle number concentration, particles/cm³

The grown particle density is then calculated by the following equation:

$$\varrho_{p2} = \left(\frac{d_{p1}}{d_{p2}} \right)^3 (\varrho_{p1}^{-1}) + 1.0 \qquad (6\text{-}3)$$

where ϱ_{p1} = initial (dry) particle density, g/cm³

The grown particle density allows one to calculate the final grown particle aerodynamic diameter with the following equation:

$$d_{pa} = d_p\ (C'\ \varrho_p)^{\frac{1}{2}} \qquad (6\text{-}4)$$

where d_p = particle physical diameter, cm

C' = Cunningham slip correction factor, dimensionless

ϱ_p = particle density, g/cm³

Collection by Diffusiophoresis

Collection by diffusiophoresis in the condenser can be calculated by means of the following equation:

$$Pt_{CD} = 1 - 0.85(f_v)\ (1-f_p) \qquad (6\text{-}5)$$

where f_v = mole fraction of gas condensing.

The total penetration in the condenser is then calculated from the product of equation (6-1) and (6-5).

$$Pt_C = Pt_{CI} \times Pt_{CD} \qquad (6\text{-}6)$$

Collection by Impaction in Scrubber

The collection of the grown particle in the scrubber is by inertial impaction. The scrubber penetration is calculated according to the method developed by Yung et al. (1978) for collection in a venturi throat. The penetration equation is as follows:

$$\frac{\ln Pt_S}{B} = \frac{1}{K_{po}\ U^* = 0.7} \times \left[4K_{po}\ U^{*1.5} + 4.2\ U^{*0.5} - 5.02\ K_{po}^{0.5} \times \left(U^* + \frac{0.7}{K_{po}}\right) \tan^{-1} \left(\frac{U^*\ K_{po}}{0.7}\right)^{0.5}\right] - \frac{1}{K_{po} + 0.7} \qquad (6\text{-}7)$$

$$x \left[4\, K_{po} + 4.2 - 5.02\, K_{po}^{0.5} \left(1 + \frac{0.7}{K_{po}} \right) \tan^{-1} \left(\frac{K_{po}}{0.7} \right)^{0.5} \right]$$

where $$B = \frac{Q_L\, \rho_L}{Q_G\, \rho_G\, C_{Do}}$$

$$K_{po} = \frac{d_{pa}^2\, (u_G - u_d)}{9 \mu_G\, d_d}$$

$$U^* = 1.0 - 2\, [1 - x^2 + (x^4 - x^2)^{0.5}]$$

$$x = \frac{3\, C_{Do}\, \rho_G}{16\, d_d\, \rho_L} + 1$$

Q_L/Q_G = liquid to gas volumetric ratio, dimensionless
C_{Do} = drop drag coefficient at throat entrance, dimensionless
d_d = drop diameter, cm
u_d = drop velocity at throat entrance, cm/s
u_G = gas velocity at throat entrance, cm/s
= throat length, cm
ρ_G = gas density, g/cm³
ρ_L = liquid density, g/cm³

TABLE 6-1. INPUT VARIABLES FOR PREDICTION OF SCRUBBER OF SCRUBBER PERFORMANCE

gas velocity through condenser	180 cm/s
void fraction of packing	0.97
liquid hold up fraction	0
packing depth	122 cm
packing diameter	5 cm
particle condensation fraction	0.15
particle number concentration	1 x 10^8 particles/cm^3
particle density	3.0 g/cm^3
condensation ratio	0.15 g H_2O/g D.G.
scrubber throat length	13 cm
scrubber liquid to gas ratio	0.002 m^3/m^3
scrubber throat velocity	5,000 cm/s

TABLE 6-2. EXAMPLE CALCULATIONS

Initial Particle Aerodynamic Diameter μmA	Grown Particle Aerodynamic Diameter μmA	Penetration, fraction Condenser Pt_c	Scrubber Pt_s	Total Pt
0.4	0.93	0.88	0.18	0.16
0.5	0.93	0.81	0.18	0.16
0.6	0.95	0.86	0.18	0.15
0.8	1.02	0.85	0.14	0.12
1.0	1.1	0.83	0.12	0.10
1.25	1.25	0.81	0.07	0.06
1.5	1.5	0.78	0.04	0.03
2.0	2.0	0.72	0.02	0.01
3.0	3.0	0.56	0.01	mil
5.0	5.0	0.25	0.01	mil
10.0	10.0	0.01	0.01	-0

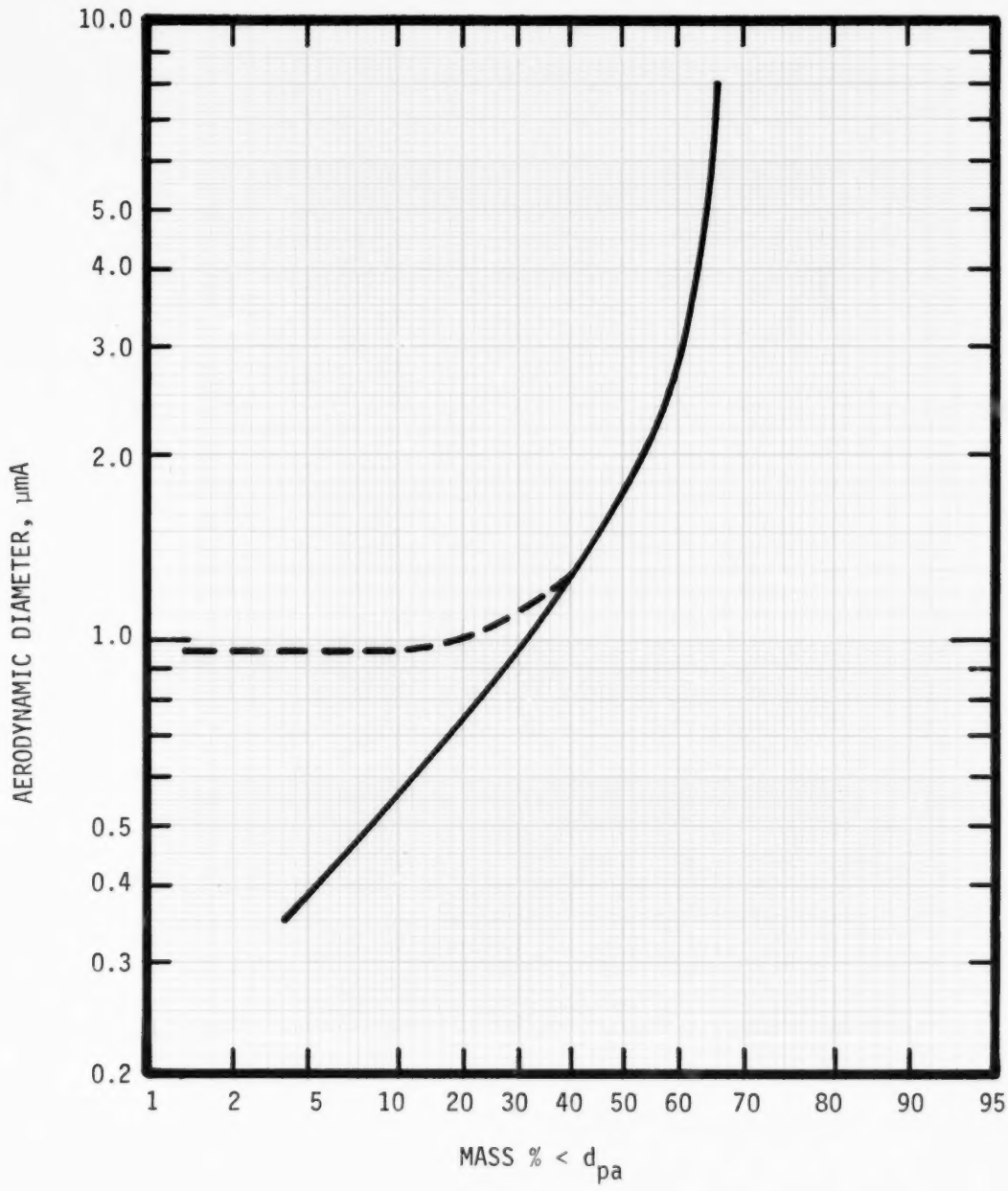

Figure 6-2. Example of initial and grown size distributions.

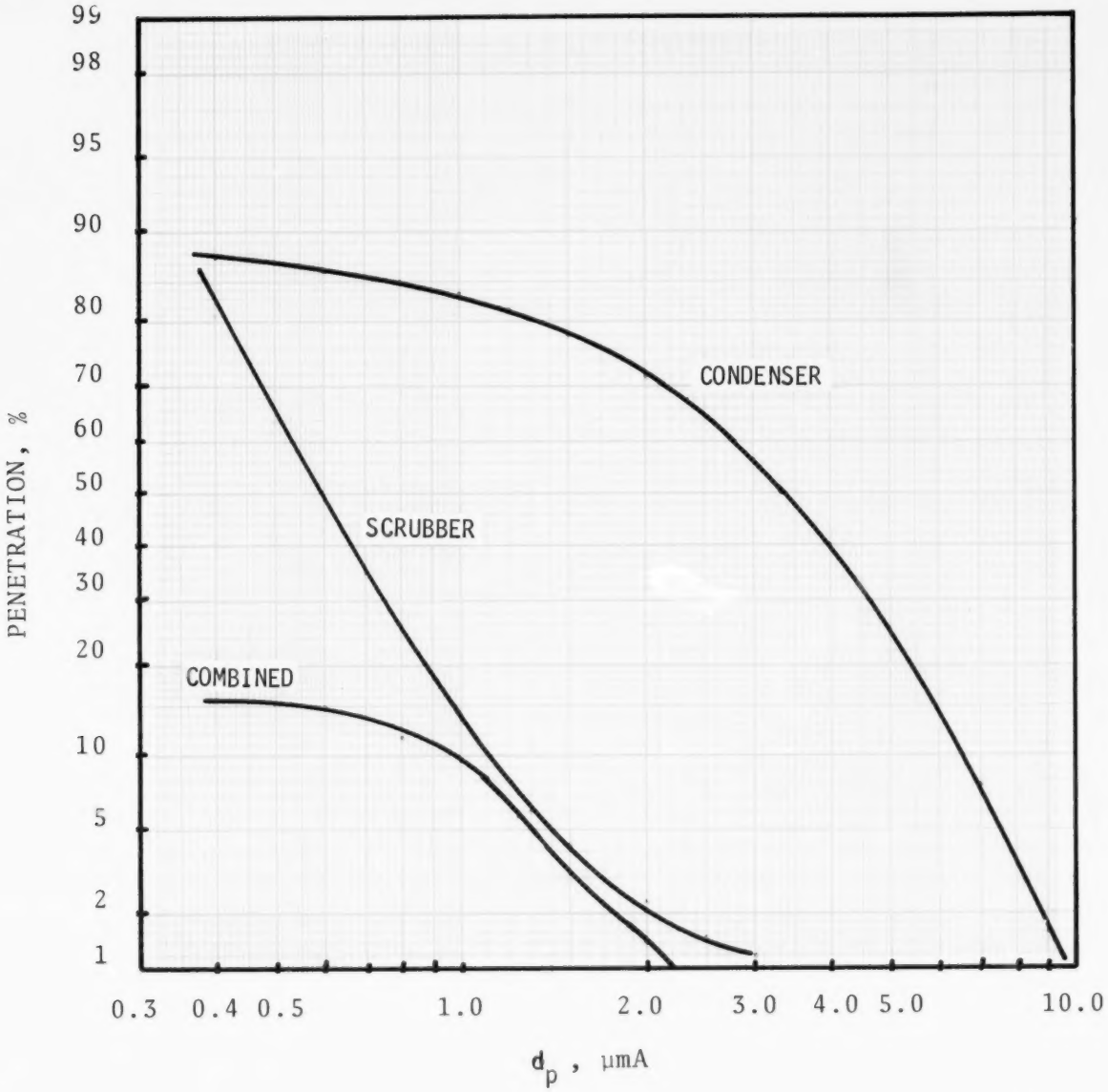

Figure 6-3. Example of Condenser, Scrubber, and Combined Penetration.

The penetration in the F/C system can then be obtained from the product of the condenser and scrubber penetrations:

$$Pt = Pt_C \times Pt_S \qquad (6\text{-}8)$$

$$Pt = Pt_{CI} \times Pt_{CD} \times Pt_S \qquad (6\text{-}9)$$

A computer program has been written to perform these calculations. The program allows prediction of the scrubber performance as a function of particle size. The input required for the program is listed in Table 6-1 along with numbers for a sample calcualtion.

Figure 6-2 shows the initial and grown size distributions for the sample case. Figure 6-3 shows the penetration as a function of particle size for the condenser, gas atomized scrubber and the combined system. The penetrations are plotted vs dry particle size. The actual scrubber penetration is based on the grown particle size distribution as shown in Table 6-2.

Calculation of Particle Number Concentrations

Particle number concentration was computed from the particle size distribution by mass. The size distribution is bimodal, a combination of small condensation aerosol and large particles formed by comminution. It is necessary to account for the fact that the great majority of the particle number population is in the submicron range. We have shown previously (Calvert et al, 1977) that the particle number concentration can be computed from the mass distribution below 1 μm diameter by fitting a log-probability distribution to it and using the hypothetical "d_{pg}" and "σ_g" as discussed below.

The particle number concentration is related to the mass concentration and mass mean diameter by the following equation:

$$n_p = \frac{6C}{\pi \rho_p d_m^3} \qquad (6\text{-}10)$$

where C = particle mass concentration, g/cm^3

d_m = mass mean diameter, cm

The mass mean diameter is related to the mass median diameter by the following equation:

$$\ln d_m = \ln d_{pg} - 1.5 \ln \sigma_g^2 \qquad (6\text{-}11)$$

where d_{pg} = mass median diameter, cm

σ_g = geometric standard deviation

For several runs the number concentration calcualted in this manner was found to be excessively high. For example aerosol systems with number concentration in excess of 10^9 particles/cm^3 can not exist over short periods of time before agglomeration of individual particles begins to reduce the particle number concentration. Coagulation theory describes the rate of particle agglomeration as:

$$\frac{d_{np}}{dt} = -Kn_p^2 \qquad (6\text{-}12)$$

where K = coagulation constant, cm^3/s

For iron oxide, which is the major constituent of the cupola particulate, K can be estimated to be 1×10^{-9} cm^3/s at the afterburner burner temperature of 1,200°K (Green and Lane, 1964).

Integration of equation (6-12) for various initial particle concentrations shows that a steady state particle concentration is reached after a few seconds, independent of the initial particle concentration. The residence time of the exhaust gas in the system upstream of the saturator is about two seconds.

An upper limit particle number concentration can then be estimated as 5×10^8 particles/cm^3. This limit was used instead of the calculated number concentrations when the calculated initial number concentration exceeded 5×10^8 particles/cm^3.

SECTION 7
COMPARISON OF EXPERIMENTAL RESULTS AND PERFORMANCE MODEL

TEST OPERATING CONDITIONS

The primary F/C scrubber system operating parameters of condenser liquid flow, scrubber pressure drop and condensation ratio are shown in Tables 7-1 and 7-2 for the two months of optimum performance. The "36 series" of tests was made in the induced draft configuration while the "37 series" was run in the forced draft mode.

The gas temperatures, flow rate and condensation ratio are shown in Tables 7-3 and 7-4 for these runs. The hot gas temperature leaving the afterburner was, for most of the runs, significantly lower than anticipated. The design-basis hot gas temperature was 1,000°C, as measured in preliminary tests. The maximum temperature measured was about 850°C.

The reasons for this discrepancy were as follow:

1. The foundry modified the cupola from conventional refractory lined to water cooled during the early stage of our program.
2. The type of metal charged was changed from large castings to small steel scrap.
3. After changes no. 1 and 2 were made the gas flowing from the cupola burden was not always burning, as it had previously been, without need for an ignition (pilot) burner.
4. Attempt to fabricate a suitable closure for the charging door and to have the cupola operators use it were not successful, so air leaked in the door at an excessive rate.

5. It was not possible to get a pilot burner installed before the test period was over.

The low gas temperature resulted in a reduction in the condensation ratio which could be achieved. The maximum condensation ratio obtained was about 0.20 g H_2O/g D.G. I had been anticipated that a condensation ratio of 0.30 g H_2O/g D.G. could be achieved with the higher gas temperature. The higher condensation ratio would further improve particle collection due to condensation effects.

TABLE 7-1. F/C SCRUBBER SYSTEM
OPERATING PARAMETERS FOR 36 SERIES

Run No.	Condenser Flow l/s	Condensation Ratio g H_2O/g Dry Gas	Scrubber Δp cm W.C.
36/1	47.3	0.13	43
36/2	47.3	0.21	48
36/3	47.3	0.18	51
36/4	47.3	0.06	66
36/5	47.3	0.23	64
36/6	47.3	0.19	76
36/7	47.3	0.14	76
36/8	25.2	0.03	76
36/9	25.2	0.12	74
36/10	25.2	0.08	53
36/11	25.2	0.10	53
36/12	25.2	0.10	64
36/13	25.2	0.16	61
36/14	47.3	0.17	38
36/15	47.3	0.17	38
36/16	25.2	0.13	41
36/17	44.2	0.15	58
36/18	47.3	0.03	66
36/19	47.3	0.12	66
36/20	47.3	0.05	51
36/21	47.3	0.18	53
36/22	25.2	0.11	53

TABLE 7-2. F/C SCRUBBER SYSTEM OPERATING PARAMETERS FOR 37 SERIES

Run No.	Condenser Flow l/s	Condensation Ratio g H_2O/g Dry Gas	Scrubber Δp cm W.C.
37/1	68	0.15	79
37/2	66	0.11	51
37/3	67	0.17	53
37/4	67	0.06	41
37/5	47	0.09	64
37/6	47	0.05	38
37/7	47	0.02	38
37/8	47	0.16	76
37/9	47	0.09	76
37/10	25	0.14	61
37/11	25	0.10	61
37/12	25	0.04	38
37/13	25	0.04	38
37/14	47	0.10	51
37/15	25	0.03	69
37/16	25	0.03	71
37/17	38	0.02	66
37/18	38	0.00	64
37/19	47	0.11	51
37/20	25	0.05	64
37/21	47	0.01	76
37/22	25	0.11	76
37/23	25	0.16	76
37/24	47	0.19	64
37/25	73	0.12	64
37/26	82	0.02	51

TABLE 7-3. GAS FLOW RATES, TEMPERATURES AND MEASURED CONDENSATION RATION FOR 36 SERIES

Run No.	Gas Flow Rate DNm^3/s	Sat. Inlet Temp. °C	Cond. Inlet Temp. °C	Cond. Outlet Temp. °C	Cond. Ratio g H_2O/g D.G.
36/1	7.88	566	66	41	0.13
36/2	7.13	855	70	48	0.21
36/3	7.13	741	73	43	0.18
36/4	7.13	700	71	41	0.06
36/5	7.13	766	74	42	0.23
36/6	6.80	713	72	45	0.19
36/7	6.80	733	67	43	0.14
36/8	6.80	585	66	52	0.03
36/9	6.56	780	75	59	0.12
36/10	6.56	766	74	61	0.08
36/11	6.56	677	70	59	0.10
36/12	6.42	858	74	61	0.10
36/13	6.42	749	71	59	0.16
36/14	6.18	583	66	38	0.17
36/15	6.18	619	69	38	0.17
36/16	7.97	649	71	58	0.13
36/17	6.00	792	75	59	0.15
36/18	7.00	460	65	59	0.03
36/19	6.60	683	70	56	0.12
36/20	6.08	605	70	59	0.05
36/21	5.90	648	73	57	0.18
36/22	5.94	639	71	56	0.11

TABLE 7-4. GAS FLOW RATES, TEMPERATURES AND MEASURED CONDENSATION RATIO FOR 37 SERIES

Run No.	Gas Flow Rate DNm^3/s	Sat. Inlet Temp. °C	Cond. Inlet Temp. °C	Cond. Outlet Temp. °C	Cond. Ratio g H_2O/g D.G.
37/1	6.09	645	74	57	0.15
37/2	7.27	649	74	58	0.11
37/3	6.98	705	70	54	0.17
37/4	7.22	574	73	60	0.06
37/5	7.74	719	77	63	0.09
37/6	6.61	500	66	66	0.05
37/7	7.22	452	67	58	0.02
37/8	7.98	836	77	60	0.16
37/9	8.11	498	61	51	0.09
37/10	6.18	802	75	61	0.14
37/11	5.14	816	76	75	0.10
37/12	5.43	840	75	70	0.04
37/13	5.80	714	73	71	0.04
37/14	7.13	662	77	60	0.10
37/15	6.42	649	71	65	0.03
37/16	6.42	621	70	65	0.03
37/17	5.14	671	69	69	0.02
37/18	5.14	688	70	68	0.00
37/19	5.14	496	64	52	0.11
37/20	6.89	483	63	56	0.05
37/21	6.61	219	51	48	0.01
37/22	5.68	796	77	63	0.11
37/23	5.80	740	73	60	0.16
37/24	5.00	752	73	55	0.19
37/25	6.50	690	74	56	0.12
37/26	5.64	610	76	60	0.02

PARTICULATE MASS CONCENTRATIONS AND SIZE DISTRIBUTIONS

The particulate mass concentrations were measured both with total filters and cascade impacters. Tables 7-5 and 7-6 show the measured particle mass concentrations. The average particle mass concentration at the inlet to the condenser was found to be 2.4 g/DNm³. The design basis mass concentration was 1.8 g/DNm³, the average mass concentration was therefore found to be 33% higher than the design basis.

The mass concentration varied significantly from run to run, which reflects sampling during various periods in the charging cycle. Figure 7-1 is a histogram showing the variation in the measured mass concentrations at the inlet to the condenser. The results of the first several preliminary tests showed that insignifiant mass was caught in the impingers. This is expected because of the nature of the source. As a consequence of these results the impinger catch was not routinely analyzed for mass, only for volume of condensed water.

The measured particle size distributions are shown in Appendix "A" for the runs in series 36 and 37. These results also show variation from run to run. When scrubber penetrations were computed on the basis of the inlet and outlet samples for each run there was great and random variation in the results. We postulated that the variation was due to the fact that inlet sampling times had to be much shorter than outlets because the inlet concentrations were so high. Consequently, one inlet sample would not be representative of the period over which the outlet sample was taken.

A statistical analysis was performed to obtain an average condenser inlet size distribution for use in determining the grade penetration curves. The averaging calculations were

performed numerically using a computer program developed by Dr. Leslie Sparks of the U.S. Environmental Protection Agency. Figure 7-2 shows the resulting average condenser inlet size distribution. Figure 7-3 shows the cumulative particle mass concentration versus particle aerodynamic diameter.

The average cumulative mass concentration distribution for the inlet was used in combination with the individual cumulative mass concentration distribution for the outlet of each run to compute the grade penetration relationship for that run. Figures 7-4 through 7-47 present the experimental and predicted grade penetration curves for runs in series 36 and 37. Series 36 was carried out with I.D. and series 37 was F.D., except for the last six runs, as shown in Tables 7-1 and 7-2.

Study of the grade penetration curves shows that predictions and experiment compare well in some cases but not in others. There is a tendency of the experimental penetrations at around 1μmA diameter to be higher than predictions, and this is true for both F/C and non-F/C conditions.

The performance in the F.D. mode was not improved as much by condensation as it was in the I.D. mode. It is possible that some of the condensed water may have been evaporated in the fan so that the particles entering the scrubber were smaller than those entering the fan. It was not possible to resolve this question within the test period.

The variation of computed penetrations appears to be caused by the uncertainty about the inlet size distribution. The agreement between predictions and experiment for many of the series 36 runs is considered good for these field experimental conditions, where the equipment is being modified and the source process is cyclic.

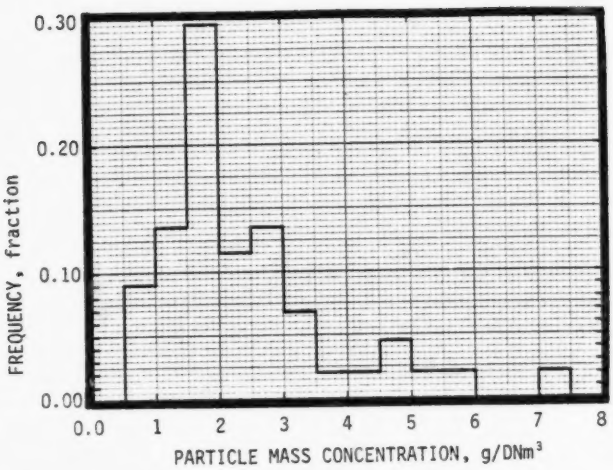

Figure 7-1. Histogram of Condenser Inlet Mass Concentration.

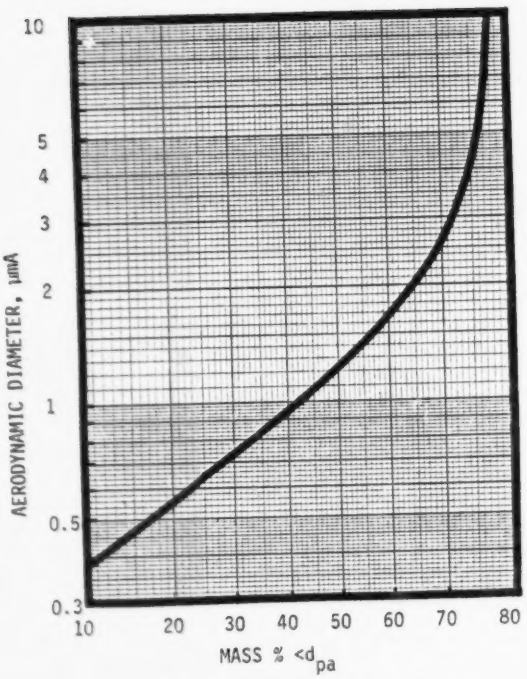

Figure 7-2. Average Condenser Inlet Size Distribution.

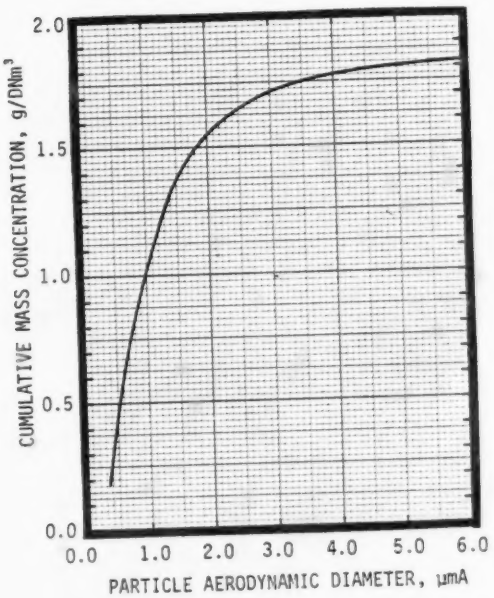

Figure 7-3. Average Condenser Inlet Cumulative Size Distribution.

TABLE 7-5. PARTICULATE MASS CONCENTRATIONS

Run No.	MASS CONCENTRATIONS, g/DNm³		
	Cond. Inlet	Scrubber Inlet	Scrubber Outlet
36/1	1.27	-	0.40
36/2	4.32	-	0.72
36/3	-	-	0.50
36/4	2.50	-	0.52
36/5	2.63	-	0.73
36/6	2.57	1.13	0.47
36/7	-	0.77	0.57
36/8	1.00	0.85	0.41
36/9	1.51	1.33	0.40
36/10	1.07	0.77	0.45
36/11	-	0.73	0.45
36/12	1.58	-	0.51
36/13	1.17	-	0.37
36/14	4.84	-	0.15
36/15	1.56	-	0.71
36/16	2.74	1.19	0.73
36/17	2.77	-	0.77
36/18	2.15	-	0.54
36/19	2.02	0.97	0.34
36/20	5.16	1.29	0.65
36/21	3.23	-	0.31
36/22	1.82	-	0.46

TABLE 7-6. PARTICULATE MASS CONCENTRATIONS

Run No.	MASS CONCENTRATIONS, g/DNm³		
	Cond. Inlet	Scrubber Inlet	Scrubber Outlet
37/1	1.53	-	0.11
37/2	2.13	-	0.49
37/3	2.51	2.03	0.62
37/4	1.22	-	0.45
37/5	1.20	-	0.28
37/6	2.34	0.76	0.50
37/7	1.55	0.62	0.35
37/8	1.75	-	0.51
37/9	3.43	-	0.26
37/10	1.86	-	0.53
37/11	3.84	-	0.57
37/12	0.89	-	0.45
37/13	1.87	-	0.50
37/14	-	-	0.62
37/15	0.82	-	0.25
37/16	1.42	-	0.54
37/17	4.88	-	1.87
37/18	0.56	1.53	0.30
37/19	1.97	-	0.42
37/20	1.62	-	0.42
37/21	3.10	-	0.40
37/22	2.40	-	-
37/23	1.94	-	0.54
37/24	5.62	-	0.70
37/25	7.23	1.72	0.77
37/26	1.74	-	0.60

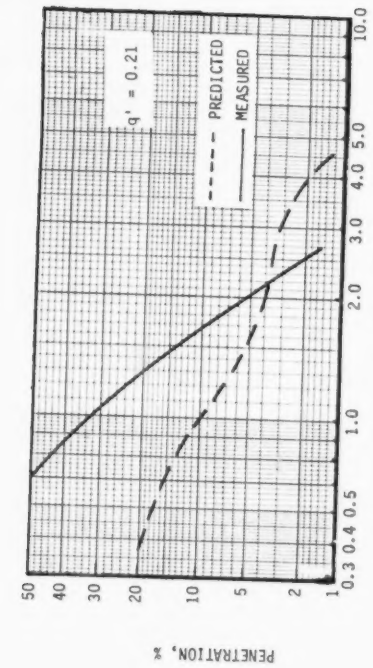

Figure 7-5. Particle Penetration, Run 36/2

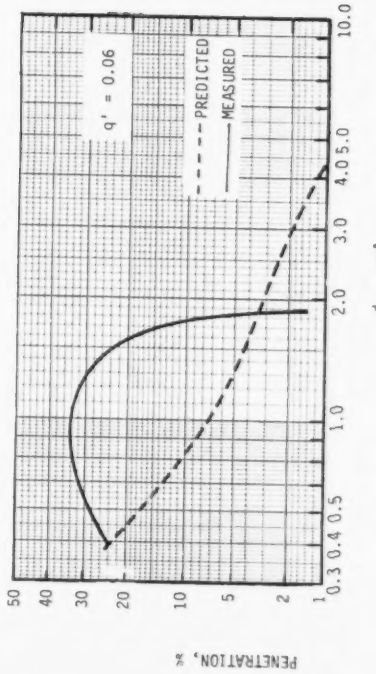

Figure 7-7. Particle Penetration, Run 36/4

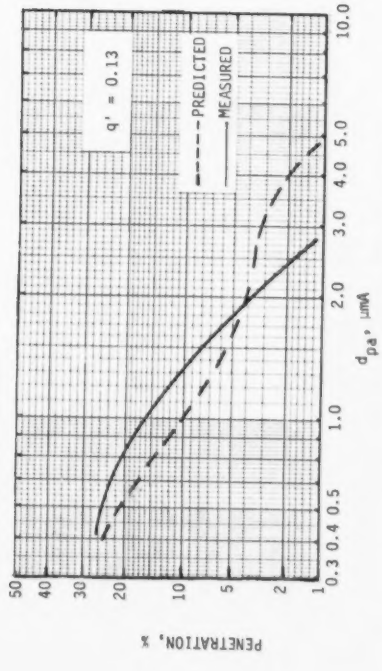

Figure 7-4. Particle Penetration, Run 36/1

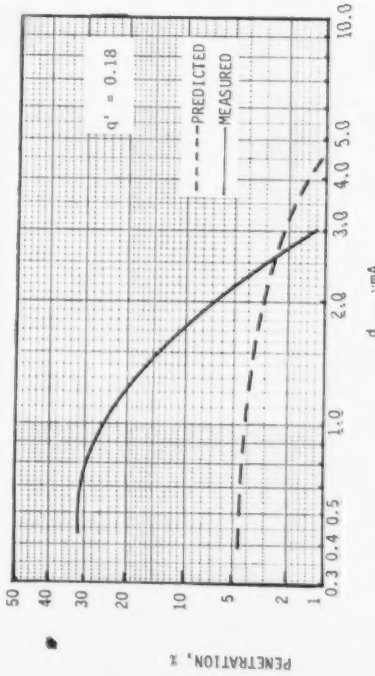

Figure 7-6. Particle Penetration, Run 36/3

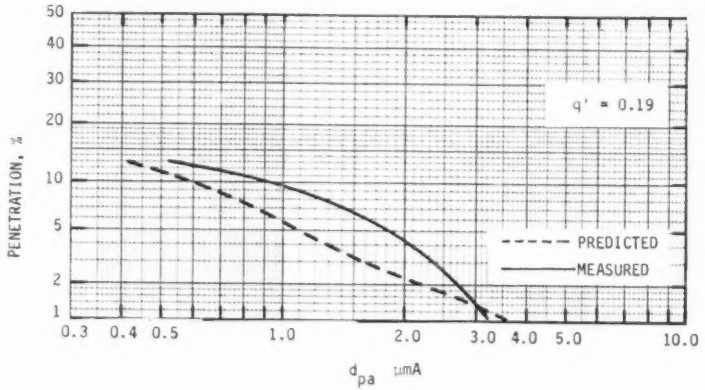

Figure 7-8. Particle Penetration, Run 36/6

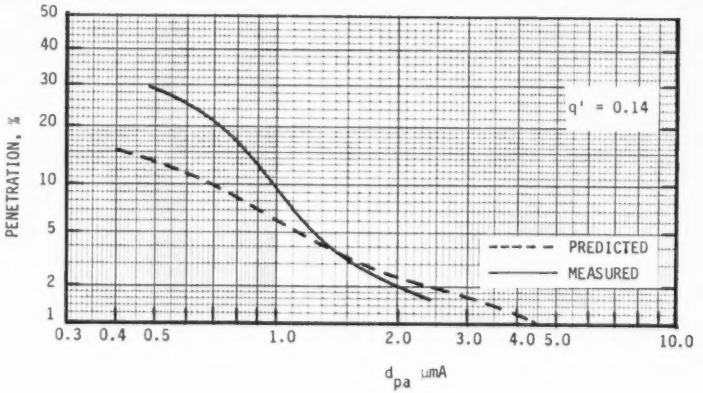

Figure 7-9. Particle Penetration, Run 36/7

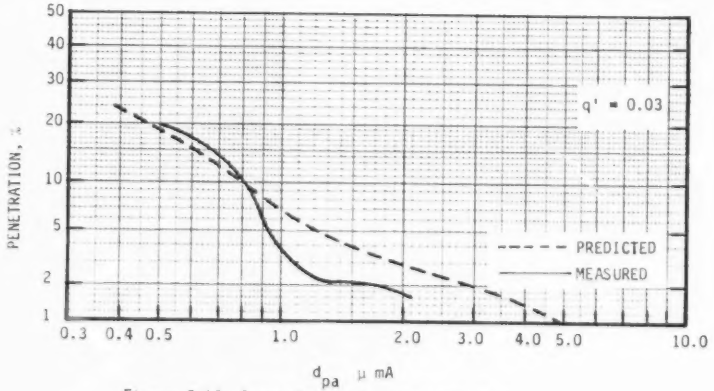

Figure 7-10. Particle Penetration, Run 36/8

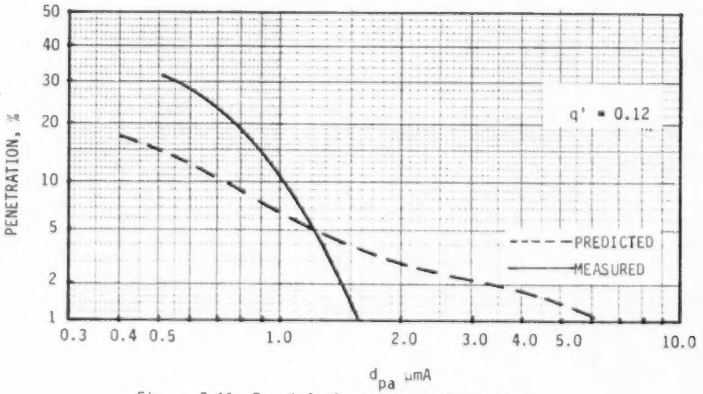

Figure 7-11. Particle Penetration, Run 36/9

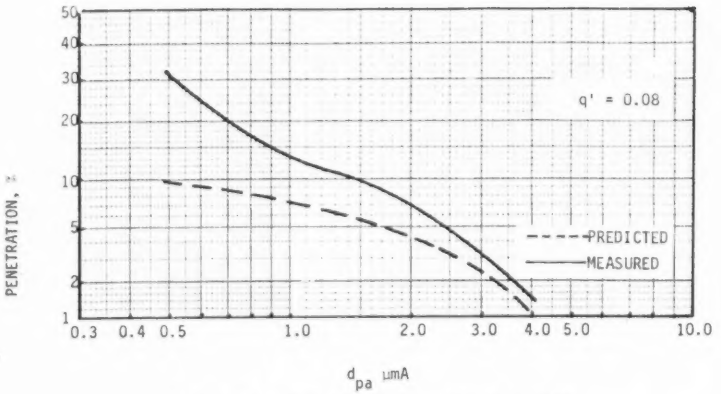

Figure 7-12. Particle Penetration, Run 36/10

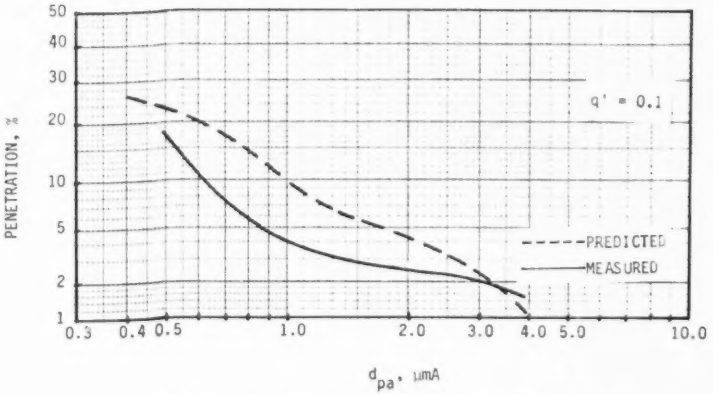

Figure 7-13. Particle Penetration, Run 36/11

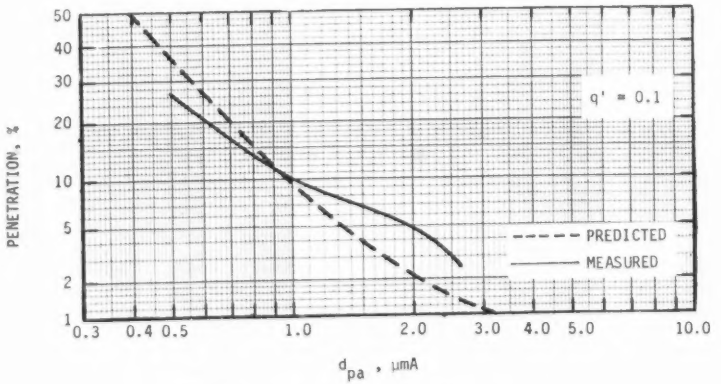

Figure 7-14. Particle Penetration, Run 36/12

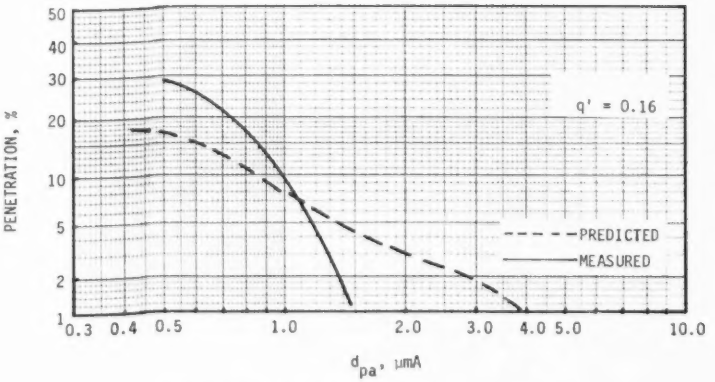

Figure 7-15. Particle Penetration, Run 36/13

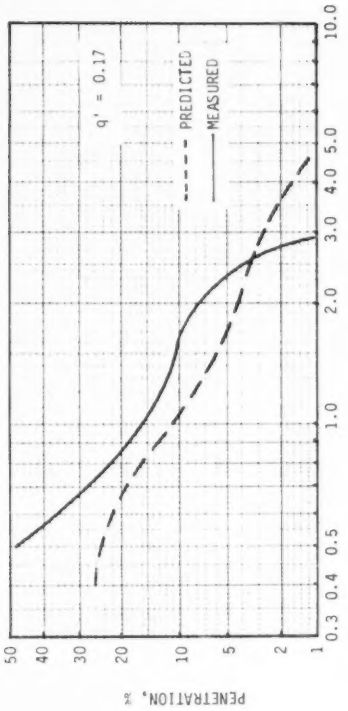

Figure 7-17. Particle Penetration, Run 36/15

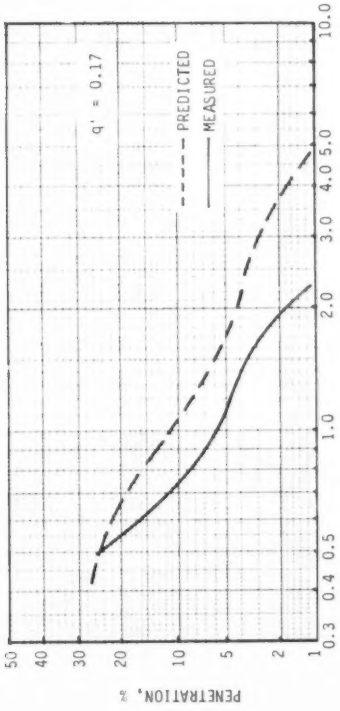

Figure 7-16. Particle Penetration, Run 36/14

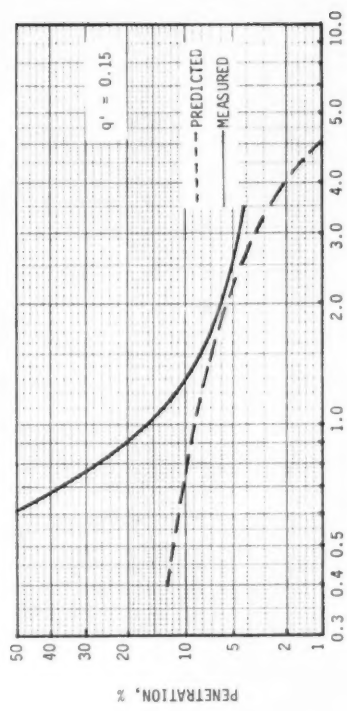

Figure 7-19. Particle Penetration, Run 36/17

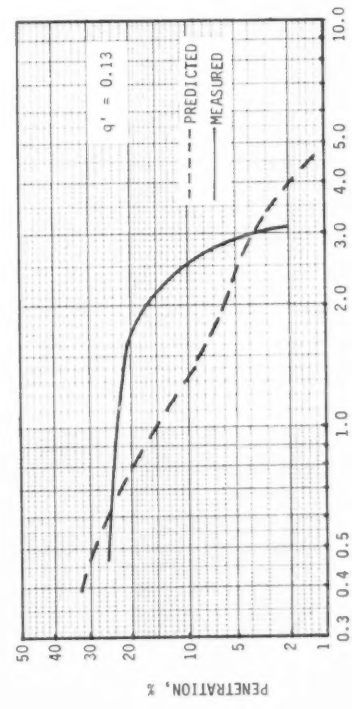

Figure 7-18. Particle Penetration, Run 36/16

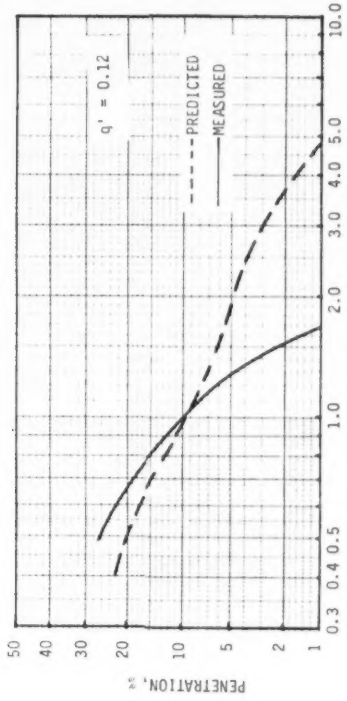

Figure 7-21. Particle Penetration, Run 36/19

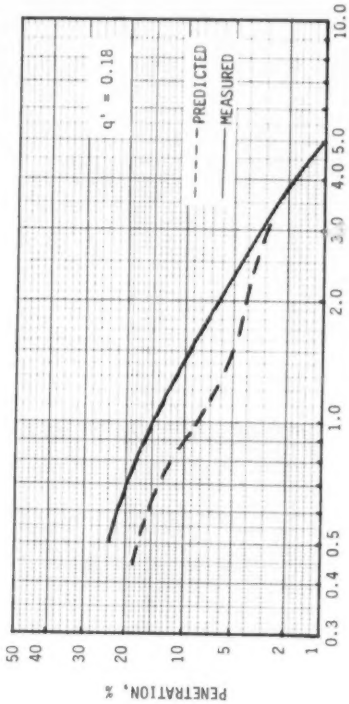

Figure 7-23. Particle Penetration, Run 36/21

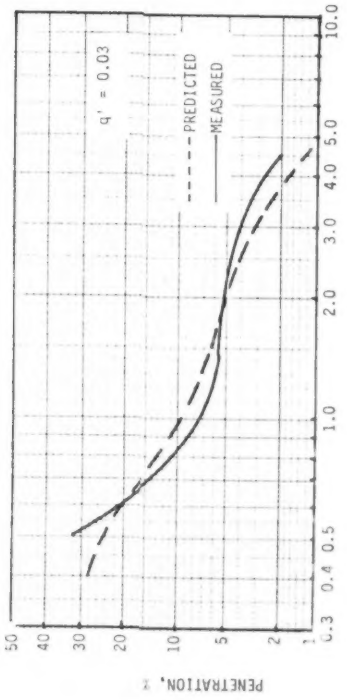

Figure 7-20. Particle Penetration, Run 36/18

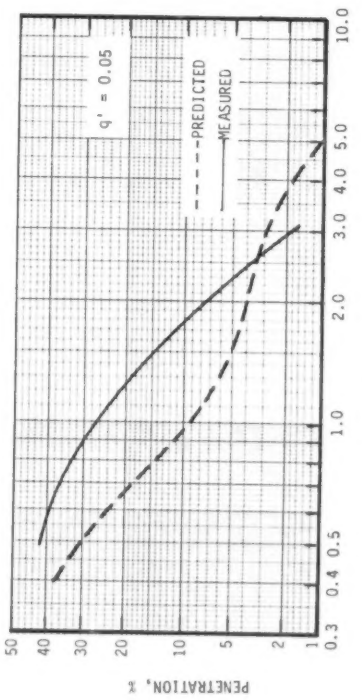

Figure 7-22. Particle Penetration, Run 36/20

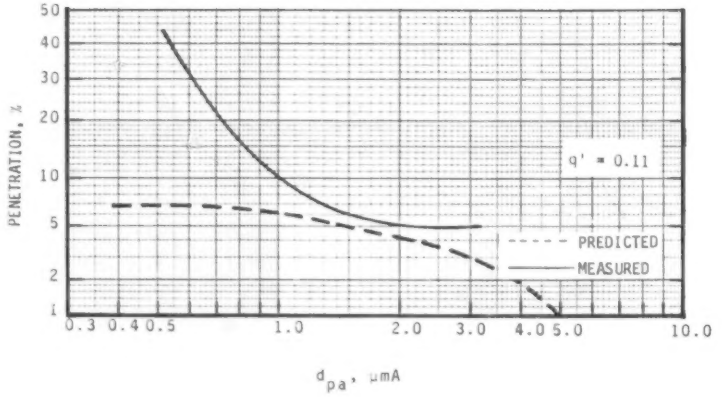

Figure 7-24. Particle Penetration, Run 36/22

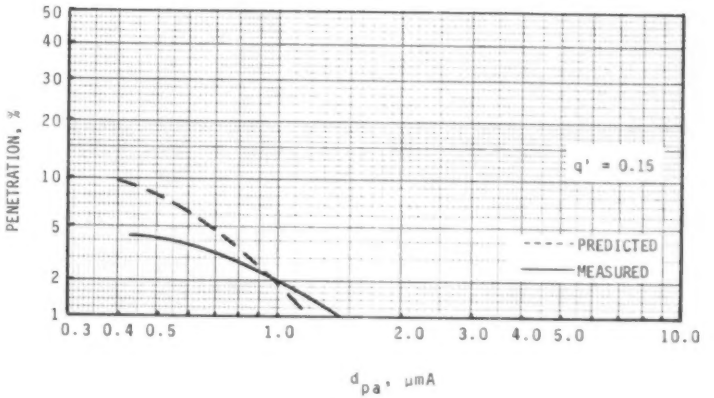

Figure 7-25. Particle Penetration, Run 37/1

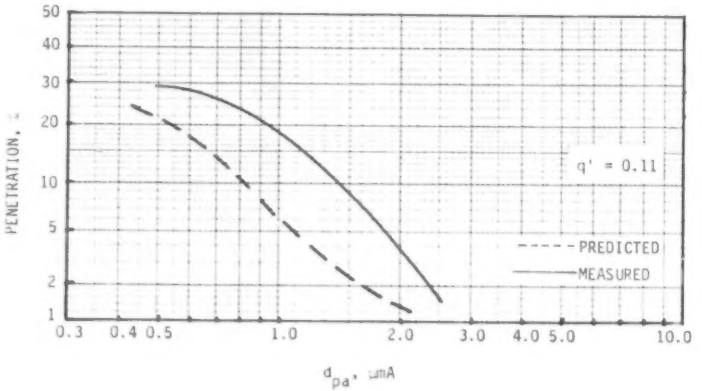

Figure 7-26. Particle Penetration, Run 37/2

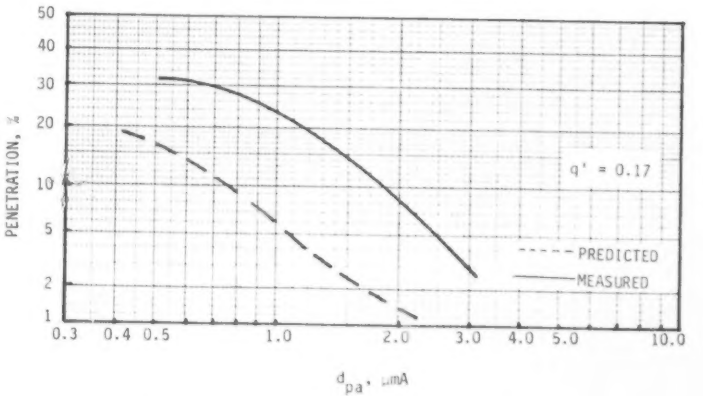

Figure 7-27. Particle Penetration, Run 37/3

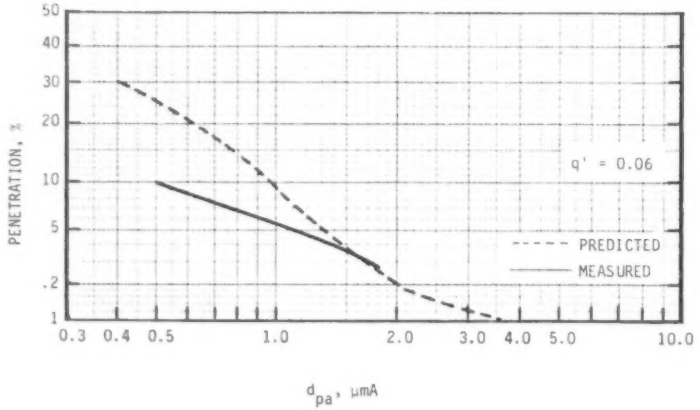

Figure 7-28. Particle Penetration, Run 37/4

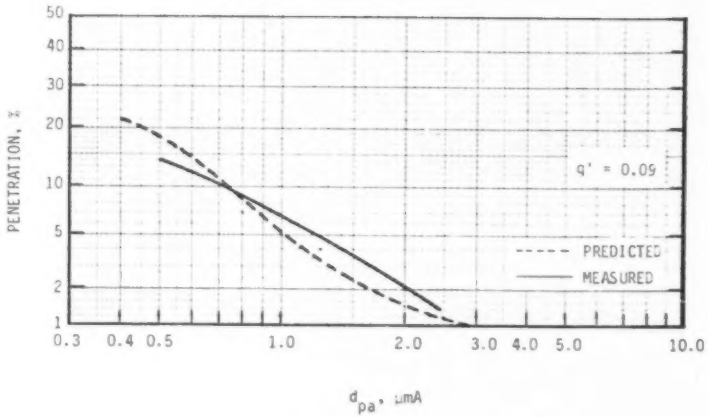

Figure 7-29. Particle Penetration, Run 37/5

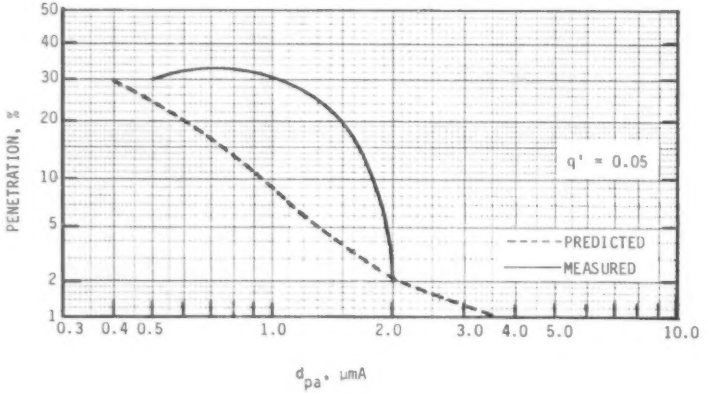

Figure 7-30. Particle Penetration, Run 37/6

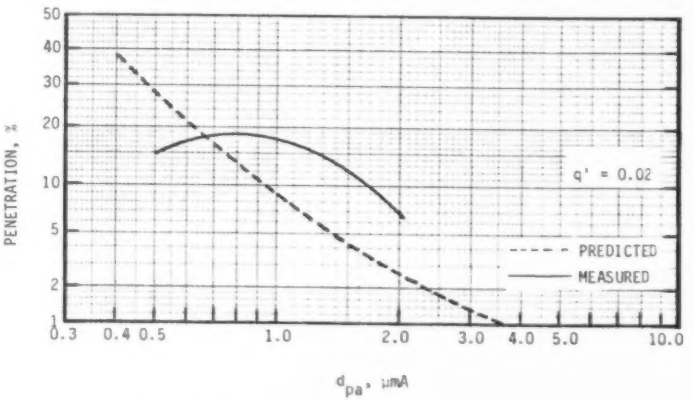

Figure 7-31. Particle Penetration, Run 37/7

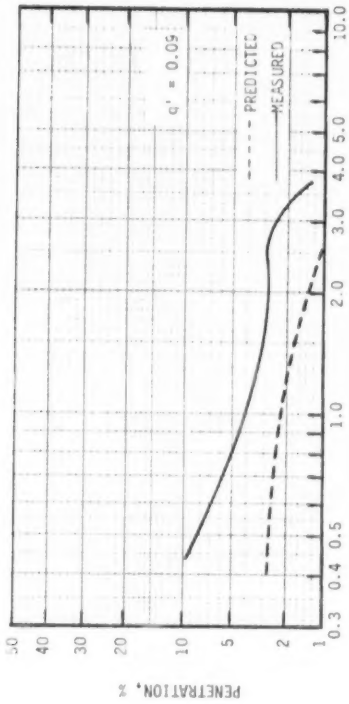

Figure 7-33. Particle Penetration, Run 37/9

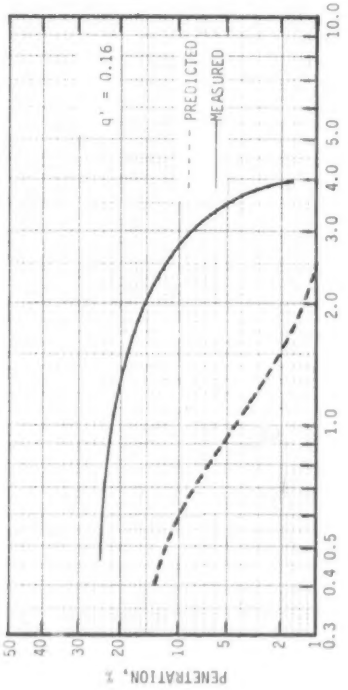

Figure 7-32. Particle Penetration, Run 37/8

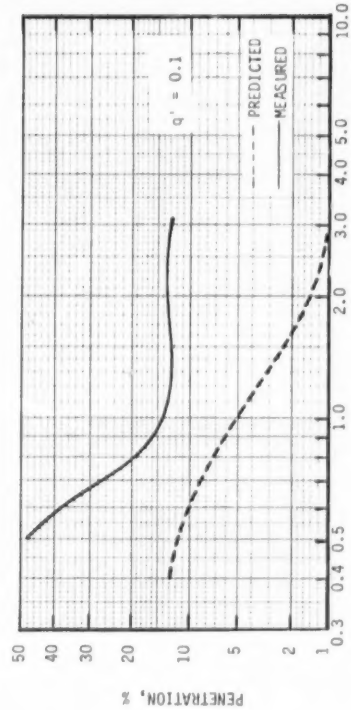

Figure 7-35. Particle Penetration, Run 37/11

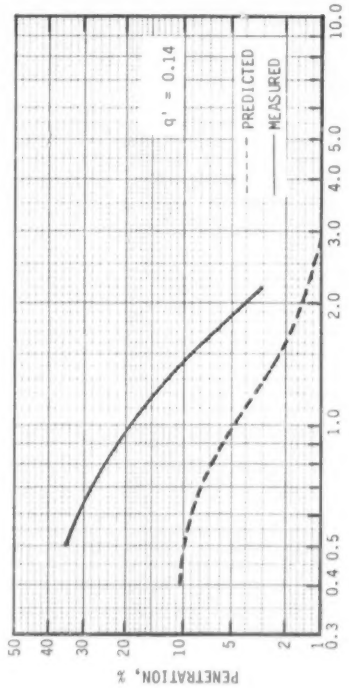

Figure 7-34. Particle Penetration, Run 37/10

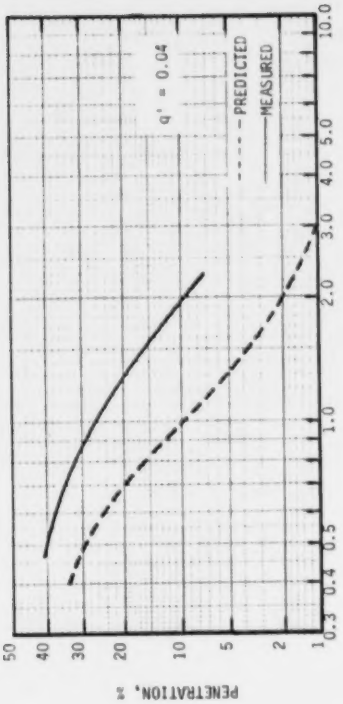

Figure 7-37. Particle Penetration, Run 37/13

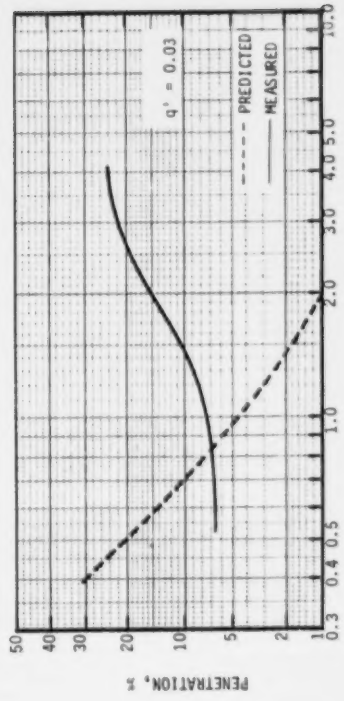

Figure 7-39. Particle Penetration, Run 37/16

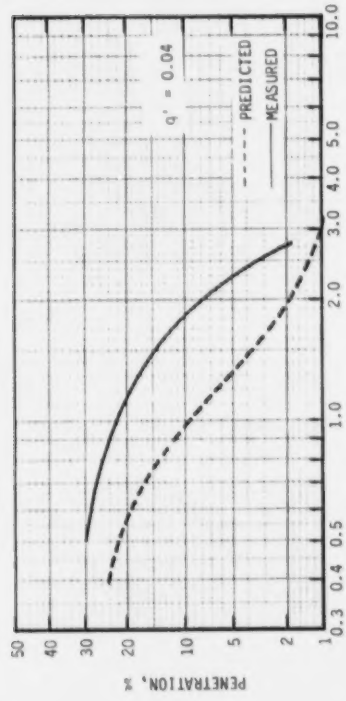

Figure 7-36. Particle Penetration, Run 37/12

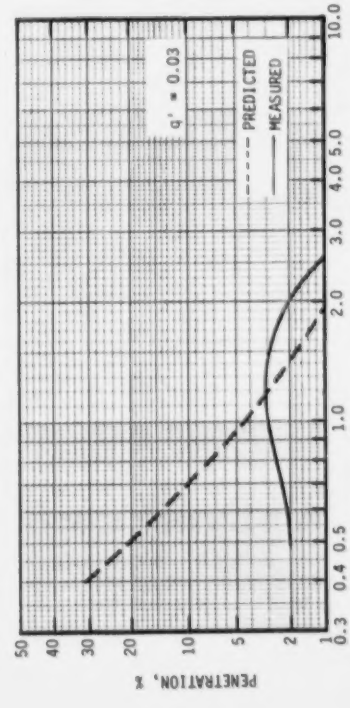

Figure 7-38. Particle Penetration, Run 37/15

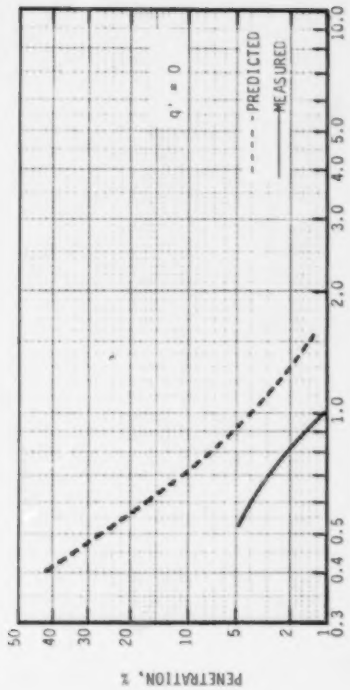

Figure 7-41. Particle Penetration, Run 37/18

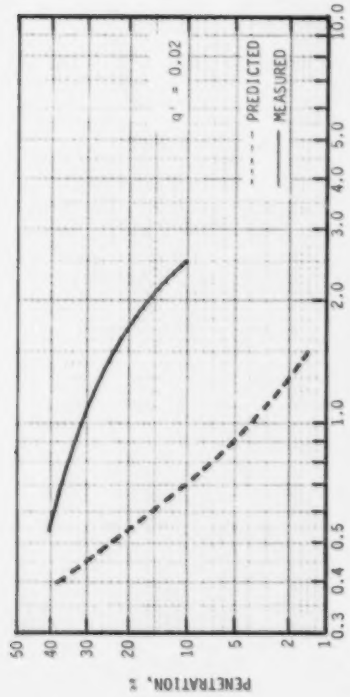

Figure 7-40. Particle Penetration, Run 37/17

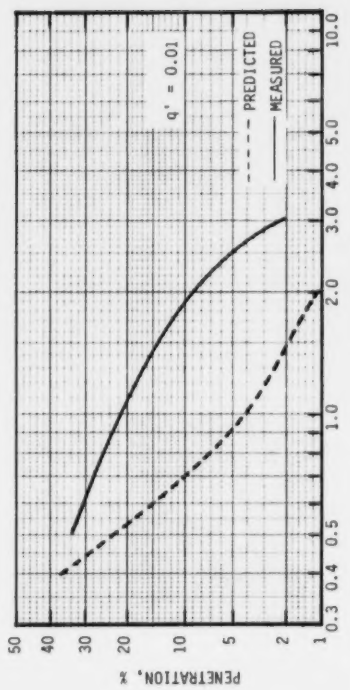

Figure 7-43. Particle Penetration, Run 37/21

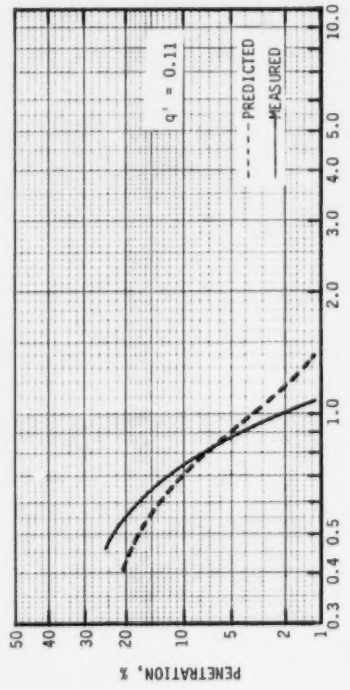

Figure 7-42. Particle Penetration, Run 37/19

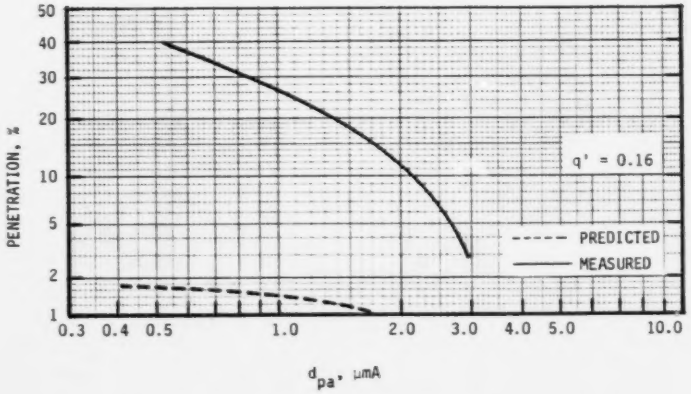

Figure 7-44. Particle Penetration, Run 37/23

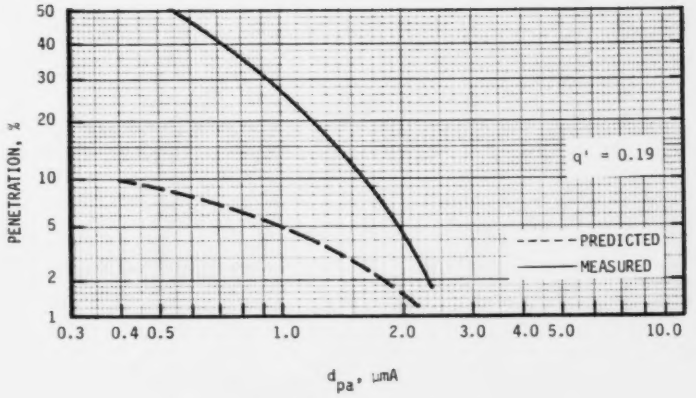

Figure 7-45. Particle Penetration, Run 37/24

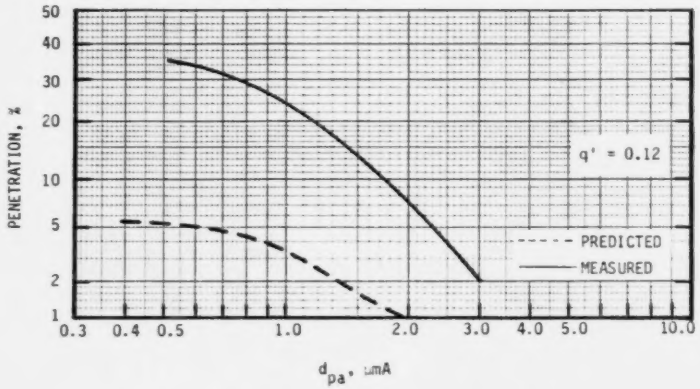

Figure 7-46. Particle Penetration, Run 37/25

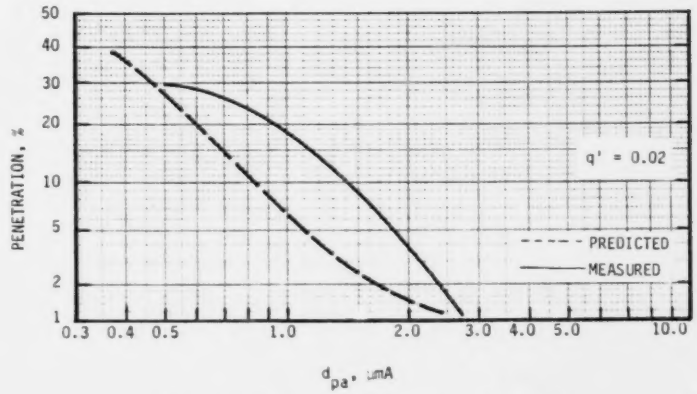

Figure 7-47. Particle Penetration, Run 37/26

SECTION 8
ECONOMIC ANALYSIS

OPTIMUM SYSTEM DESIGN

The optimum F/C scrubber system design for this application would not be significantly different from the demonstration plant and the process design would remain substantially unchanged. The major modifications recommended for an optimum system involve equipment redesign and specification to reduce capital expense and to ensure that the gas temperature would be high. Figure 8-1 shows a flow sheet for an optimum F/C system.

The major area where redesign can provide significant cost savings is a single combined condenser/scrubber vessel. The diameter can be reduced from the size used in the demonstration plant by increasing the superficial velocity through the packing section. The depth of the packing can be reduced to approximately 1 m, based on the results obtained in the demonstration plant.

The second item which can result in cost savings is an alternate choice in cooling towers. The cooling tower chosen for the demonstration plant was dictated by space requirements. The cooling tower had to be elevated on a platform above the saturator and sump. Consequently the most compact tower was chosen, which was not the most economical or energy efficient.

In the course of the project, bids were obtained from other manufacturers. A wood-filled cooling tower would be the most likely choice if space were not at a premium. Such a tower would require only 30 HP, compared to 60 HP for the tower used on the demonstration plant. The wood packing may have some advantage over epoxy coated steel in terms of corrosion resistance. A second circulating water pump would be required for the system

but the total cost would be less because an expensive structural steel platform would not be needed.

The saturator design would be changed in an optimum system. The saturator was designed to allow the equipment to be fit into the available space at the foundry. An optimum system would have a smaller, more compact saturator.

The settler used on the demonstration system provided acceptable performance, however the condenser, scrubber and sump all were subject to deposition of fine sandy material which required removal at frequent intevals. The material which settled out was fairly large, which is apparent from the fact that it settled out in these process vessels. Sloped bottoms should be used in all of these vessels.

It is also recommended that a moving belt filter be used instead of the gravity settler to remove this sandy material. These can be purchased at a lower cost than the settler which was used on the demonstration plant.

Conventional System

In order to evaluate the potential benefits of an F/C scrubber system as compasred to a conventional one, we estimated the costs for a Venturi scrubber system. The process conditions and emission criteria were the same for both systems.

CAPITAL COST ESTIMATES

The capital cost of an optimum F/C system would consist of the total equipment costs and other direct costs such as installation, piping, electrical, etc., along with indirect costs such as engineering, construction overhead, contingencies, etc. The total equipment costs were calculated as described below. For equipment identical or similar to that purchased for the demonstration plant, costs were scaled up from those incurred for

those incurred for the purchased component. For the condenser/scrubber vessel, cost estimates were prepared with standard techniques and then compared to purchased cost for the demonstration plant scrubber and condenser vessels. The fan and motor costs were obtained from the data presented by Neveril et al. (1978). Tables 8-1 and 8-2 show the total equipment costs for the F/C system and high energy scrubber respectively.

The other direct costs were computed by means of ratio factors obtained from Peters (1968) which are based on equipment costs. These fasctors were confirmed using cost data from the Demonstration Plant. The indirect costs have been estimated in the same manner with factors suggested by Peters (1968). Tables 8-3 and 8-4 show the direct and indirect costs for the F/C system and the high energy scrubber. All costs were adjusted to December 1979 by means of the M&S cost index.

OPERATING COSTS

The operating costs for the air pollution control system consist of the annual cost of the utilities (power and water), raw material and maintenance. Table 8-5 shows the power requirement for both the F/C scrubber system and a conventional scrubber. The F/C scrubber system would require only 65% of the power of the conventional scrubber. The exhaust fan for the conventional scrubber would require more than twice the power of the F/C system.

The total operating costs are summarized in Table 8-6. The power cost was estimated at 6.5 cents/kW hr and water at 3.5 cents/1,000 l. The raw material included soda ash for neutralizing the scrubber liquor at 26.5 cents/kg and flocculant to improve water treatment at $1.15/l.

Maintenance costs were based on the estimating factors given by Neveril, et al. (1978), with some modification. Maintenance

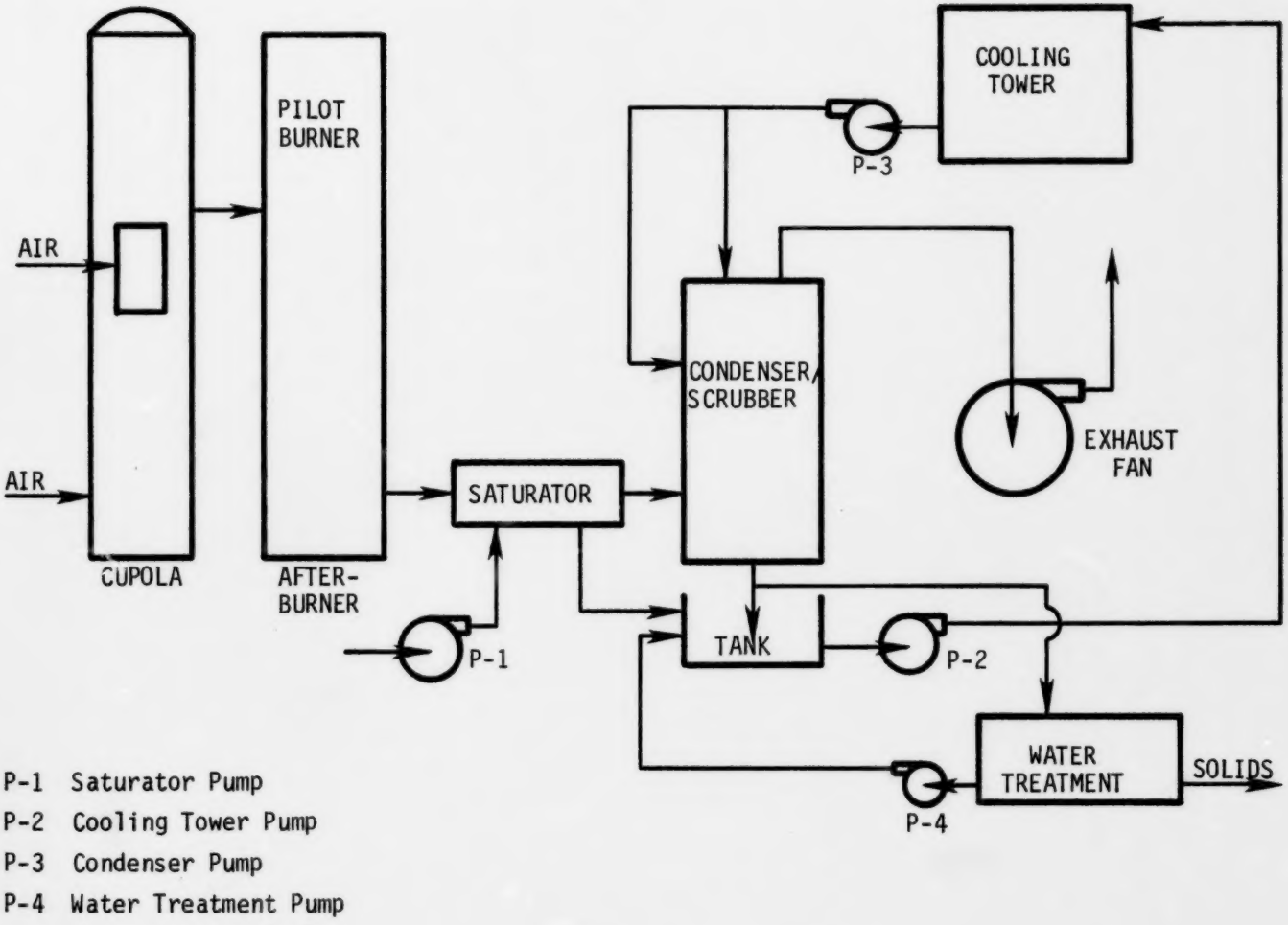

Figure 8-1. Optimum F/C scrubber system flow diagram.

TABLE 8-1. SUMMARY OF ESTIMATED EQUIPMENT COSTS
F/C SCRUBBER SYSTEM

	Unit Cost	Total Cost
Saturator pump & motor	$ 2,290	
starter	240	$ 2,530
Cooling loop pumps & motors	6,950	
starters	580	7,530
Exhaust fan	3,890	
motor & starter	8,290	12,180
Cooling tower	29,370	
fan starter	280	29,650
Saturator shell	3,650	
internals	1,300	4,960
Condenser/scrubber shell	20,000	
internals	8,000	28,000
Tank	4,630	4,630
Belt filter	12,900	12,900
TOTAL EQUIPMENT COST		$102,380

TABLE 8-2. SUMMARY OF ESTIMATED EQUIPMENT COSTS
CONVENTIONAL SCRUBBER SYSTEM

	Unit Cost	Total Cost
Saturator pump & motor	$ 2,290	
starter	240	$ 2,530
Scrubber pump & motor	3,880	
starter	195	4,075
Saturator vessel	3,650	
internals	1,300	4,960
Exhaust fan	5,350	
motor & starter	18,450	23,800
Scrubber vessel	14,600	
internals	10,900	25,500
Belt filter	12,900	12,900
TOTAL EQUIPMENT COST		$73,765

materials were estimated at 3% of fixed capital investment rather than equal to maintenance labor cost, in order to reflect the greater complexity of the F/C system. Maintenance labor was estimated as 1 man-day/wk for each shift of operation; or 2 man-days/wk for 2-shift operation. Operating labor was estimated as 3 hr/day, which is lower than Neveril's range of 2-8 hours per shift, for both systems on 2-shift operation.

The total operating cost for the F/C scrubber system was found to be $131,230 compared to $150,300 for the conventional scrubber. The annual operating cost of the F/C scrubber system would be about $19,100 less than the cost for a conventional scrubber for the conditions of this application.

TABLE 8-3. DIRECT AND INDIRECT COST F/C SYSTEM

Direct	Ratio	Cost, $
Equipment	1.00	$102,380
Installation	0.40	40,952
Instruments	0.10	10,238
Piping and Ducting	0.40	40,952
Electrical	0.10	10,238
Site Preparation	0.05	5,119
Total Direct Cost	2.05	$209,879
Indirect		
Engineering	0.40	40,952
Construction Overhead	0.45	46,071
Contractors Fee	0.10	10,238
Contingency	0.40	40,952
Total Indirect Costs	1.35	$138,213
Fixed Capital Investment	3.40	$348,092

TABLE 8-4. DIRECT AND INDIRECT COST CONVENTIONAL SCRUBBER

Direct	Ratio	Cost, $
Equipment	1.00	$ 73,765
Installation	0.40	29,506
Instruments	0.10	7,377
Piping and Ducting	0.40	29,506
Electrical	0.10	7,377
Site Preparation	0.05	3,687
Total Direct Cost	2.05	$151,218
Indirect		
Engineering	0.40	29,506
Construction Overhead	0.45	33,194
Contractors Fee	0.10	7,377
Contingency	0.40	29,506
Total Indirect Costs	1.35	$ 99,582
Fixed Capital Investment	3.40	$250,800

TABLE 8-5. SUMMARY OF POWER REQUIREMENTS

	Power, kW (HP)			
	F/C Scrubber		Conventional Scrubber	
Exhaust fan	156	(210)	322	(445)
Saturator pump	10	(13)	10	(13)
Scrubber pump	2	(2)	3	(4)
Cooling water pumps	33	(44)	-	
Cooling tower fan	22	(30)	-	
Total Power Required	223	(299)	345	(462)

TABLE 8-6. SUMMARY OF ANNUAL OPERATING COSTS

Item	Unit Cost	F/C Scrubber System	Conventional Scrubber
Capital Cost	@ 10% of F.C.I.	$ 34,809	$ 25,080
Maintenance	materials @3% of FCI	10,440	7,524
Labor	@8 hr/wk shift, $9/hr	7,200	7,200
Operating Labor	@12 hr/wk shift, $9/hr	10,800	10,800
Power Cost*	6.5 cents/kWhr	57,980	89,700
Water Use	3.5 cents/1,000 l	2,000	2,000
Raw Materials	soda ash 26.5 cents/kg		
	flocculant $1.15/l	8,000	8,000
	TOTAL OPERATING COST	$131,230	$150,300

*Power cost estimated at 4,000 hours per year.

REFERENCES

A. G. Amelin, Theory of Fog Condensation, Second Edition, Jerusalem, Israel Program for Scientific Translations, 1967. pp. 33-39.

Calvert, S., J. Goldshmid, D. Leith, N. Jhaveri. Feasibility of Flux Force/Condensation Scrubbing for Fine Particle Collection. A.P.T., Inc. EPA Contract No. 68-02-0256. NTIS #PB 227 307. October 1973.

Calvert, S., J. Goldshmid, D. Leith, N. Jhaveri. Scrubber Handbook. A.P.T., Inc. EPA Contract No. CPA-70-95. NTIS #PB 213 016. August 1972.

Calvert, S., S. Gandhi. Fine Particle Collection By a Flux-Force/Condensation Scrubber: Pilot Demonstration. A.P.T., Inc. EPA Contract No. 68-02-1869. NTIS #EPA-600/2-77-238. December 1977.

Calvert, S., N. Jhaveri, T. Huisking. Study of Flux Force/Condensation Scrubbing of Fine Particles. A.P.T., Inc. EPA Contract No. 68-02-1082. NTIS # EPA-600/2-75-018 August 1975.

Calvert, S., N. Jhaveri, Flux Force/Condensation Scrubbing, JAPCA, 24, 946 (1974).

R. J. Davis and J. Truitt, "Using Condensing Steam for Air Cleaning", Instruments and Control Systems, 1972. pp.68-70.

F. Fahnoe, A. E. Lindroos, and R. J. Abelson, "Aerosol build-up techniques," Ind. Eng. Chem. 43: 1336 (1951).

P. Goldsmith and F. G. May. "Diffusiophoresis and Thermophoresis in Water Vapor Systems", In: Aerosol Science, C. N. Davies (ed.). Academic Press, New York, 1966. pp. 163-194.

Green, H. L., W. R. Lane, Particulate Clouds E. & F. N. Spon Ltd. London, 1964.

G. M. Hidy and J. R. Brock, The Dynamics of Aerocolloidal Systems, Pergamon Press, New York, 1970, 379 pp.

B. W. Lancaster and W. Strauss, "A study of stream injection into wet scrubbers", Ind. Eng. Chem. Fundamentals 10(3): 362 (1971).

A. T. Litvinov, "Influence of condensation on the effectiveness of capture of fine particles during cleaning of gases by the wet method", Zh. Priklad. Khim. 40(2):353(1967).

McCain, J. D., Clinard, G. I., Flix L. G., Johnson J. W., A Data Reduction System for Cascade Impactors. EPA No. 600/7-78-132a, July 1978.

Neveril, R. B., J. V. Price and K. L. Engdahl, Capital and Operating Costs of Selected Air Pollution Control Systems Parts II and IV. J. Air Pollution Control Association V28 N9 P963, September 1978 and V28 N10, October 1978.

Peters, M. S., K. D. Timmerhaus, Plant Design and Economics for Chemical Engineers, McGraw-Hill Book Company, 1968.

C. B. Prakash and f. E. Murray, "Particle Conditioning by Steam Condensation", Preprint of paper presented in 1973.

A. M. Rozen and V. M. Kostin, "Collection of finely dispersed aerosols in plate columns by condensation enlarjgement", Internat. Chem. Eng. 7:464(1967).

P. J. Schauer, "Condensation Technique4s for Dust Detection and Collection", cited by A. Bralove in Chapt. 40 of Air Pollution, L. C. McCabe. McGraw-Hill Co., New York, 1952.

L. E. Sparks and M. J. Pilat, "Effect of diffusiophoresis on particle collection by wet scrubbers", Atmos. Environ. 4: 1 (1970).

R. A. Stinchombe and P. Goldsmith, "Removal of iodine from the atmosphere by condensing steam", J. Nuclear Energy 20:261 (1966).

A. N. Terebenin and A. P. Bykov, "Aerosol sedimentation mechanisms in water vapor diffusion fields", Zh. Priklad Khim. 45:1012 (1972).

L. Waldmann and K. H. Schmitt, "Thermophoresis and Diffusiophoresis of Aerosols", In: Aerosol Science, C. N. Davies (ed.) Academic Press, New York, 1966. pp. 137-161.

Whitmore, P. J., Diffusiophoretic Deposition Under Turbulent Conditions, PhD Thesis, University of British Columbia, 1976.

Yung, S., S. Calvert, H. Barbarika, Venturi Scrubber Performance Model. Environmental Science and Technology V 12 p. 456, April 1978.

APPENDIX A

CASCADE IMPACTOR DATA

Table A-1. Cascade Impactor Data for Run 36/1

Impactor Stage Number	Inlet		Outlet	
	W_{cum} (mg/DNm³)	d_{pc} (µmA)	W_{cum} (mg/DNm³)	d_{pc} (µmA)
1	1,275	24.2	395	19.1
2	988	10.6	395	8.35
3	976	4.10	394	3.22
4	927	2.07	394	1.60
5	844	1.20	389	0.96
6	758	0.65	354	0.52
7	581	0.24	204	0.22
Filter	347		94	
Sample Volume DNm³	0.131		0.249	

Table A-2. Cascade Impactor Data for Run 36/2

Impactor Stage Number	Inlet		Outlet	
	W_{cum} (mg/DNm³)	d_{pc} (µmA)	W_{cum} (mg/DNm³)	d_{pc} (µmA)
1	4,326	21.3	719	20.0
2	2,228	9.33	719	8.78
3	2,480	3.60	718	3.40
4	2,164	1.82	718	1.69
5	2,047	1.05	711	1.01
6	1,892	0.57	610	0.55
7	987	0.20	263	0.23
Filter	426		104	
Sample Volume DNm³	0.030		0.103	

Table A-3. Cascade Impactor Data for Run 36/3

Impactor Stage Number	Inlet		Outlet	
	W_{cum} (mg/DNm^3)	d_{pc} (µmA)	W_{cum} (mg/DNm^3)	d_{pc} (µmA)
1	375	36.5	501	18.4
2	224	16.0	501	8.05
3	221	6.19	501	3.11
4	218	3.22	499	1.60
5	214	1.96	489	0.93
6	208	1.03	426	0.51
7	63	0.49	182	0.22
Filter	34		47	
Sample Volume DNm^3	0.065		0.163	

Table A-4. Cascade Impactor Data for Run 36/4

Impactor Stage Number	Inlet		Outlet	
	W_{cum} (mg/DNm^3)	d_{pc} (µmA)	W_{cum} (mg/DNm^3)	d_{pc} (µmA)
1	2,497	25.5	515	18.4
2	1,813	11.2	450	8.05
3	1,768	4.31	449	3.11
4	1,618	2.18	448	1.55
5	1,441	1.25	442	0.93
6	1,230	0.66	174	0.51
7	400	0.14	133	0.23
Filter	234		46	
Sample Volume DNm^3	0.086		0.152	

Table A-5. Cascade Impactor Data for Run 36/5

Impactor Stage Number	Inlet		Outlet	
	W_{cum} (mg/DNm^3)	d_{pc} (μmA)	W_{cum} (mg/DNm^3)	d_{pc} (μmA)
1	2,631	42.7	733	19.1
2	2,496	3.76	604	8.35
3	2,466	2.29	604	3.23
4	2,435	1.23	604	1.66
5	2,396	0.64	598	0.96
6	2,297	0.39	106	0.52
7	1,410	0.18	77	0.23
Filter	1,006		76	
Sample Volume DNm^3	0.026		0.154	

Table A-6. Cascade Impactor Data for Run 36/6

Impactor Stage Number	Inlet		Outlet	
	W_{cum} (mg/DNm^3)	d_{pc} (μmA)	W_{cum} (mg/DNm^3)	d_{pc} (μmA)
1	2,570	53.9	463	19.0
2	2,225	4.75	324	8.32
3	2,213	2.90	324	3.22
4	2,167	1.55	321	1.66
5	2,095	0.81	318	0.96
6	2,011	0.49	277	0.52
7	865	0.22	153	0.23
Filter	755		41	
Sample Volume DNm^3	0.015		0.154	

Table A-7. Cascade Impactor Data for Run 36/7

Impactor Stage Number	Inlet		Outlet	
	W_{cum} (mg/DNm^3)	d_{pc} (µmA)	W_{cum} (mg/DNm^3)	d_{pc} (µmA)
1	450	45.5	571	19.4
2	206	4.02	473	8.48
3	175	2.45	473	3.28
4	162	1.31	473	1.69
5	146	0.68	473	0.97
6	131	0.42	469	0.52
7	82	0.23	365	0.19
Filter	31		234	
Sample Volume DNm^3	0.039		0.109	

Table A-8. Cascade Impactor Data for Run 36/8

Impactor Stage Number	Inlet		Outlet	
	W_{cum} (mg/DNm^3)	d_{pc} (µmA)	W_{cum} (mg/DNm^3)	d_{pc} (µmA)
1	996	49.7	407	17.7
2	886	4.38	170	7.74
3	868	2.67	170	2.99
4	856	1.43	170	1.54
5	835	0.74	167	0.89
6	758	0.45	158	0.48
7	256	0.22	46	0.21
Filter	68		18	
Sample Volume DNm^3	0.040		0.154	

Table A-9. Cascade Impactor Data for Run 36/9

Impactor Stage Number	Inlet		Outlet	
	W_{cum} (mg/DNm^3)	d_{pc} (µmA)	W_{cum} (mg/DNm^3)	d_{pc} (µmA)
1	1,510	44.0	404	17.2
2	420	3.88	343	7.54
3	409	2.37	342	2.91
4	395	1.27	342	1.50
5	377	0.66	340	0.87
6	340	0.40	319	0.47
7	196	0.19	132	0.19
Filter	127		38	
Sample Volume DNm^3	0.083		0.152	

Table A-10. Cascade Impactor Data for Run 36/10

Impactor Stage Number	Inlet		Outlet	
	W_{cum} (mg/DNm^3)	d_{pc} (µmA)	W_{cum} (mg/DNm^3)	d_{pc} (µmA)
1	1,075	45.4	448	18.0
2	879	3.83	328	7.87
3	860	2.31	324	3.04
4	825	1.31	322	1.57
5	649	0.76	302	0.91
6	545	0.42	235	0.49
7	208	0.20	63	0.21
Filter	4		24	
Sample Volume DNm^3	0.026		0.114	

Table A-11. Cascade Impactor Data for Run 36/11

Impactor Stage Number	Inlet		Outlet	
	W_{cum} (mg/DNm^3)	d_{pc} (µmA)	W_{cum} (mg/DNm^3)	d_{pc} (µmA)
1	600	41.6	453	22.9
2	442	3.51	287	10.0
3	437	2.11	280	3.88
4	423	1.20	275	1.99
5	405	0.70	271	1.15
6	385	0.38	253	0.62
7	141	0.20	89	0.22
Filter	54		13	
Sample Volume DNm^3	0.040		0.045	

Table A-12. Cascade Impactor Data for Run 36/12

Impactor Stage Number	Inlet		Outlet	
	W_{cum} (mg/DNm^3)	d_{pc} (µmA)	W_{cum} (mg/DNm^3)	d_{pc} (µmA)
1	1,580	45.9	506	18.2
2	1,298	3.87	436	8.00
3	1,297	2.34	435	3.08
4	1,292	1.32	428	1.58
5	1,282	0.77	414	0.91
6	1,252	0.42	369	0.49
7	560	0.17	133	0.19
Filter	318		34	
Sample Volume DNm^3	0.020		0.071	

Table A-13. Cascade Impactor Data for Run 36/13

Impactor Stage Number	Inlet		Outlet	
	W_{cum} (mg/DNm³)	d_{pc} (μmA)	W_{cum} (mg/DNm³)	d_{pc} (μmA)
1	1,168	42.0	365	18.1
2	694	3.70	358	7.91
3	684	2.26	356	3.06
4	666	1.21	355	1.55
5	655	0.63	350	0.89
6	476	0.39	329	0.49
7	283	0.19	198	0.18
Filter	171		74	
Sample Volume DNm³	0.064		0.169	

Table A-14. Cascade Impactor Data for Run 36/14

Impactor Stage Number	Inlet		Outlet	
	W_{cum} (mg/DNm³)	d_{pc} (μmA)	W_{cum} (mg/DNm³)	d_{pc} (μmA)
1	4,838	22.3	145	19.7
2	4,462	9.77	133	8.62
3	4,177	3.78	133	3.33
4	3,931	1.88	133	1.71
5	3,793	1.12	128	0.99
6	3,300	0.61	101	0.54
7	1,724	0.26	31	0.21
Filter	700		0	
Sample Volume DNm³	0.023		0.152	

Table A-15. Cascade Impactor Data for Run 36/15

Impactor Stage Number	Inlet		Outlet	
	W_{cum} (mg/DNm^3)	d_{pc} (µmA)	W_{cum} (mg/DNm^3)	d_{pc} (µmA)
1	1,560	24.9	713	19.3
2	1,271	10.9	702	8.44
3	1,256	4.21	699	3.26
4	1,219	2.19	693	1.65
5	1,159	1.32	675	0.95
6	1,075	0.68	612	0.52
7	503	0.28	305	0.20
Filter	287		147	
Sample Volume DNm^3	0.087		0.116	

Table A-16. Cascade Impactor Data for Run 36/16

Impactor Stage Number	Inlet		Outlet	
	W_{cum} (mg/DNm^3)	d_{pc} (µmA)	W_{cum} (mg/DNm^3)	d_{pc} (µmA)
1	2,735	25.2	728	16.4
2	1,448	11.0	709	7.18
3	1,434	4.27	707	2.77
4	1,347	2.12	697	1.43
5	1,221	1.27	627	0.82
6	1,023	0.70	459	0.44
7	474	0.33	126	0.18
Filter	243		36	
Sample Volume DNm^3	0.055		0.171	

Table A-17. Cascade Impactor Data for Run 36/17

Impactor Stage Number	Inlet		Outlet	
	W_{cum} (mg/DNm^3)	d_{pc} (µmA)	W_{cum} (mg/DNm^3)	d_{pc} (µmA)
1	2,772	30.6	773	19.0
2	2,044	13.4	765	8.31
3	2,040	5.18	760	3.21
4	1,974	2.69	758	1.65
5	1,832	1.63	741	0.96
6	1,640	0.85	664	0.53
7	516	0.36	384	0.25
Filter	210		148	
Sample Volume DNm^3	0.053		0.138	

Table A-18. Cascade Impactor Data for Run 36/18

Impactor Stage Number	Inlet		Outlet	
	W_{cum} (mg/DNm^3)	d_{pc} (µmA)	W_{cum} (mg/DNm^3)	d_{pc} (µmA)
1	2,154	29.6	540	18.93
2	1,601	13.0	460	8.29
3	1,594	5.01	454	3.21
4	1,525	2.49	450	1.62
5	1,276	1.50	432	0.94
6	1,095	0.83	402	0.52
7	568	0.42	247	0.22
Filter	242		69	
Sample Volume DNm^3	0.070		0.117	

Table A-19. Cascade Impactor Data for Run 36/19

Impactor Stage Number	Inlet		Outlet	
	W_{cum} (mg/DNm^3)	d_{pc} (µmA)	W_{cum} (mg/DNm^3)	d_{pc} (µmA)
1	2,016	28.0	344	19.8
2	1,410	12.3	313	8.69
3	1,398	4.74	313	3.36
4	1,346	2.46	312	1.73
5	1,190	1.49	309	1.00
6	1,071	0.77	285	0.55
7	948	0.31	148	0.26
Filter	629		65	
Sample Volume DNm^3	0.027		0.127	

Table A=20. Cascade Impactor Data for Run 36/20

Impactor Stage Number	Inlet		Outlet	
	W_{cum} (mg/DNm^3)	d_{pc} (µmA)	W_{cum} (mg/DNm^3)	d_{pc} (µmA)
1	5,165	30.6	654	19.8
2	2,074	13.4	597	8.66
3	1,655	5.18	595	3.35
4	1,509	2.69	592	1.73
5	1,272	1.64	571	1.01
6	1,082	0.88	495	0.57
7	827	0.45	251	0.32
Filter	507		58	
Sample Volume DNm^3	0.063		0.099	

Table A-21. Cascade Impactor Data for Run 36/21

Impactor Stage Number	Inlet		Outlet	
	W_{cum} (mg/DNm^3)	d_{pc} (µmA)	W_{cum} (mg/DNm^3)	d_{pc} (µmA)
1	3,231	29.3	313	21.5
2	478	12.8	290	9.40
3	475	4.97	287	3.64
4	453	2.47	285	1.87
5	412	1.49	276	1.09
6	360	0.84	235	0.62
7	304	0.48	134	0.35
Filter	166		52	
Sample Volume DNm^3	0.092		0.166	

Table A-22. Cascade Impactor Data for Run 36/22

Impactor Stage Number	Inlet		Outlet	
	W_{cum} (mg/DNm^3)	d_{pc} (µmA)	W_{cum} (mg/DNm^3)	d_{pc} (µmA)
1	1,820	31.2	459	20.4
2	1,165	13.6	437	8.93
3	1,158	5.28	434	3.46
4	1,044	2.75	432	1.75
5	900	1.67	419	1.02
6	728	0.89	387	0.58
7	426	0.46	231	0.28
Filter	193		49	
Sample Volume DNm^3	0.094		0.167	

Table A-23. Cascade Impactor Data for Run 37/1

Impactor Stage Number	Inlet		Outlet	
	W_{cum} (mg/DNm^3)	d_{pc} (µmA)	W_{cum} (mg/DNm^3)	d_{pc} (µmA)
1	1,529	29.9	107	21.8
2	1,045	13.1	29	9.53
3	877	5.06	28	3.69
4	798	2.63	28	1.89
5	724	1.60	28	1.11
6	505	0.83	25	0.63
7	464	0.37	23	0.34
Filter	239		19	
Sample Volume DNm^3	0.069		0.227	

Table A-24. Cascade Impactor Data for Run 37/2

Impactor Stage Number	Inlet		Outlet	
	W_{cum} (mg/DNm^3)	d_{pc} (µmA)	W_{cum} (mg/DNm^3)	d_{pc} (µmA)
1	2,134	29.5	493	21.4
2	1,739	12.9	425	9.38
3	1,680	5.00	421	3.63
4	1,505	2.48	421	1.84
5	1,406	1.49	414	1.07
6	1,185	0.82	375	0.59
7	982	0.42	200	0.25
Filter	566		61	
Sample Volume DNm^3	0.099		0.253	

Table A-25. Cascade Impactor Data for Run 37/3

Impactor Stage Number	Inlet		Outlet	
	W_{cum} (mg/DNm³)	d_{pc} (µmA)	W_{cum} (mg/DNm³)	d_{pc} (µmA)
1	2,506	24.2	617	20.7
2	1,817	10.6	589	9.05
3	1,791	4.10	589	3.50
4	1,718	2.04	587	1.82
5	1,484	1.22	571	1.10
6	1,411	0.66	474	0.58
7	1,341	0.28	310	0.27
Filter	595		97	
Sample Volume DNm³	0.048		0.258	

Table A-26. Cascade Impactor Data for Run 37/4

Impactor Stage Number	Inlet		Outlet	
	W_{cum} (mg/DNm³)	d_{pc} (µmA)	W_{cum} (mg/DNm³)	d_{pc} (µmA)
1	1,219	27.4	445	20.7
2	792	12.0	326	9.08
3	792	4.64	314	3.52
4	754	2.39	314	1.83
5	747	1.39	272	1.11
6	746	0.77	245	0.59
7	577	0.40	233	0.28
Filter	284		149	
Sample Volume DNm³	0.101		0.237	

Table A-27. Cascade Impactor Data for Run 37/5

Impactor Stage Number	Inlet		Outlet	
	W_{cum} (mg/DNm^3)	d_{pc} (µmA)	W_{cum} (mg/DNm^3)	d_{pc} (µmA)
1	1,195	25.8	281	21.8
2	1,064	11.3	261	9.55
3	1,050	4.38	261	3.69
4	1,013	2.18	261	1.87
5	955	1.31	259	1.09
6	909	0.72	252	0.61
7	772	0.37	202	0.28
Filter	428		101	
Sample Volume DNm^3	0.060		0.236	

Table A-28. Cascade Impactor Data for Run 37/6

Impactor Stage Number	Inlet		Outlet	
	W_{cum} (mg/DNm^3)	d_{pc} (µmA)	W_{cum} (mg/DNm^3)	d_{pc} (µmA)
1	2,337	50.4	497	19.3
2	1,570	22.1	479	8.44
3	1,559	8.54	474	3.27
4	1,526	4.25	472	1.10
5	1,486	2.56	468	1.03
6	1,427	1.43	379	0.54
7	1,277	0.79	159	0.25
Filter	983		68	
Sample Volume DNm^3	0.028		0.194	

Table A-29. Cascade Impactor Data for Run 37/7

Impactor Stage Number	Inlet		Outlet	
	W_{cum} (mg/DNm^3)	d_{pc} (µmA)	W_{cum} (mg/DNm^3)	d_{pc} (µmA)
1	1,552	48.4	349	19.46
2	902	21.2	314	8.52
3	902	8.21	314	3.30
4	902	4.08	314	1.67
5	898	2.46	268	0.97
6	871	1.38	184	0.54
7	712	0.75	87	0.24
Filter	470		27	
Sample Volume DNm^3	0.029		0.214	

Table A-30. Cascade Impactor Data for Run 37/8

Impactor Stage Number	Inlet		Outlet	
	W_{cum} (mg/DNm^3)	d_{pc} (µmA)	W_{cum} (mg/DNm^3)	d_{pc} (µmA)
1	1,754	44.0	512	21.7
2	1,436	19.3	498	9.49
3	1,228	7.46	498	3.67
4	1,199	3.84	496	1.91
5	1,188	2.23	460	1.16
6	1,151	1.25	376	0.61
7	1,020	0.66	219	0.28
Filter	972		85	
Sample Volume DNm^3	0.028		0.095	

Table A-31. Cascade Impactor Data for Run 37/9

Impactor Stage Number	Inlet		Outlet	
	W_{cum} (mg/DNm^3)	d_{pc} (µmA)	W_{cum} (mg/DNm^3)	d_{pc} (µmA)
1	3,434	52.8	257	21.7
2	2,799	23.1	214	9.50
3	2,710	8.94	214	3.68
4	2,710	4.61	205	1.91
5	2,710	2.68	190	1.16
6	1,784	1.49	190	0.61
7	1,022	0.78	178	0.29
Filter	249		52	
Sample Volume DNm^3	0.030		0.195	

Table A-32. Cascade Impactor Data for Run 37/10

Impactor Stage Number	Inlet		Outlet	
	W_{cum} (mg/DNm^3)	d_{pc} (µmA)	W_{cum} (mg/DNm^3)	d_{pc} (µmA)
1	1,858	24.4	529	19.2
2	1,578	10.7	369	8.41
3	1,553	4.13	569	3.25
4	1,501	2.12	368	1.69
5	1,420	1.23	362	1.02
6	1,340	0.67	316	0.53
7	827	0.31	112	0.23
Filter	179		56	
Sample Volume DNm^3	0.048		0.051	

Table A-33. Cascade Impactor Data for Run 37/11

Impactor Stage Number	Inlet		Outlet	
	W_{cum} (mg/DNm^3)	d_{pc} (µmA)	W_{cum} (mg/DNm^3)	d_{pc} (µmA)
1	3,839	25.3	571	17.7
2	2,901	11.1	549	7.76
3	2,885	4.28	542	3.00
4	2,787	2.12	538	1.52
5	2,601	1.28	482	0.88
6	2,341	0.70	443	0.49
7	1,314	0.34	250	0.21
Filter	230		80	
Sample Volume DNm^3	0.057		0.127	

Table A-34. Cascade Impactor Data for Run 37/12

Impactor Stage Number	Inlet		Outlet	
	W_{cum} (mg/DNm^3)	d_{pc} (µmA)	W_{cum} (mg/DNm^3)	d_{pc} (µmA)
1	889	24.5	463	18.2
2	763	10.7	445	7.95
3	762	4.16	442	3.08
4	746	2.07	440	1.56
5	646	1.24	420	0.90
6	514	0.68	273	0.50
7	406	0.34	111	0.22
Filter	111		27	
Sample Volume DNm^3	0.064		0.161	

Table A-35. Cascade Impactor Data for Run 37/13

Impactor Stage Number	Inlet		Outlet	
	W_{cum} (mg/DNm^3)	d_{pc} (µmA)	W_{cum} (mg/DNm^3)	d_{pc} (µmA)
1	1,874	24.3	496	18.8
2	1,656	10.7	445	8.23
3	1,651	4.12	442	3.18
4	1,558	2.12	439	1.65
5	1,187	1.23	429	1.00
6	1,048	0.67	301	0.53
7	909	0.30	80	0.24
Filter	168		28	
Sample Volume DNm^3	0.103		0.191	

Table A-36. Cascade Impactor Data for Run 37/15

Impactor Stage Number	Inlet		Outlet	
	W_{cum} (mg/DNm^3)	d_{pc} (µmA)	W_{cum} (mg/DNm^3)	d_{pc} (µmA)
1	823	26.3	251	23.4
2	769	11.5	158	10.3
3	752	4.45	154	3.97
4	746	2.21	148	2.01
5	713	1.33	146	1.16
6	601	0.73	131	0.62
7	524	0.35	131	0.19
Filter	396		131	
Sample Volume DNm^3	0.090		0.108	

Table A-37. Cascade Impactor Data for Run 37/16

Impactor Stage Number	Inlet		Outlet	
	W_{cum} (mg/DNm^3)	d_{pc} (µmA)	W_{cum} (mg/DNm^3)	d_{pc} (µmA)
1	1,423	26.7	535	35.1
2	1,149	11.7	535	15.4
3	1,115	4.53	481	5.94
4	1,082	2.35	427	3.01
5	1,012	1.42	373	1.74
6	871	0.72	319	0.96
7	737	0.27	274	0.41
Filter	576		229	
Sample Volume DNm^3	0.030		0.022	

Table A-38. Cascade Impactor Data for Run 37/17

Impactor Stage Number	Inlet		Outlet	
	W_{cum} (mg/DNm^3)	d_{pc} (µmA)	W_{cum} (mg/DNm^3)	d_{pc} (µmA)
1	4,879	51.9	1,879	21.1
2	3,253	22.7	1,497	9.24
3	3,105	8.77	1,314	3.57
4	2,859	4.50	1,176	1.81
5	2,686	2.58	962	1.05
6	2,440	1.34	779	0.58
7	2,292	0.82	596	0.25
Filter	2,095		367	
Sample Volume DNm^3	0.040		0.007	

Table A-39. Cascade Impactor Data for Run 37/18

Impactor Stage Number	Inlet		Outlet	
	W_{cum} (mg/DNm^3)	d_{pc} (µmA)	W_{cum} (mg/DNm^3)	d_{pc} (µmA)
1	560	26.6	300	22.5
2	111	11.6	248	9.84
3	87	4.50	234	3.80
4	78	2.24	228	1.97
5	68	1.35	224	1.19
6	61	0.74	220	0.61
7	51	0.38	203	0.22
Filter	38		161	
Sample Volume DNm^3	0.092		0.121	

Table A-40. Cascade Impactor Data for Run 37/19

Impactor Stage Number	Inlet		Outlet	
	W_{cum} (mg/DNm^3)	d_{pc} (µmA)	W_{cum} (mg/DNm^3)	d_{pc} (µmA)
1	1,973	26.5	420	15.5
2	996	11.6	396	6.78
3	785	4.48	387	2.62
4	632	2.26	387	1.35
5	543	1.30	387	0.78
6	453	0.68	387	0.42
7	428	0.42	85	0.18
Filter	345		70	
Sample Volume DNm^3	0.016		0.033	

Table A-41. Cascade Impactor Data for Run 37/20

Impactor Stage Number	Inlet		Outlet	
	W_{cum} (mg/DNm^3)	d_{pc} (µmA)	W_{cum} (mg/DNm^3)	d_{pc} (µmA)
1	1,624	29.2	421	15.5
2	1,124	12.8	417	6.78
3	1,115	4.94	407	2.62
4	1,112	2.56	407	1.35
5	1,087	1.55	407	0.78
6	1,026	0.79	407	0.42
7	947	0.28	89	0.18
Filter	921		73	
Sample Volume DNm^3	0.084		0.033	

Table A-42. Cascade Impactor Data for Run 37/21

Impactor Stage Number	Inlet		Outlet	
	W_{cum} (mg/DNm^3)	d_{pc} (µmA)	W_{cum} (mg/DNm^3)	d_{pc} (µmA)
1	3,142	34.1	401	20.7
2	1,310	15.0	381	9.07
3	1,251	5.79	377	3.51
4	1,245	3.08	375	1.75
5	1,217	1.83	346	1.05
6	1,175	0.98	273	0.59
7	211	0.50	105	0.34
Filter	183		17	
Sample Volume DNm^3	0.076		0.242	

Table A-43. Cascade Impactor Data for Run 37/23

Impactor Stage Number	Inlet		Outlet	
	W_{cum} (mg/DNm^3)	d_{pc} (µmA)	W_{cum} (mg/DNm^3)	d_{pc} (µmA)
1	1,924	36.5	543	19.8
2	1,602	16.0	537	8.70
3	1,521	6.19	535	3.36
4	1,416	3.19	532	1.68
5	1,311	1.86	522	1.01
6	1,230	1.05	442	0.57
7	882	0.59	225	0.33
Filter	170		75	
Sample Volume DNm^3	0.012		0.191	

Table A-44. Cascade Impactor Data for Run 37/24

Impactor Stage Number	Inlet		Outlet	
	W_{cum} (mg/DNm^3)	d_{pc} (µmA)	W_{cum} (mg/DNm^3)	d_{pc} (µmA)
1	5,622	30.2	704	22.1
2	2,197	13.2	646	9.70
3	2,147	5.11	646	3.76
4	2,020	2.66	646	1.90
5	1,917	1.62	646	1.11
6	1,822	0.87	593	0.63
7	1,708	0.45	325	0.31
Filter	523		69	
Sample Volume DNm^3	0.071		0.054	

Table A-45. Cascade Impactor Data for Run 37/25

Impactor Stage Number	Inlet		Outlet	
	W_{cum} (mg/DNm³)	d_{pc} (μmA)	W_{cum} (mg/DNm³)	d_{pc} (μmA)
1	7,230	29.6	765	20.7
2	6,319	13.0	748	9.09
3	6,297	5.01	743	3.52
4	5,921	2.58	740	1.75
5	5,263	1.51	727	1.06
6	4,309	0.85	627	0.50
7	2,191	0.48	311	0.34
Filter	441		88	
Sample Volume DNm³	0.049		0.188	

Table A-46. Cascade Impactor Data for Run 37/26

Impactor Stage Number	Inlet		Outlet	
	W_{cum} (mg/DNm³)	d_{pc} (μmA)	W_{cum} (mg/DNm³)	d_{pc} (μmA)
1	1,744	28.3	601	20.7
2	1,509	12.4	599	9.08
3	1,498	4.80	596	3.51
4	1,437	2.50	594	1.75
5	1,263	1.52	587	1.05
6	1,074	0.81	552	0.60
7	684	0.42	312	0.34
Filter	210		142	
Sample Volume DNm³	0.064		0.218	